October 2019

THE ROLE OF AGULHAS LEAKAGE IN PLIOCENE CLIMATE CHANGE

Neil Patel

THE ROLE OF AGULHAS LEAKAGE IN PLIOCENE CLIMATE CHANGE

A Dissertation Presented

by

Neil Patel

Submitted to the Graduate School of the
University of Massachusetts Amherst in partial fulfillment
of the requirements for the degree of

DOCTOR OF PHILOSOPHY

September 2019

Geosciences

THE ROLE OF AGULHAS LEAKAGE IN PLIOCENE CLIMATE CHANGE

A Dissertation Presented

by

NEIL PATEL

Approved as to style and content by:

_____
Robert M. DeConto, Chair

_____
Alan Condron, Member

_____
Mark Leckie, Member

_____
Julie Brigham-Grette, Member

_____
Richard Palmer, Member

_____
Julie Brigham-Grette, Department Head
Department of Geosciences

DEDICATION

To my parents, Faith and Pravin

ACKNOWLEDGEMENTS

I'd like to acknowledge and thank all the people who have guided me on my journey in completing this thesis. The entire UMass Geosciences Department, both students and faculty, helped in creating a welcoming environment for getting acquainted with a new field. In particular, the enthusiasm of all the people at the Climate Center helped spark great discussions and increased my understanding of the broader significance of my work.

But foremost, I would like to thank my advisor, Professor Robert DeConto, for his guidance for my entire time in the program. His broad knowledge of both climate modeling and paleoclimate was invaluable in helping me brainstorm ideas. He was also incredibly patient when I got stuck, which happened frequently in this complicated modeling experiment. I would also like to thank Professor Alan Condron for helping me setup the MITgcm and in diagnosing its frequent crashes. Additionally, his advice on climate modeling was very useful.

ABSTRACT

THE ROLE OF AGULHAS LEAKAGE IN PLIOCENE CLIMATE CHANGE

SEPTEMBER 2019

NEIL P. PATEL, B.A., CORNELL UNIVERSITY

M.S., UNIVERSITY OF MASSACHUSETTS AMHERST

Ph.D., UNIVERSITY OF MASSACHUSETTS AMHERST

Directed by: Professor Robert DeConto

The late Pliocene (2.6-3.3 Myr) was an epoch of gradual cooling, with expanding Antarctic ice sheets and sea ice preceding a general Northern Hemisphere glaciation. A decline in the strength of the Atlantic Meridional Circulation (AMOC) in the late Pliocene may have decreased Southern Hemisphere oceanic heat transport into the Northern Hemisphere; pre-conditioning it for glaciation. A common explanation for a weakening of the AMOC in paleoclimate is freshwater forcing into the North Atlantic. In this thesis, I posit that a northward shift in the Southern Hemisphere westerlies in the late Pliocene, due to an expanded Antarctic ice sheet, weakens the Agulhas Leakage — a narrow current flowing past the Cape of Good Hope that connects the Indian and Atlantic Ocean basins. Since the Agulhas Leakage transports relatively salty waters from the Indian Ocean into the South Atlantic, it could alter the AMOC by changing the density stratification in North Atlantic deep-water formation sites. To test this hypothesis, I use a high-resolution (1/6°) ocean model, the MITgcm, with passive and Lagrangian particle-based tracers to quantify changes in Agulhas Current leakage. Following a spin-up simulation, I run two experiments, an experiment with a prescribed 6° northward shift in the southern westerlies and a control experiment with unchanged winds, both run for 58

model-years. I found a quick (< 10 year) decline in Agulhas Leakage volume in the northward wind perturbation experiment that, by the experiment end, led to changes in North Atlantic surface densities, including in areas of North Atlantic deep water formation (NADW), with an increase in vertical stratification in the perturbation experiment suggesting a weakening of the NADW. The findings from my research indicate that Agulhas Leakage water has a pathway into the North Atlantic and that the northward wind perturbation decreased the influx of Agulhas water into the North Atlantic, with corresponding implications for salt and heat transport. A northward shift in the southern westerlies is therefore a plausible mechanism for inter-hemisphere heat transport, altering the surface branch of the AMOC and inter-hemisphere heat transport and as such likely played a role in altering climate during the late Pliocene.

TABLE OF CONTENTS

Page

LIST OF TABLES

Table Page

LIST OF FIGURES

Figure Page

CHAPTER 1

INTRODUCTION

The mid-Pliocene (~3.3 Myr) was a period with an average Earth surface temperature ~2-3°C warmer than today, while atmospheric CO_2 was similar to today at ~400 ppm (Raymo and Mitrovica 2012). Antarctic ice sheet volume was smaller than today with global sea levels estimated to be at least 6m higher than today, and possibly 20m or more (Dutton et al., 2015; Miller et al., 2012; Rovere et al., 2014).

The transition from the warm Pliocene climate to a cooler Pleistocene climate with glacial cycles was accompanied by a reorganization of the global wind belts, a larger meridional temperature gradient, and expanding ice sheets (Brierley and Fedorov, 2010; Ravelo et al., 2004). Paleoclimate evidence shows the expansion of the Antarctic ice sheet was accompanied by increased sea ice and a change in deep water masses, in particular Antarctic Bottom Water replacing North Atlantic Deep Water (McKay et al., 2012). The subsequent cooling was followed by expanded Northern Hemisphere continental ice sheets, including the first large ice sheet over North America, similar to the Laurentide of the Last Glacial Maximum (Bailey et al., 2013; Shackleton, 1995, Haug et al., 2005).

One little-explored trigger for Northern Hemisphere glaciation is the growth of the Antarctic Ice Sheet during the late Pliocene. McKay et al. (2012) found detailed evidence for substantial Antarctic Ice sheet expansion, which was accompanied by coastal sea surface temperature cooling (~2.5°C) as well as expanded sea ice. These changes were found to be correlated with a northward shift in the southern westerlies, which are

observed in the paleo-record (Lee et al., 2011), and with a weakened Atlantic Meridional Overturning Circulation (AMOC).

Both modeling (Sijp and England, 2008) and paleoclimate proxy evidence (Bard and Rickaby, 2009) suggest a northward shift in the southern westerlies would have numerous consequences on the global ocean basin. The northward migration of the southern westerlies leads to a mis-alignment between the center of the Antarctic westerlies and the core of the Antarctic Counter-Current, whose latitude is topographically constrained by the Drake Passage, leading to a weakening in the Antarctic Counter-Current (Sijp and England, 2004, 2008). This decreased wind forcing on the Southern Ocean has the potential to impact the upwelling of NADW and reduce AABW formation (Spence et al., 2017; Gent et al.,2015). This upwelling is part of the southern limb of the AMOC; a slowdown of the upwelling would result in a slowdown of the entire AMOC (Kuhlbrodt et al., 2007).

An additional mechanism by which a shift in the southern westerlies could trigger changes in hemispheric oceanic heat transport is via changes in the leakage magnitude of the Agulhas Current. The Agulhas Current is a western boundary current that flows along the east coast of southern Africa. Most of it retroflects back into the Indian Ocean, while a portion leaks past the Cape of Good Hope into the South Atlantic, contributing salt and heat into the Southern Ocean as the Agulhas Leakage (Figure 2.1). This salt and heat contribution affects the Atlantic Meridional Overturning Circulation, so Agulhas variability may control AMOC variability (Sijp and England 2008; Beal et al., 2011; van Sebille et al., 2015; de Boer et al., 2008).

Like all western boundary currents, the Agulhas Current is wind-driven (Hermes et al. 2007; Beal et al., 2011). The Indian Ocean north of 30°S is under the influence of southeast trade winds. To the south lie the southern westerlies belt, which extends south to 60° across the globe. This wind configuration results in a positive wind stress curl (reflecting the change in wind speed with latitude) over the Agulhas Region down to the Cape of Good Hope (Figure 2.1). Through Ekman pumping, positive wind stress curl keeps the western boundary current in place within the South Indian Ocean gyre with counter-clockwise rotation (de Boer et al., 2013). At the position of maximum westerlies, the wind stress curl is zero and the Agulhas Current is free to exit the gyre as Leakage (Beal et al., 2011). How much Indian Ocean water “leaks” in to the North Atlantic is controlled by the position of the southern westerlies and the inertia, or the strength of the Agulhas Current.

Here, I investigate the potential for a northward shift in the southern westerlies to weaken the hemispheric south - north heat transport using the MITgcm, a high-resolution eddy-permitting numerical ocean model. In particular, I focus on how wind-driven alterations of the Agulhas Leakage strength would change the inter-hemispheric heat transport. Much of the Agulhas Leakage is carried by fine structures such as eddies or "Agulhas rings" (Schouten et al., 2000; Loveday et al., 2014; Cheng et al., 2016), so a sufficiently high-resolution ocean model is needed to resolve eddies, which is what I used in the study.

Climate models can isolate how sensitive the Agulhas Leakage is to plausible northward shifts in the southern westerlies of a late Pliocene atmosphere. A modeling study can also

quantify global shifts in water masses to a northward wind perturbation. While modeling studies have been performed on how the Agulhas Leakage may impact a present-day ocean (Biastoch and Böning, 2013; Durgadoo et al., 2013) to date, none have been conducted to test how it modulated the AMOC in the Pliocene. My experiment will help ascertain whether a northward shift in the southern westerlies in the late Pliocene, reflecting expanded an Antarctic ice sheet and sea ice, could have transferred high-latitude southern hemisphere cooling to the North Atlantic via Agulhas Leakage. This question can be split into two main hypotheses:

1. The northward shift in southern westerlies at the end of the Pliocene results in a significant decrease in Agulhas Leakage volume

2. This decrease in Agulhas Leakage volume results in a slowdown of the AMOC

In this work, I will use the results of a high-resolution ocean simulation to provide evidence supporting both of these ideas. In chapter 2, I'll discuss the general background of both of the above hypotheses: the current knowledge of the geography and mechanics of the controls on the southern westerly strength and position, as well as the climate of the Pliocene. In particular, I will discuss prior paleo-climate proxies and modeling research on shifts in the southern westerlies and the Agulhas Leakage in the past and future, which inform my experimental setup. In chapter 3, I will discuss details of the modeling experiment setup and motivative my choice of wind forcing. Subsequently, I will discuss results, which are separated into chapters 4 and 5. Chapter 4 discuses on global ocean property changes, focusing on ones relevant to AMOC changes to determine whether there is any slowdown in the AMOC in response to my perturbation. Chapter 5

discusses my methods for measuring Agulhas Leakage volume changes and the observed decrease in Agulhas Leakage in response to the wind perturbation, answering the first hypothesis (listed above). Chapter 6 discusses the results and the role the Agulhas Leakage decline could played in affecting the AMOC.

CHAPTER 2

BACKGROUND

2.1 Introduction

Both the controls and impacts of the Agulhas Leakage have been an area of expanding research interest (Beal et al., 2011; Weijer and van Sebille 2014; Castellanos et al., 2017; Kelly et al., 2016). Most Agulhas Leakage modeling studies have investigated how Agulhas Leakage changes could have a global impact under future global warming, rather than during past climate change. Paleoclimate proxy evidence shows the Agulhas Leakage underwent major fluctuations during the Pleistocene, many of these fluctuations correspond to transitions to interstadial or stadial conditions (van Sebille et al., 2015; Caley et al., 2014; Turney and Jones, 2010). At many stadial and interstadial terminations, Agulhas Leakage changes precede global climate change, implying that the Agulhas Leakage was one of the triggers of global climate change, although the precise timing of the changes remain poorly resolved, hampering conclusions regarding the actual role of the current. (Brummer et al., 2004; Bard and Rickaby, 2009; Marino et al., 2013; Flores et al., 1999)

Both model future forecasts of southern hemisphere westerly winds and past proxy evidence suggest westerlies have shifted zonally with global temperature change. In the first half of this section, I'll discuss in more detail the dynamics of the Agulhas Leakage, the Westerly winds, and prior research on wind-driven impacts on the Agulhas. Subsequently, I'll summarize the climate of the Pliocene and Pliocene-Pleistocene transition.

2.2 The Agulhas Leakage

The Agulhas Current is a western boundary current in the subtropical Indian Ocean. A portion of the current 'leaks' into the South Atlantic just south of the Cape of Good Hope as the so-called *Agulhas Leakage*, while most (about 80%) of the Agulhas Current water recirculates back into the Indian Ocean (Figure 2.1). This leakage water is warmer and saltier than the background South Atlantic water at similar depths, so Agulhas Leakage changes have the potential to modify the properties of the South Atlantic and therefore Atlantic Ocean circulation, with potential further global consequences. Some of the leakage water remains in the South Atlantic gyre (Figure 2.1), while some returns back to the Indian Ocean via the South Atlantic Current (Dencausse et al, 2010; Gordon, 2003), but the remainder goes into the surface component (Richardson, 2007) of the Atlantic Meridional Overturning Circulation (AMOC) of the North Atlantic. The salt transport is of greater importance in affecting ocean currents than the heat transport, as heat more easily diffuses, or is lost to the atmosphere by evaporation. In contrast, the extra salinity remains in the ocean (Weijer et al., 2002). Some of the additional salt is transported into the Gulf Stream, increasing its density and therefore the strength of buoyancy forcing on the overturning circulation. The Atlantic Meridional Overturning Circulation refers to the overall zonal component of Atlantic Ocean currents, extending from the Southern Ocean to Arctic sections of the Atlantic. The net surface flow is northward and contains relatively warm and saline water, resulting in a net heat and salt transport into the North Atlantic. A return flow of cold water flows in the deep Atlantic . (Lumpkin and Speer, 2007; see Figure 2.2) Connecting the surface flow to the deep water flow are regions of upwelling and downwelling in the cold, dense high-latitude seas where a weak density

stratification allows water to sink or rise. The main deep water formation sites are in the subpolar North Atlantic, while upwelling mostly occurs within the Southern Ocean in zones of wind divergence at the site of the Antarctic Circumpolar Current (Hogg et al., 2016; Morrison et al., 2014) The AMOC is an important modulator of the Earth's global climate by creating a net oceanic heat transport from the southern hemisphere to the northern hemisphere (Buckley and Marshall 2015; Cunningham and Marsh 2010). In particular, the AMOC has a particularly large influence on the high latitude North Atlantic temperatures (Vellinga and Wood, 2002).

Recently, there has been increased scientific interest in the potential impact of Agulhas Leakage changes in amplifying global climate change (Beal et al., 2011; Biastoch and Böning 2013; Weijer and van Sebille 2014; Rouault et al., 2009). One particular motivation is the impact of the Agulhas Leakage salt transport to the South Atlantics on the strength of the AMOC (Biastoch et al., 2015; Lübbecke et al., 2015; Weijer et al., 2002; McCarthy et al., 2012; Simon et al., 2015). In addition, the heat transported by the Agulhas Leakage into the Atlantic may also play role in modulating the overturning circulation (Kelly et al., 2016). These transports could allow the Agulhas Leakage to transfer climate changes in the southern hemisphere to the northern hemisphere. Recent studies have found an increase in the Agulhas Leakage and tied it to a recent southward shift in the westerlies. Climate change projections suggest the Agulhas Leakage will continue to increase in the future (Biastoch et al., 2009; Beal et al., 2011)

2.3 Agulhas Leakage Controls

The Agulhas Leakage results from a complicated interaction between a western boundary

current, a changing coastal geography and mesoscale structures such as eddies. This makes determining the details of the Agulhas Leakage response to an alteration in the wind configuration not straightforward, but observations plus general dynamic arguments give some clues. Paleo-climate evidence suggests the Agulhas Leakage strength is correlated to a more southerly position of the southern westerlies (list references). Wind dynamics sets the boundaries of the Agulhas System, allowing us to make some inferences on the effect of the southern westerlies. The counter-clockwise motion of the Indian Ocean gyre, of which the Agulhas Current is a part of, is imparted by a positive wind stress curl. At the southern edge of the Indian Ocean gyre, the wind stress curl, eventually reaching zero. At zero wind stress curl, the Agulhas Current has no rotational forcing and is free to exit the gyre (Biastoch et al., 2009). From these wind forcings, the primary controls can be described by two factors (Beal et al., 2011):

1) The position of zero wind stress curl in the Agulhas Region

2) The inertia of the Agulhas Current itself

The position of zero stress curl is where the southern westerlies are at their maximum magnitude. A change in southern westerly magnitude would not affect the position of zero wind stress curl, however, depending on the shape of the magnitude change the wind stress forcing is altered. Some Agulhas modeling work has looked at the effects of a change in the southern westerly magnitude (Biastoch et al., 2009; Durgadoo et al., 2013). However, I focus on a shift in the southern westerlies, as it is easier to tie with paleo-climate evidence (McKay et al., 2012).

Most work and modeling studies posit (de Ruijter et al., 1999) a higher inertia, or higher Agulhas Current speed, results in more Agulhas Current retaining its velocity and staying within the gyre. A lower inertia allows more of the current to leak out of its circular path (Van Sebille et al., 2009; Beal et al., 2011). The Agulhas Current speed is partially controlled by the strength of the trade winds. However, modern observations (Dencausse, et al., 2010; Loveday et al., 2014) and past reconstructions (Franzese et al., 2006) show that changes in inertia have only a limited effect on the Agulhas Leakage position, while the southern westerlies are more important.

Since the Agulhas Current is free to leak westward only where the wind stress curl is near zero (latitude of maximum westerlies), the position of maximum westerlies has a strong effect on the magnitude of leakage. At one extreme, if the westerlies moved so far north that the latitude of maximum wind stress was north of the Cape of Good Hope, it would be unable to leak westwards as land blocks it. If the westerlies moved far south of the Cape of Good Hope, the Agulhas Leakage would experience less wind stress at the Cape of Good Hope from the east. Therefore, I expect a southward shift in the southern westerlies would result in more leakage and a northward shift; less leakage.

While most recent work (Rouault et al., 2009; Biastoch et al., 2009; Sijp and England, 2008) on the Agulhas Leakage shows a northward migration of the southern westerlies is accompanied by a weakening of the Agulhas Leakage (and a southward migration with a strengthening), since the Agulhas Leakage contains many small-scale features, the simulated response is model dependent. One high-resolution modeling study (Durgadoo et al., 2015), found an increase in Agulhas Leakage from a model prescribed northward

shift in southern westerlies. This unexpected result was due to the wind shift increasing wind stress curl in the Cape of Good Hope region. In addition, they found that increasing the magnitude of the westerlies leads to a transient increase in Agulhas Leakage, but after several model -decades the Agulhas Leakage magnitude returns to its prior value before the westerly increase.

The range of Agulhas Leakage responses to a shift in the southern westerlies in the scientific literature makes it hard to evaluate its consequences. However, both current changes and paleoclimate evidence (Section 2.6) suggest a southward shift in the westerlies results in a strengthening of the Agulhas Leakage while a northward shift in the westerlies results in a weakening of the leakage. In recent decades, the southern westerlies have been moving southward. Several simulations have tied the recent southward movement in the westerlies to an increase in Agulhas Leakage (Biastoch and Böning, 2013). Biastoch (2009) ran an ocean model hindcast (from 1958–2004) forced with the recent wind changes and compared the results to a control simulation based on wind stresses prior to the beginning of the shift and found a statistically significant increase in the Agulhas Leakage. (Rouault et al., 2009) tied the recent warming of the Agulhas Current to a strengthening of the southern westerlies. The discrepancy between the work of Durgadoo et al. (2013) with recent observations and hindcast could be a result of the ocean not reaching equilibrium, however, other work suggests a more lasting response, especially when more global oceanic dynamic effects are considered.

2.4 Future Trends in Westerlies

Numerous modeling projections suggest that the westerlies will shift even further south

with a continued increase in global temperatures via an intensification and widening of the Hadley Cell (Russell et al., 2006). However, global climate change is not the sole cause of recent trends in the southern westerlies. Besides global warming, ozone hole depletion has been found responsible for some of the shift via an alteration of the Southern Annular Mode (Yang et al., 2007). While the ozone-dependent changes should decline in the near future, global warming induced poleward movement of the westerlies should continue. There is substantial uncertainty in southern westerly forecast, with model forecasts underestimating southern westerly wind changes; for example, a comparison study by Swart and Fyfe (2012) found models show a modest strengthening in the westerlies and a slight summer southward shift (0.4°) in mean summer position in 1979-2010 in the CMIP5 model average. In contrast, reanalysis observational data found a more significant change; with almost double (0.8°) the summer southward shift in even though a larger shift has been observed. But there is general consensus that there has already been a significant but small trend in the southern westerlies.

In the future, climate change projections predict a continued strengthening and southward movement in the southern westerlies due to global warming, despite a diminished impact from ozone (Wang et al., 2014), with the more extreme scenarios forecasting a large southern shift in the westerlies. The IPCC 5th assessment (IPCC, 2014) defined its potential climate futures by the future greenhouse gas concentration or Representative Concentration Pathway (RCP). Each of the RCPs are labeled by the radiative forcing in Watts per meter squared, with RCP 8.5 the most extreme "business as usual" scenario and RCP 2.6 the scenario involving the largest reduction in human emission. In RCP 8.5 (Riahi et al., 2011; Meinshausen et al., 2011; van Vuuren et al., 2011), the NCAR

CCSM4 forecasts a poleward movement of the southern westerlies of roughly 3° by the end of the 22nd century (Meehl and Washington, 2012) and shown in Figure 2.3. By the end of the 21st century, the RCP 8.5 scenario is the only scenario that shows a significant southward shift in the annual mean position. However, all scenarios have changes in westerly strength except RCP 2.6, the scenario representing the most carbon emissions mitigation (Swart and Fyfe, 2012). Part of the reason for the relatively weak predicted change is due to ozone recovery counteracting the effects of global warming.

By absorbing of UV radiation, ozone warms the stratosphere (Son et al., 2010; Wang et al., 2014). Depleting stratospheric ozone cools the stratosphere while its recovery results in a slow, gradual warming of the stratosphere. Southern polar stratospheric cooling increases the temperature contrast between the tropopause and lower troposphere, raising the tropopause height. In the mid-atmosphere, this creates a weaker tropical to poles pressure difference (Son et al., 2009). The lower pressure gradient results in an expanded Hadley circulation and a southward shift in the southern westerlies. As the ozone layer recovers in the 21st century, the ozone recovery will induce southern westerlies to migrate northwards, partly counteracting poleward induced global warming (Swart and Fyfe, 2012; Son et al., 2010).

The 22nd century is forecast to see stronger changes in wind, as the ozone recovery would be nearly complete. It is possible that model predictions may underestimate the scale of westerly shifts, as both the CMIP3 and CMIP5 models have predicted less westerly wind change than the observed wind shift of the last few decades (Swart and Fyfe, 2012).

2.5 Southern westerly wind shifts in the past

Proxy and modeling data of the Earth's past informs us how the southern westerlies have varied and may vary in the future. Additionally, they also inform the possible magnitude of the westerlies impact on the Agulhas Leakage. Paleoclimate proxy evidence shows during colder periods of Earth's history, the southern westerlies shifted northward. The most recent cold period, and therefore the easiest accessible evidence, is the last glacial period in the Pleistocene, from 115 ka to 12 ka; with the peak of the cold, Last Glacial Maximum (LGM), roughly around 22 ka. Some prior interglacial-glacial periods of the Pleistocene can also provide evidence of westerly wind shifts and the Agulhas system response. However, the lines of evidence on glacial period southern westerly position are a challenge to interpret and can be somewhat conflicting. For example, the most accepted interpretation of LGM southern western westerly wind proxies is that the westerlies were more intense and were located further northward relative to present day. Rojas et al. (2009), however, concluded a weakening with no latitude shift while Russell et al. (2006) interpreted an equatorward shift. Atmospheric modeling does not provide much insight in narrowing down the possibilities, as most GCMs (Global Climate Models) have a large variation in the position of the southern westerlies during the LGM (Rojas et al., 2009, Sime et al., 2013, Chavaillaz et al., 2013). Many models show little LGM shift of the southern westerlies relative to present day. For example, the NCAR CCSM winds show only a slight difference in the position of the westerlies between the LGM and present-day, barely more than the discrepancy between the CCSM4 model position of the present-day southern westerlies compared to the observed winds **(**Figure 5 in Rojas et al., 2009).

Given the drastic differences in climate between the LGM and present-day, a small difference in westerly position may appear surprising. However, the LGM climate changes may have induced opposing shifts in the southern westerlies. The two main climatic differences between the last glacial period and today that had the biggest impact on the southern hemisphere westerly wind position are:

1) Equator-ward movement of the Hadley cell due to a cooler high latitude climate

2) Strengthened katabatic (polar easterly) winds and sea ice extent around Antarctica

If these two effects are nearly equal, then there would be little change in the southern westerlies during the LGM. During deglaciation, the two factors may have changed at different times, leading to large equatorial or poleward shifts in the southern westerlies (Kohfeld et al., 2013, Kohfeld private communication). So, even if there was little shift in the westerlies at the LGM compared to modern day, during deglaciation there may have been large shifts in the southern westerlies. Proxy-based reconstructions show that these large shifts in the position of the southern westerlies of the Agulhas Leakage during recent glacial-deglacial transitions coincide with the largest excursion in the magnitude of the Agulhas Leakage.

2.6 Paleo-Agulhas Evidence

Paleoclimate proxy data in Beal (2011) and Caley (2012) presented reconstructions of the Agulhas Leakage and the Subtropical Wind Front (shown in Figure 2.4) during the LGM. The Agulhas Leakage reconstruction was based on the abundance of tropical

foraminiferal species in marine sediments corresponding to warmer Agulhas Leakage water, measured right near the Cape of Good Hope (Figure 1 from Caley 2014). To the south lies the cold Southern Ocean, creating a sharp transition in marine species. The paleo-Subtropical Front position was defined to correspond to this species transition, reflected in the relative fraction of subtropical compared to sub-Antarctic species. From this reconstruction, the magnitude of the Agulhas Leakage was found at the times of glacial terminations to exhibit large, sudden changes (Marino et al., 2013; Caley et al., 2014). In addition, Caley (2014) found changes in the strength of Agulhas Leakage corresponded with orbital cycles, as well as the ~1500 year D-O events during the LGM. These peaks were found to be correlated with shifts in the subtropical front or southern westerly position, further confirming a linkage between the southern westerlies, the Agulhas Leakage, and climate change over a range of timescales.

Paleoclimate proxy evidence of the Agulhas region gives many indications that changes in the Agulhas Leakage corresponded with global climate changes by modulating the AMOC strength. Due to dating uncertainties, it is difficult to postulate a lead or lag between the Agulhas Leakage and the AMOC for proxy studies in the Pleistocene and Pliocene, however a few studies have to attempted to do so. A marine core inter-comparison study of the last interglacial by Turney and Jones (2010) found a time lag. The study analyzed at a high-resolution marine record of two sites underneath the position of the Agulhas retroflection, one in the Indian Ocean the other off of South Africa. They found warming in the Agulhas Leakage warming region led the global $\delta^{18}O$ record, indicating a possible contributing mechanism to global climate and ice volume. Other sites, such as in the North Pacific displayed no lead, suggesting that the Agulhas

Leakage or an associated southern hemisphere climate change may have been a cause of global climate change. An early warming was also found in the Southern Ocean and Indian Ocean but not the North Atlantic, suggesting an increase in Agulhas throughflow preceded North Atlantic and global temperature amplification (Turney and Jones 2010). Other observations, while unable to distinguish the event order, show strong evidence of a correlation between the Agulhas Leakage and glacial-interglacial cycles. For example, Marino (2013) found the resumption of the AMOC at the end of glacial stadials coincided with short-lived period of high Agulhas Leakage volume, suggesting an ability of the Agulhas Leakage to modulate AMOC strength

Bard and Rickaby (2009) noted a connection between MIS 10 and MIS 12, two unusually cold glacial periods, and a northward migration of the southern westerlies. In particular, MIS 10 and MIS 12 had higher productivity ocean waters and rather cool subtropical sea surface temperatures. Yet, orbital insolation and atmospheric CO_2 levels were similar to other glacial periods. However, the subtropical winds were unusually far north, with the potential to choke off the Agulhas Leakage. In particular, a site in the Indian Ocean normally bathed with warm Agulhas Current waters had fauna that reflected cooler waters, suggesting the Agulhas Current was prevented from reaching south to the leakage position. A possible mechanism noted by Bard and Rickaby (2009) is that the removal of Agulhas Leakage waters caused a weakening of the AMOC, cooling the climate. Adding credence to this hypothesis is a lower $\delta^{13}C$ contrast between the Atlantic and Pacific (Bard and Rickaby, 2009) reflecting a weaker dominance of the Atlantic in the overturning circulation, or weaker overturning in general. One important implication of a connection between the Southern Hemisphere westerlies, Agulhas Leakage, and the

AMOC, is that it provides a mechanism for the Antarctic region to have a global climatic influence on a range of timescales.

2.7 Agulhas Leakage in the Pliocene

The first occurrence of the periodic glacial-interglacial cycles with large-scale Northern Hemisphere ice sheets in the geological record is 2.7 Myr ago in the late Pliocene (Raymo, 1994; Shackleton, 1995; Willeit, 2015; de Schepper, 2013). Before that, the earth was substantially warmer (2-3°C) than today globally (Pagani et al., 2010; Zhang et al., 2013; Haywood 2016). Because it was accompanied by elevated carbon dioxide levels above pre-industrial levels (pre-industrial atmospheric CO_2 concentrations of 280 ppm; Pliocene CO_2 estimates range from 400-500 ppm) but similar to current or near-future levels, it is often considered a good analog for a future global warming climate when all climate feedbacks have filtered into the climate system (Zachos et al., 2008, Haywood et al., 2010, Lunt et al., 2009, Burke et al., 2018). At its warmest, the Antarctic Ice Sheets were much smaller than today; with strong evidence for a collapsed West Antarctic Ice Sheet during the warmest Temperatures (Naish et al., 2009; Pollard and DeConto, 2009). At its warmest, Pliocene sea level was 22±10 m higher than modern (Miller et al., 2012) Unlike earlier times deeper in Earth's history, the continental configuration was similar to today, with a few differences: the Panamanian Seaway was open and the Hudson Bay was subaerial (Haywood et al., 2013, Lunt et al., 2010). Otherwise, similar continental configuration makes it easier to model and compare with present-day climate compared to earlier time periods. However, Hill et al. (2015), suggested the aggregate of numerous paleogeographic differences result in the Pliocene

in being an imperfect analog to a future warming world; resulting in a different geography of warming and less meridional temperature gradients.

The mid-Pliocene, which contains the warmest times of the Pliocene, at the peak of its warmth had tropical sea surface temperatures expanded over a much greater area than today (Dowsett et al., 2013; Haywood et al., 2013). It is also probable there was an expanded warm pool over the entire tropical Pacific, often termed a "permanent El Niño-like state" (Dekens et al., 2007), although this is a subject of an energetic debate (Brierly and Federov, 2010; Watanabe et al., 2011). Overall, there was less zonal variation in the tropics; implying either upwelling zones were warmer or there was less upwelling. Both paleo-data and model evidence show expanded warm temperatures into the subtropics; with little sea surface temperature contrast between the subtropics and the tropics. The mid-latitude and high-latitude temperatures were warmer than today, with one reconstruction showing 3-6°C (Brierley and Fedorov, 2010) warmer.

How much warmer higher latitude Pliocene sea temperatures were compared to modern-day is unclear, as modeling and proxy data yield conflicting results. Models fail to simulate the very warm sea surface temperatures of the northern high latitudes found in proxy data, which show a warming as much as 10°C, even when matching the rest of the ocean well (Brierley and Fedorov, 2010; Haywood et al., 2013; Haywood et al., 2016; Haywood et al., 2010; Salzmann et al., 2008). Both the models are subject to weak constraints, making comparison to paleo-proxies difficult while interpreting the high-latitude proxies as there are uncertainties in the seasons they represent. The PRISM3D dataset used for proxy-based SST reconstructions of the mid-Pliocene (Robinson et al.,

2010) averages over 240,000 years; including multiple orbital cycles, resulting in smoothing over multiple Pliocene climate states, making a model comparison to one climate state less straightforward.

Model simulations of the Pliocene (Xiangyu et al., 2015) show a range of wind shifts of the southern westerlies; but most coupled GCMs have a moderate (3°) poleward shift of the southern westerlies . An inter-model comparison chart of Pliocene southern hemisphere westerlies is shown in Figure 2.5. One unexpected inconsistency is that climate model predictions of the Pliocene show little to no wind shifts relative to modern, despite the Pliocene having similar global temperatures to the middle of the road global warming scenarios, which do predict a significant southward shift in the westerlies. Other factors (e.g. ice sheet topography) must explain the discrepancy. Climate models also indicate that a reduced tropical-subtropical SST contrast of the Pliocene led to a weaker Hadley circulation (Brierley and Fedorov 2010) . Numerous paleo observations such as dust (Naafs et al., 2012) and a more southward Benguela upwelling zone (Petrick et al., 2015), agree with a more southerly westerly wind belt in the Pliocene. Observations also show the end of the Pliocene led to a shift of the westerlies from the mid-Pliocene position (McKay et al., 2012).

The cooling of the late Pliocene marks the first appearance of the northern hemisphere glacial cycles of the last 2.7 million years (Shackleton, 1995; Raymo, 1994). The triggers for these glacial cycles are important for understanding the earth's climate system, as it is a transition from the warm conditions of the early Pliocene to cold glacial / mild interglacial phases more similar to the Pleistocene but with a 41 kyr cycle. Both the

subtropics and the poles cooled; the tropical warm pool (area of the sea with temperature as warm or warmer than non-upwelling regions of the tropics today; roughly at or above 24°C) shrunk in size to a state closer to modern day. Simultaneously, the Pacific shifted from a "permanent El-Niño state" to something more resembling the modern climate state. The transition from the warm Pliocene climate to a cooler Pleistocene climate with glacial cycles was accompanied by a reorganization of the global wind belts, a larger meridional temperature gradient and expanding ice sheets (Brierley and Fedorov 2010). Paleoclimate evidence shows that during the expansion of the Antarctic ice sheet (McKay et al., 2012; Hill et al, 2017), Antarctic sea ice increased and an alteration in the origin of deep-water masses, in particular Antarctic Bottom Water replacing North Atlantic Deep Water.

The increased Antarctic ice sheets and sea ice likely led to numerous positive feedbacks. The southern westerly wind belt and circumpolar current moved northwards, along with a higher meridional temperature gradient, resulting in a reorganization of the Hadley cell circulations. In addition, the northward southern westerly shift would have impacted the Agulhas Leakage. The change in Southern Ocean water mass led to less ocean ventilation. A decrease in ocean ventilation would promote a subsequent drawdown in atmospheric carbon dioxide, leading to further cooling. The growth of northern hemisphere ice sheets occurred after the M2 Antarctic ice sheet expansion (McKay et al., 2012), suggesting the feedbacks resulting from a cooling high-latitude southern hemisphere could be responsible for a cooling northern hemisphere. A flowchart diagram for the feedbacks involved in my hypothesis is shown in Figure 2.6.

One positive feedback in particular that has the potential for cooling the northern hemisphere is a change in the AMOC via a weakening of the Agulhas Leakage. Both modeling and $\delta^{13}C$ evidence support a mid-Pliocene AMOC not unlike modern (Zhang et al., 2013). The modern AMOC has a net heat transport from the South Atlantic to the North Atlantic, while glacial periods had an AMOC much weaker than modern (Muglia and Schmittner, 2015; Arzel et al., 2008). In the transition to the cooler, more variable Pleistocene, a weakening Agulhas Leakage could have been responsible for an overall, long term weakening of the AMOC. This weakening of the AMOC could have resulted in less heat transported to the northern hemisphere, leading to a cooler high-latitude northern hemisphere.

The most common explanation for an AMOC slowdown during glacial periods is forcing from North Atlantic meltwater (Vellinga and Wood 2002); here, I investigated a southern hemisphere induced mechanism: the Agulhas Leakage. In this section, I have discussed paleoclimate proxy evidence showing the Agulhas Leakage frequently declined during transitions from warmer interglacials to glacial periods, with the decline accompanied by a northward shift in the southern westerlies. Ekman dynamics imply that a shift in the southern westerlies impacts the extent of the South Indian Ocean gyre, altering the circulation near the Agulhas Retroflection. Modeling studies, discussed previously, have showed this results in a change in Agulhas Leakage volume although the studies disagree on the resulting change from a southern westerly shift. The magnitude of the southern westerlies shift in the late Pliocene is uncertain; however, paleoclimate proxies and modeling help narrow the range of likely wind shifts. These previous modeling and paleoclimate proxy studies suggest both of the hypothesis I wish to test are plausible: (1)

a northward shift in the southern westerlies can decrease the Agulhas Leakage in the Pliocene (2) a decrease in the Agulhas Leakage weakens the AMOC. The details of the experiment setup to test these hypotheses are discussed in the next chapter.

2.8 Figures

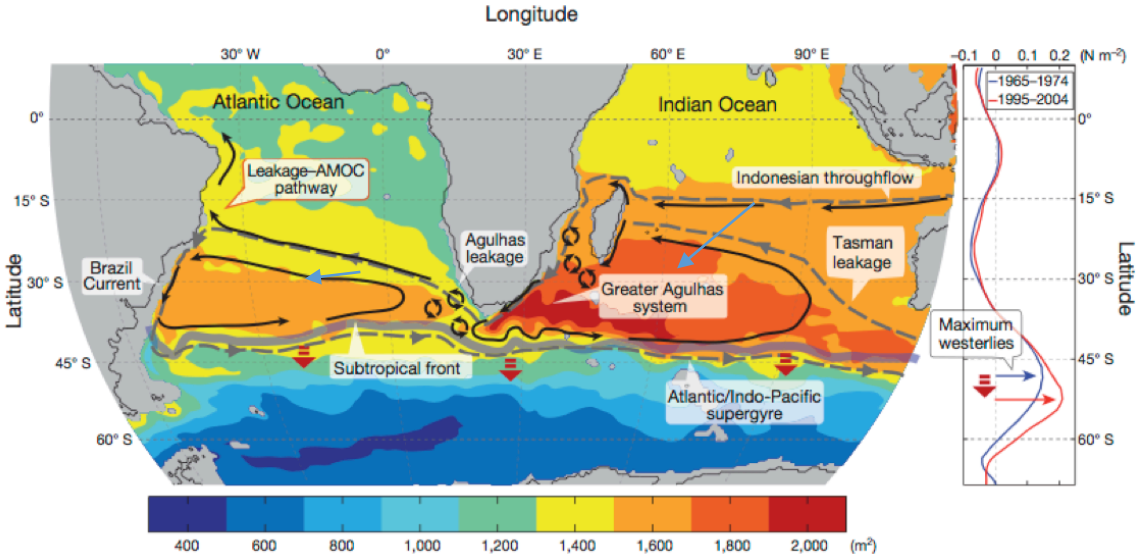

Figure 2.1 Map of the Agulhas system, taken from Beal (2011). Map colors show the mean subtropical gyre circulation, depicted by climatological dynamic height. Line graph represents the zonal wind stress averaged between longitudes 20°E and 110°E. The arrows of the greater Agulhas systemin the map show the prevailing circulation is counter-clockwise, with the retroflection position just south of the Cape of Good Hope, which is set by the subtropical front position

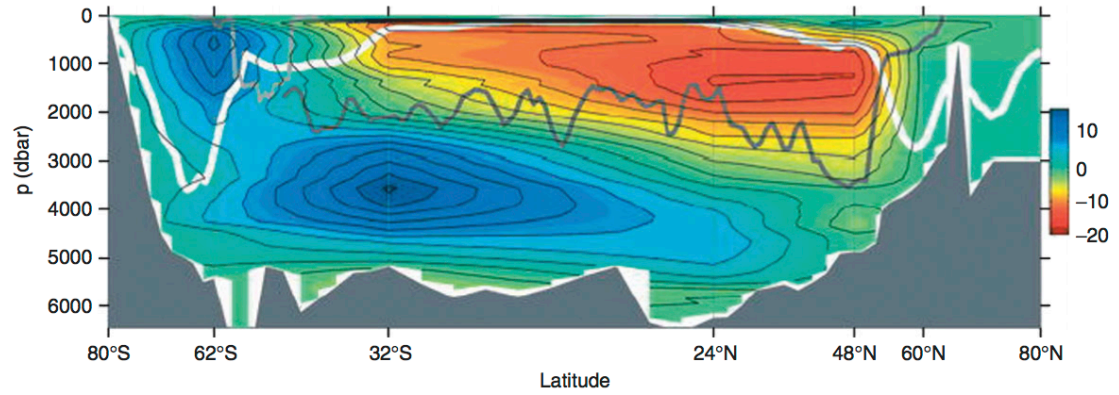

Figure 2.2 Observed AMOC taken from figure 2 of Lumpken and Speer 2007. Southward depth-integrated transport in Sv (meridional overturning function). White line typical winter mixed layer depths; gray line mean depth of ocean ridge crests. Peak northward volume transport occurs at about 30°N in the upper 1500 m.

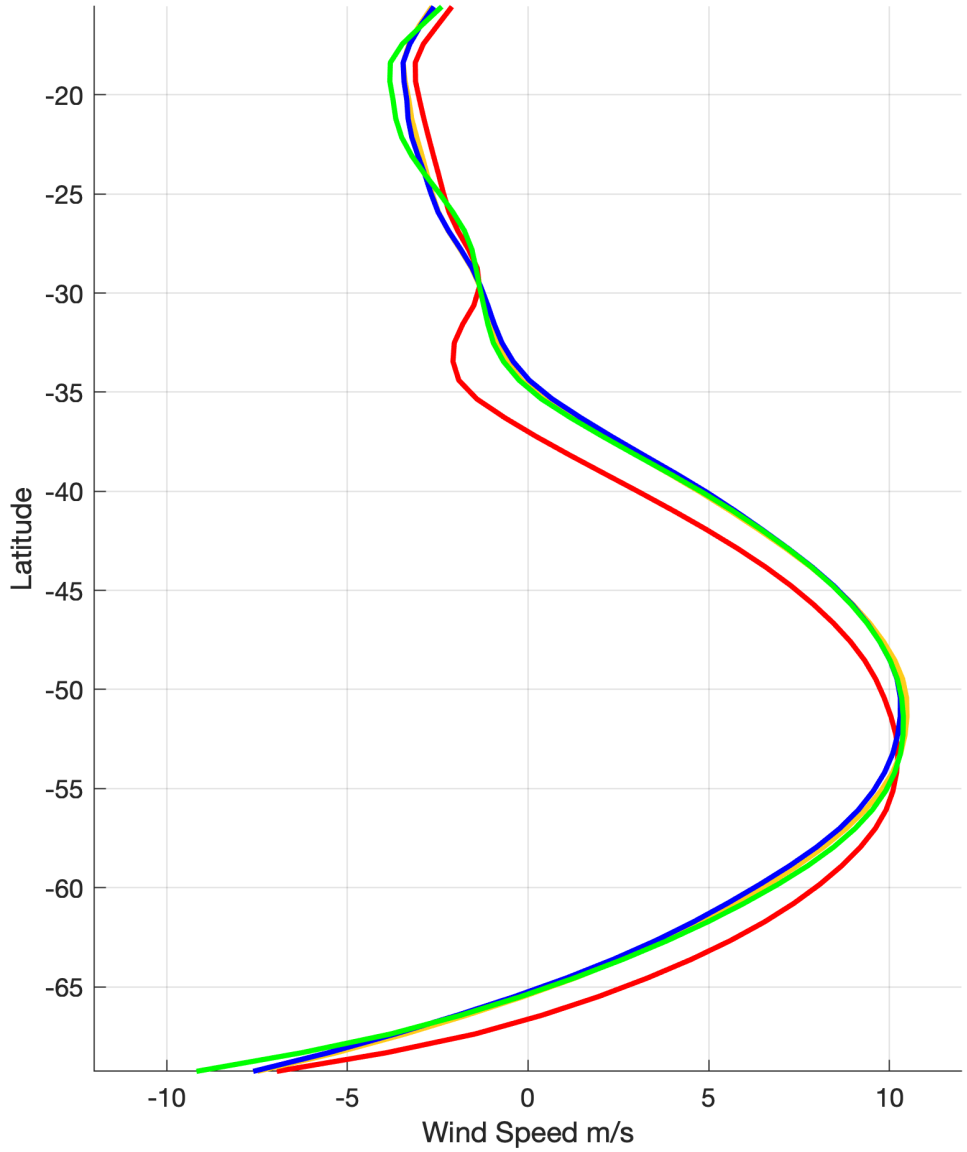

Figure 2.3 Zonal wind speed averaged between 5°E and 40°E (longitude of the Agulhas Region) in the CCSM4 model output. comparing different time periods in the southern hemisphere summer. Red presents the RCP 8.5 scenario in the 23rd century. Yellow, modern (1970-2000). Blue, pre-industrial (1870-1900). Green, Pliocene. The winds mid-Pliocene in equilibriums is little different from present-day.

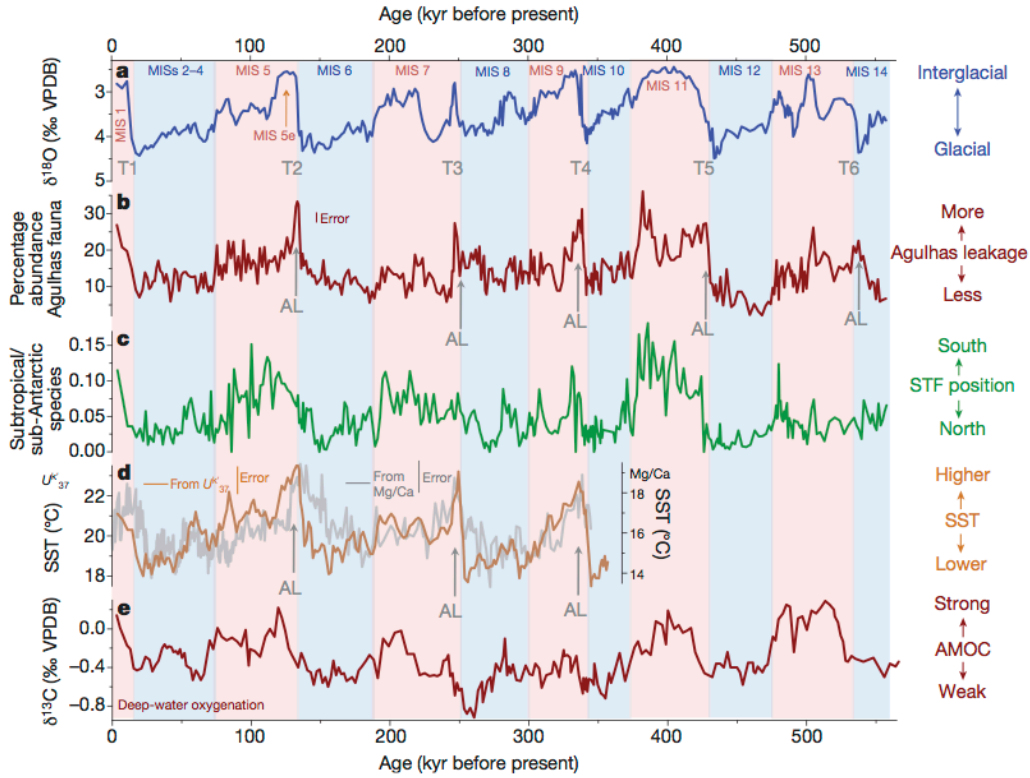

Figure 2.4 Paleoceanographic data of the Agulhas Region in the last 600 kyr. (b) refers to abundances of tropical planktonic foraminferal species associated with the Agulhas Leakage (c) Subtropical front position (d) Sea Surface Temperatures (SSTs) derived from the $U^{k'}_{37}$ biomarker. Highest SSTs are at glacial terminations, occurring at the same time as Agulhas Leakage (e) benthic $\delta^{13}C$ in the deep Pacific, reflecting deep Pacific ventilation and AMOC strength.

(a) $\delta^{18}O$ reflects ice volume and ocean temperature; showing global temperatures and Agulhas strength were well-correlated (b) reflects the strength of the Agulhas Leakage, which peaks at deglaication. SSTs (d) and $\delta^{13}C$ peak, reflecting AMOC strength shows a generally stronger AMOC during interglacials.

Image is taken from figure 4 of Beal (2011).

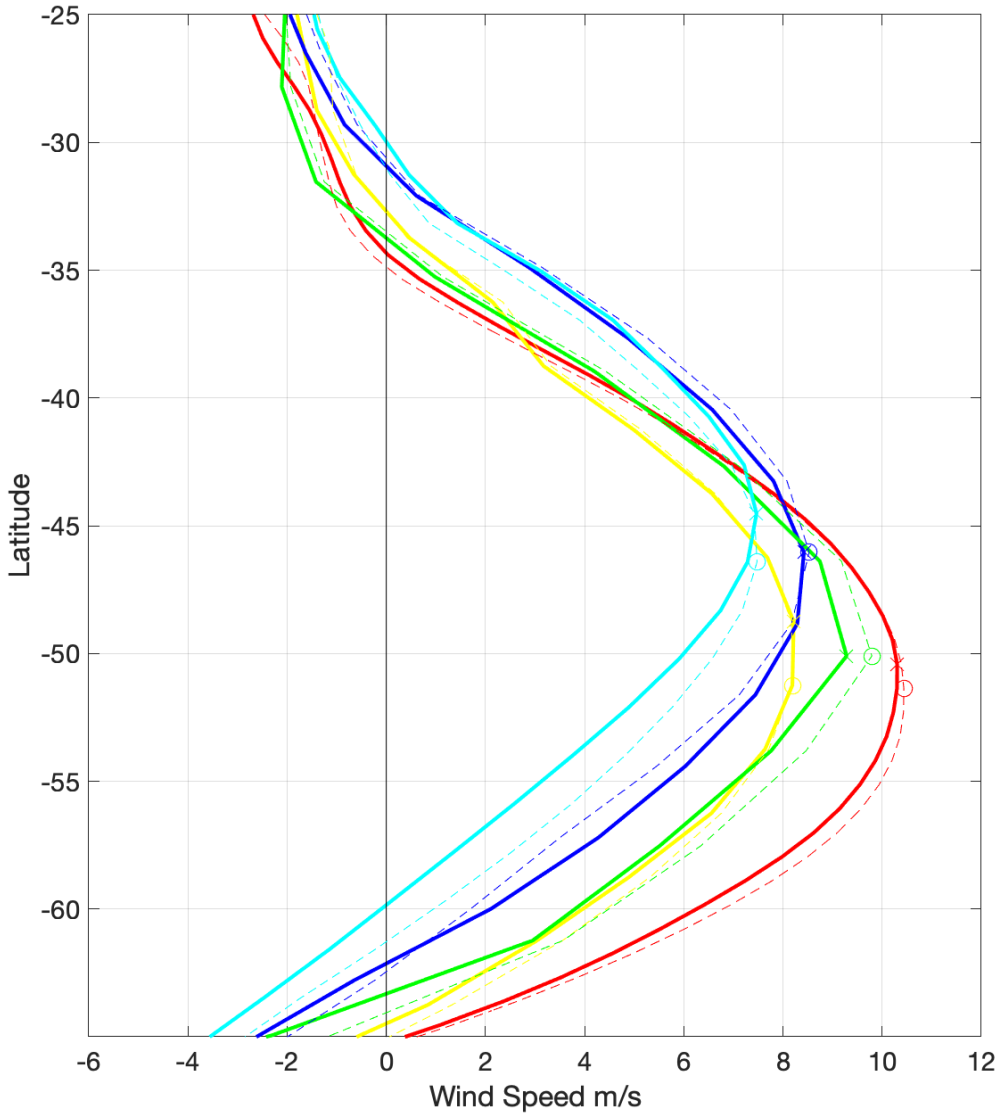

Figure 2.5 Inter-model comparison of westerly wind strength of both modern and Pliocene averaged over the longitude range containing the Agulhas retroflection, 5°E to 40°E. Solid Lines correspond to modern winds, dashed correspond with Pliocene winds. X and O corresponds to latitude of maximum westerlies for modern and Pliocene respectively. Cyan corresponds to the IPSL model, Blue, MIROC. Red, NCAR CCSM4; Green, COSMOS; Yellow, HADCM3.

Most models show a small but significant southward westerly shift between present-day and the mid-Pliocene. However, model variability is high; resulting in the inter-model difference being larger than the modern-Pliocene difference within the same model

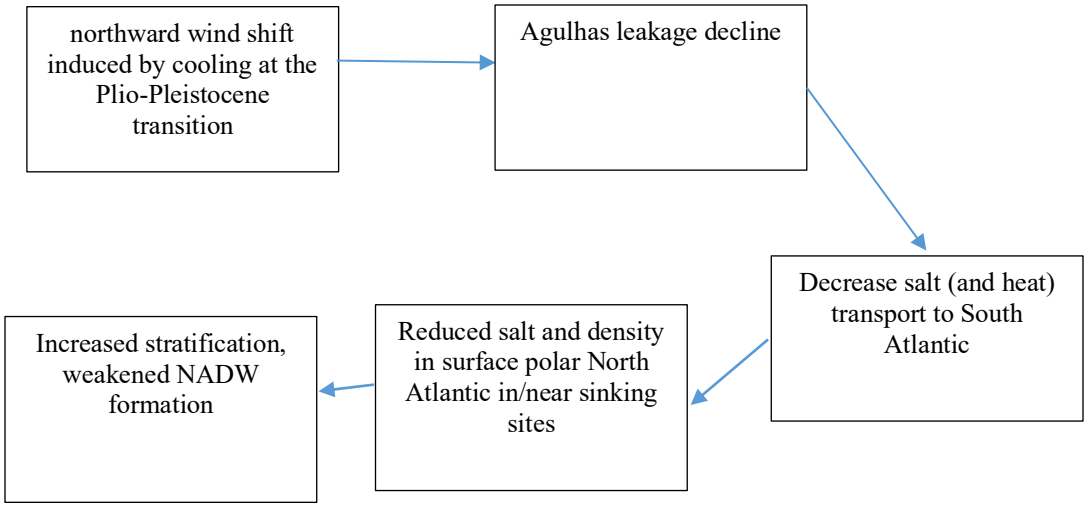

Figure 2.6 Flowchart diagram showing steps for Agulhas-driven southern hemisphere to northern hemisphere cooling

CHAPTER 3

EXPERIMENT SETUP

3.1 Introduction

To test the hypothesis that end of Pliocene northward southern westerlies shift could have induced a reduction in Agulhas Leakage and whether that reduction impacted the AMOC, a high-resolution numerical ocean model is used. The modeling experiment tests the sensitivity of the Agulhas Leakage to a latitudinal shift of the southern hemisphere westerly winds. The shift is created by an artificial perturbation of the southern westerlies; which mimics the changing wind fields at the Pliocene - Pleistocene transition. High-resolution coupled models have not simulated the glacial transitions due to the difficulty of prescribing appropriate boundary conditions. Therefore, an artificial shift is necessary as shifted westerlies are unavailable from current climate models. To ensure any ocean response does not modify the wind perturbation, I chose to run an un-coupled, high-resolution ocean-only model. A very high resolution (0.1°) is required to fully capture eddies, which carry about half of the Agulhas Leakage et al., 2015). Coarse-resolution models over-estimate the leakage by a factor of two (Cheng et al., 2016).

In this section, the details of the model experiment setup and initialization are discussed. The initial conditions are taken for the simulation results from the results a global coupled model of the Pliocene. Many global GCMs have modeled the Pliocene, however, they differ in the properties, making selecting an appropriate model to start the experiment not straightforward. The choice of starting model is justified as well as the advantage or disadvantages of various model options. Also, the ocean model setup and

wind perturbation model experiment design is discussed and justified. Choosing an appropriate model configuration involves tradeoffs between computational practically and scientific realism and I explain why the configuration fits the research goals.

3.2 MITgcm

The MITgcm is a well-tested ocean-only model with the ability to be run with a wide range of spatial resolutions for a variety oceanographic modeling experiments including ocean biogeochemistry, oceanic state estimation and paleoclimate. Using a high-resolution MITgcm setup, (Condron and Winsor, 2012; Hill and Condron, 2014) tracked the paths of Greenland meltwater during deglaciation. Point source tracking allowed the routes of icebergs to be traced from their North Atlantic origin to observed scours to the Atlantic coast of the US South. Water mass tracking showed meltwater released during deglaciation did not reach North Atlantic deep-water sinking sites further east. As I am interested in performing similar water mass tracking near AMOC sinking sites with an ocean-only model, a high-resolution MITgcm model would fit my research goals well, so I choose to use the MITgcm.

In my MITgcm setup, surface atmospheric conditions are prescribed, with the surface winds and temperatures only used to force the ocean model. A convenient cube face configuration (with 1/6° resolution) has been devised for the MITgcm, allowing the entire ocean to be simulated without drastic grid size changes in polar latitudes. While I run my ocean model at a somewhat lower resolution (1/6°) than usual (1/10°) for capturing eddies, it is sufficient to resolve eddies and capture the trends in eddies. To check if 1/6° MITgcm resolution is able to capture the Agulhas Leakage, I did a four-year test run of

the modern ocean forced with modern atmospheric re-analysis. The eddy frequency and resulting Agulhas magnitude, measured using an Eulerian "spice-based" method (Putrasahan et al., 2015), agreed with previous high-resolution model experiments of the modern ocean. Therefore, the global spatial resolution is sufficient for my purposes.

The vertical resolution in my MITgcm setup varied with depth, with levels closer to the surface not as thick as deep levels since the near surface ocean changes faster and has a finer structure. The ocean model has up to 50 vertical levels. For geographic boundary conditions, I used modern continent positions and bathymetry. Even though sea level was higher in the Pliocene, the bulk of the ocean and landmass was in a similar position as today, so the error should not be large. By the late Pliocene, the time period my experiments model, the continental configuration is much closer to modern-day than the mid-Pliocene. For example, the Panamanian seaway closed before the late Pliocene. The bulk of ocean currents of interest to my experiment would therefore be little changed using a modern rather than late Pliocene bathymetry.

To initialize my model experiment of the Agulhas Leakage in a Pliocene world, both the ocean and atmosphere must reflect Pliocene conditions. An ocean that already reflects Pliocene conditions has a faster, more stable spin-up to a model in equilibrium with the atmosphere. The chosen Pliocene atmosphere is fixed, while the Pliocene ocean is allowed to change in response to any alterations in atmospheric forcing. The atmospheric fields such as air temperature, solar radiation and wind are converted to heat and evaporation fluxes using bulk forcing formulae in the MITgcm EXF package (Large et al., 1997). Eight different coupled climate simulations of the Pliocene have been

performed as part of the PlioMIP project, containing both ocean and atmosphere Pliocene. All had much coarser resolution than my MITgcm ocean simulations, ranging from 1° to 3.5° in ocean and atmosphere. To account for these differences in resolution among the models the initial ocean was re-gridded from the coarser coupled model resolution to the resolution of the MITgcm cube face ocean. The MITgcm EXF package interpolates the atmosphere to the cube face grid. I considered either using only one PlioMIP simulation or a multi-model PlioMIP mean to initialization of my experiments. I chose to use just one model for the best model stability.

3.3 Ocean Model Biases

To determine the most appropriate Pliocene GCM simulation for initialization, the coupled Pliocene models from the PlioMIP were compared, based on resolution and model biases in present day 'control' simulations. Haywood et al. (2013) described the resulting model similarities and disagreements. The GCM ocean components mostly agree that Pliocene sea temperatures were significantly warmer than modern, and that the southern hemisphere westerlies were further south than today. However, the models have a range of warming from 1.8°C in the MRI model to 3.6°C in COSMOS. Haywood et al. (2013) showed Pliocene model simulations clustered in two groups, with some models around 2.0°C of warming while others above 3.2°C. The models have varying biases in precipitation, resulting in significant biases in salinity. To compare the model salinity biases, I created an inter-model comparison of the mean upper 400m salinity (Figure 3.1). I took an upper ocean mean rather than just the surface since the surface salinity mostly reflects local evaporation and precipitation rather than influences of ocean currents, so

measuring the ocean properties at depth is necessary to analyze changes in ocean currents. The eddies embedded within the Agulhas Leakage extend down to a depth of ~1300 m. I found that averaging down to the entire depth to cover the full extent of an Agulhas ring results in a similar pattern as the upper 400 m average but with a lower salinity contrast; therefore I chose to compare the upper 400 m.

In many cases, the difference in upper-ocean salinity between models was larger than the difference between modern and Pliocene simulations. The NCAR CCSM4 model had a much fresher Indian Ocean than modern re-analysis data (Gent and Danabasoglu, 2011; Gent et al., 2011). This salinity bias reduced the salinity contrast between the South Atlantic and Indian Ocean (Figure 3.2) so that the Agulhas Leakage had near zero net salt transport (Weijer and van Sebille 2014).

Model Name	Ocean Resolution	Δ Surface Air Temperature	Modern salinity difference	Pliocene salinity difference	Modern Westerly Position	Pliocene – Modern Westerly Shift
MIROC	1.4 x 1.4°	3.46°C	0.198	-0.066	46.0°S	0.11°
COSMOS	3.0 x 1.8 °	3.60°C	0.183	0.135	50.1°S	0.51°
CCSM4	1.0°x 1.0°	1.86°C	-0.034	-0.072	50.4°S	0.13°
HADCM3	1.25 x 1.25°	3.27°C	-0.061	-0.158	48.8°S	-0.03°
IPSL	2°, L31	2.18°C	0.455	0.397	44.5°S	0.01°
NCEP			0.155			

Table 3.1 Comparison of selected PlioMIP ocean models by their climate changes, with NCEP reanalysis for comparison. Δ in Surface Air Temperature represents the global Pliocene Modern difference. The modern and Pliocene ocean salinity difference represent the difference in Indian Ocean - South Atlantic near the Agulhas region. Indian Ocean region defined as ocean between 7°E and 19°E, South Atlantic between 19°E and 40°E, both regions between 23°S and 35°S. For the Pliocene-Modern westerly shift column, Positive westerly shift indicates a northward shift

To solve this issue of model bias, I created a bias-corrected ocean and atmosphere by adding the difference between a Pliocene and Modern GCM simulations for each field (both ocean and atmosphere) to modern NCEP reanalysis fields. For example, the

resulting atmospheric temperature would be the modern NCEP re-analysis air temperature added to the difference between the NCAR Pliocene (Rosenbloom et al., 2013) and NCAR modern air temperature. The NCAR CCSM4 model was chosen for bias-correction due to having the highest ocean resolution of the PlioMIP models. This removes most NCAR model-dependent biases (see Table 3.1). However, after running this setup in the for twenty model years, it resulted in an unstable AMOC, with large changes within a few model-years and never reached equilibrium. An extreme salinity drift in parts of the Atlantic (Figure 3.3) may have been responsible for this AMOC result. It is hard to determine the cause of this, but perhaps the bias-corrected atmosphere and ocean were initially far from equilibrium, leading to a drift in the ocean-only model. In contrast, the atmosphere and ocean from a coupled model has had at least several model centuries for the model to come to equilibrium, leading to less drift in an ocean-only model.

Since I am unable to obtain a stable MITgcm ocean with bias-corrected NCAR GCM forcing, I chose to use one, uncorrected coupled model to ensure a more stable model experiment. The HADCM3 (Bragg, Lunt, and Haywood 2012) shares in common with the NCAR CCSM4 (Danabasoglu et al., 2012) a similarly high resolution; unfortunately, it has an even larger salinity bias. The IPSL and COSMOS models have the smallest salinity biases in present day simulations. However, the IPSL contains a well-regarded ocean component so I chose to initialize a MITgcm ocean experiment with the Pliocene IPSL rather than the COSMOS.

A drawback of the IPSL model is its low-resolution (3.75° x 1.9° atmosphere, ocean 2°)

makes it a less than ideal candidate to re-grid to a higher resolution ocean model. Spinning up a high-resolution model from a lower resolution likely led to more drift, as there was more change from the initial configuration. While the IPSL simulation of modern-day has small salinity biases (see Figure 3.1) relative to observations, it simulates a much smaller AMOC strength; roughly 40% weaker than the multimodel mean (Zhang et al., 2013), which matches closely with observations. The modeled AMOC strength of the IPSL simulation is an outlier among the eight models that are part of the CMIP5 project (Heuzé, 2017; Zhang et al., 2013; Jungclaus et al., 2013), while NCAR's CCSM4 modern-day simulation matched closely with observations and is close to the multi-model AMOC mean. The CCSM4, however, had fairly high salinity biases in many ocean basins. Ideally, the Pliocene experiments should be based on a high-resolution ocean model with little salinity bias and AMOC bias. Since this ideal combination is not available; I performed two separate experiments, one based on the IPSL (low salinity bias, high AMOC bias), the other based on the NCAR simulation (high salinity bias, low AMOC bias).

3.4 Perturbation details

To gauge how big of an impact a northward wind shift could have on the Agulhas Leakage, I performed three model experiments. Each of the experiments were initialized with a Pliocene ocean and atmosphere based on the mean of a coupled model simulation of the mid-Pliocene (~3.1 Myr), either the IPSL or the NCAR. Both the shape and scale of the wind perturbation was designed to mimic the response of the wind field to a growing Antarctic ice sheet at the end of the Pliocene, as hypothesized by McKay (2012).

The only altered forcings are the southern hemisphere winds, in order to isolate the effects of high-latitude southern hemisphere cooling to trigger global climate change via circulation changes. Two of the MITgcm experiments were initialized with an unchanged ocean and unperturbed atmosphere from a Pliocene coupled model, labeled as control. The last experiment involved altered southern hemisphere westerlies. I conducted control experiments with unperturbed winds as ocean-only models have some model drift. To be scientifically meaningful, a perturbed wind experiment with the MITgcm must be compared to an unperturbed wind experiment with the same model at the same model time. The three experiments are summarized below:

1) ISPL initialized ocean and atmosphere, no wind shift:
Atmospheric forcing unchanged from the coupled IPSL model. This was run for 37 model-years.

2) NCAR CCSM4 initialized ocean and atmosphere, no wind shift:
After 17.5 model-years of spin-up, a new perturbation experiment was branched off with different wind forcings (see below) but the control experiment was run with unchanged forcings for 58 more model years.

3) NCAR CCSM4 initialized ocean and atmosphere, northward wind shift:
An imposed northward 6º shift on the entire southern westerly wind belt across the globe. After experiment #2 was run for 17.5 model years, the northward wind shift was imposed, while no other forcings from experiment 2 were changed. This perturbation experiment was then run for a subsequent 59 model-years.

The experiments were run on NCAR's supercomputers using both their Yellowstone and their Cheyenne facilities. The MITgcm was setup to run on 900 cores on t with a model integration time-step of 600 seconds after a few model-years of spin-up. Computational speed of running the MITgcm simulation on NCAR varied from different package configurations and unreliability of the supercomputer facilities, but overall 10 model-years consumed 80,000 core-hours of computer time. The total core-hours consumed was more than the model experiments described running at that speed; additional computer time was consumed debugging the MITgcm after computer crashes, a few shorter experiments were performed that I chose not to use and spin-up was run at a slower speed, using more core-hours. Altogether, nearly 2 million core-hours of supercomputer time was used.

Because the IPSL-initialized unperturbed MITgcm wind experiment suffered from much more drift than the CCSM4-initalized unperturbed MITgcm wind experiment, the bulk of the available computer model time was used for the CCSM4-initialized experiments. Subsequently in the results and discussion sections, I focus on the NCAR-initialized experiment results. I refer to the unperturbed wind CCSM4-initialized experiment as simply "the control" with the CCSM4-initialized experiment with perturbated winds as simply "the perturbation". A diagram showing the MITgcm setup and the CCSM4-initialized (including the perturbation and control split) is shown in Figure 3.4.

The IPSL experiment was run for 37 model-years from initialization. The NCAR initialized experiment was run for 17.5 years with unchanged winds as a "spin-up" in order for the MITgcm to be in model equilibrium. Then, the perturbation experiment was

started, altering the winds on this resulting spun-up ocean, while the unperturbed wind experiment was continued as a control. Both the perturbed and unperturbed wind experiment was run for an additional 59 model years. For all three experiments, monthly mean atmospheric forcing was used.

The wind perturbation (Figure 3.5) was chosen to be both realistic and large enough to produce an easily discernible model response, as the Agulhas Leakage is difficult to measure. To determine the maximum plausible meridional wind shift caused by a cooling climate accompanied by an expanding Antarctic ice sheet, I used as a reference the wind shifts in model simulations and proxy-based wind reconstructions of the LGM (Kohfeld et al., 2013, Rojas et al., 2012). Both of these lines of evidence do not support the LGM westerly position being further north than 6–7° of their present-day position. As shown in Figure 2.5, the mid-Pliocene models show a wide range of westerly wind positions; with the latitude of maximum westerlies varying by as much 5–6°; a much higher shift in westerlies is unlikely in the Plio-Pleistocene transition, as the cooling magnitude was than the magnitude of the temperature difference between the LGM and modern. The CCSM4 placed the core of the southern westerlies in the most southerly position among the eight Pliocene simulations, while the IPSL model simulated the northernmost westerly wind position. Given the high inter-model variability of maximum westerly position, a position of the westerlies 5° northward of the NCAR state is not out of line with existing climate model results of the Pliocene. Due to the northerly wind position of the westerlies in the IPSL Pliocene simulation, the winds of the IPSL experiment were not perturbed, perturbation were only imposed on the NCAR experiment. Because the winds are already fairly far north in the IPSL experiment, a northward wind perturbation

would not be physically plausible. Since the control IPSL position was already 5° north of the Pliocene CCSM wind position, the control IPSL experiment is effectively an additional northward-shifted westerly experiment.

In the wind-perturbation experiment, the westerlies were shifted northward around the entire southern hemisphere, rather than shifting the southern westerlies only over the longitudes that are affected by the Agulhas Leakage. Other Agulhas Leakage experiments have taken this later approach (Biastoch and Böning 2013; Durgadoo et al., 2013), with a wind perturbation over the source of the Agulhas (western Indian Ocean) and the longitudes of the entire Atlantic Ocean, while leaving the southern westerlies unchanged over the rest of the globe. Although this had the benefit of limiting impacts on other ocean currents, I decided against such a setup, as partially shifted westerlies is clearly unrealistic (in a zonal sense). It also had the detriment that the transition between unperturbed and perturbed southern westerlies would impact the regional wind stress, and more importantly its curl, in an unphysical way, creating an artificial current. Furthermore, the goal here was not just to perform an Agulhas Leakage sensitivity experiment, but to understand the impacts of a northward shift in the southern westerlies during a cooling southern hemisphere Pliocene. A global shift in the southern westerlies reflects this scenario better.

The wind perturbation was constructed similar to the perturbation experiment conducted by Durgadoo et al. (2013). In the shifted region, the zonal wind value of each grid cell was a weighted combination of the control value of the cell plus the control values in the cells to the immediate south, to ensure a resulting smooth and continuous wind field

(Figure 3.5). Each longitude was shifted individually. The grid cells within **3°** of the centroid of max westerlies were shifted first, with a shift of 6.3° northward. Then, winds outside but in or near the southern westerly region were shifted. The winds north of 34°S were left unchanged to minimize impacts on the Agulhas Current and winds 14° south of the latitude of peak westerlies pre-perturbation left unchanged. In between the shifted peak westerly region and the unchanged winds, a cubic spline was used to interpolate the remaining cells. The results from the experiment are now discussed in the following sections.

3.5 Figures

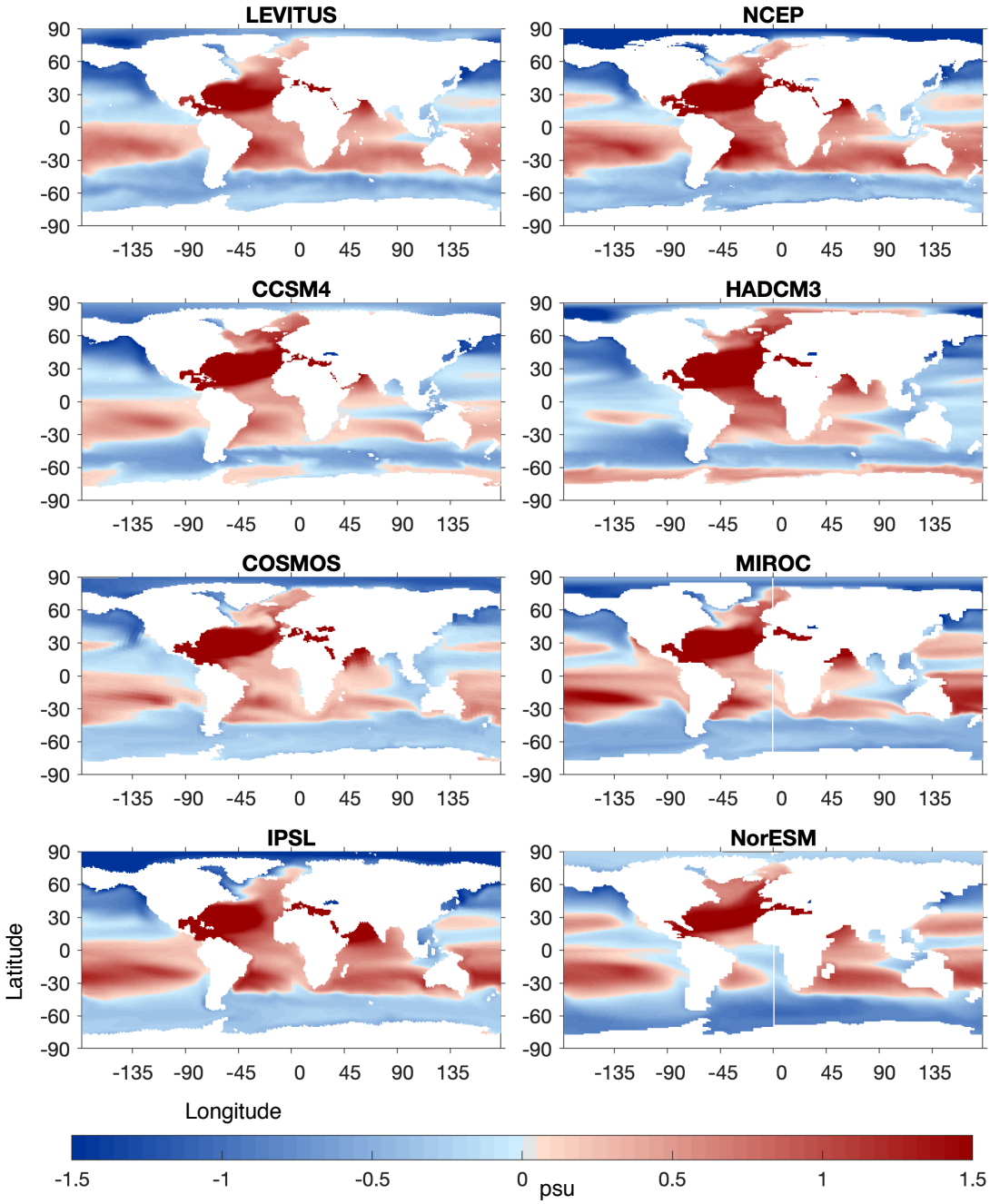

Figure 3.1 Inter-model salinity comparison of 6 modern ocean simulations and 2 modern re-analysis (Levitus and NCEP), averaged over the upper 400 m of the ocean. The salinity values in each map are relative to the global model (or reanalysis) ocean mean. Zero in this scale represents the global ocean of the model. The six ocean models have had Pliocene experiments performed as part of the PlioMIP project. The models range in their ocean salinity distributions, significantly differing from each other and the observed ocean (reanalysis). The CCSM4 shows a weakened salinity contrast between the South Atlantic and Indian Ocean as well as unusually salty compared to the global mean. The modern IPSL reproduces observed modern conditions relatively closely but with the downside of poor resolution

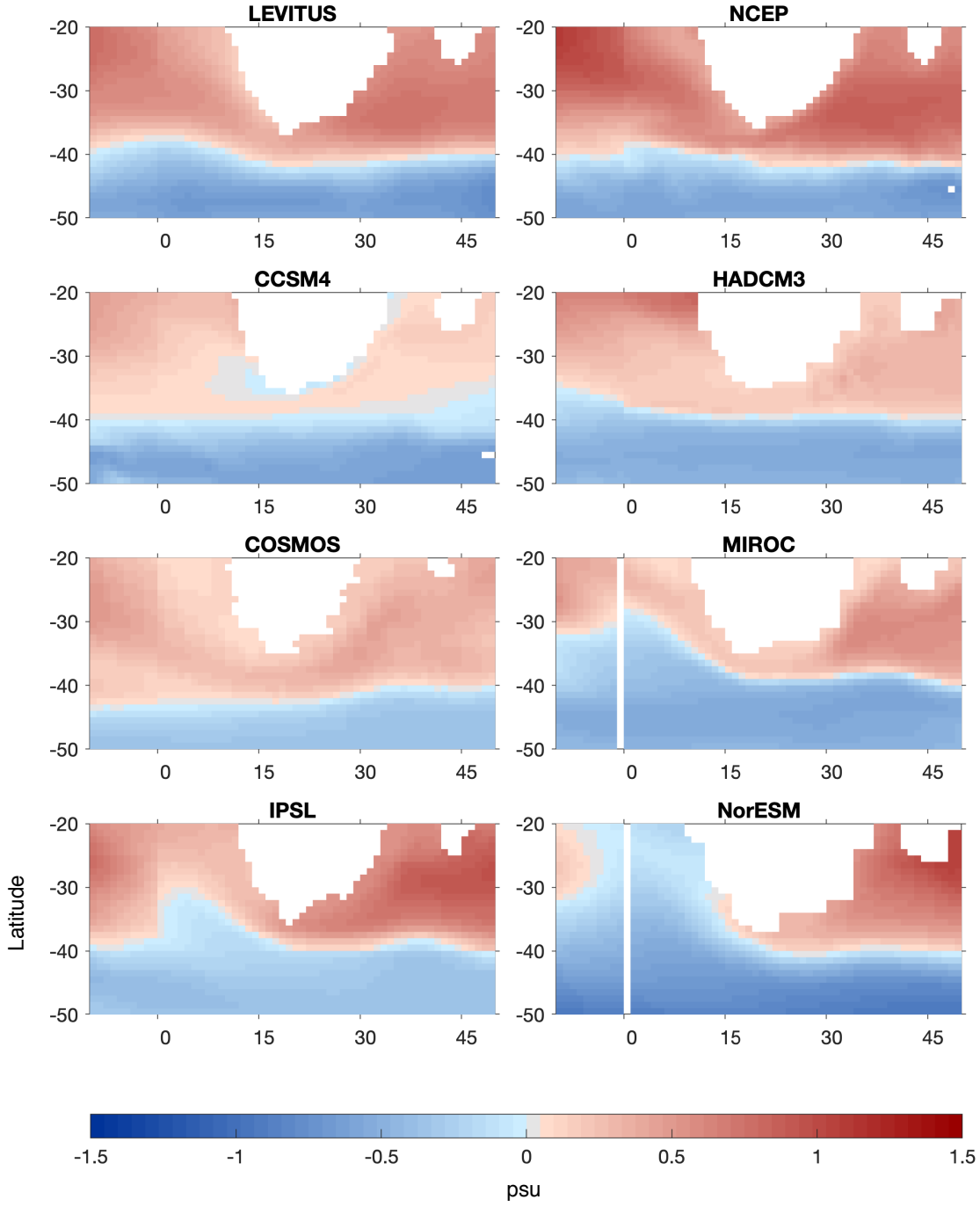

Figure 3.2 Inter-model salinity comparison of 6 modern ocean simulations and 2 modern re-analysis (Levitus and NCEP), averaged over the upper 400 m of the ocean. Same ocean data plotted as Figure 3.1 but displaying only the Agulhas Region

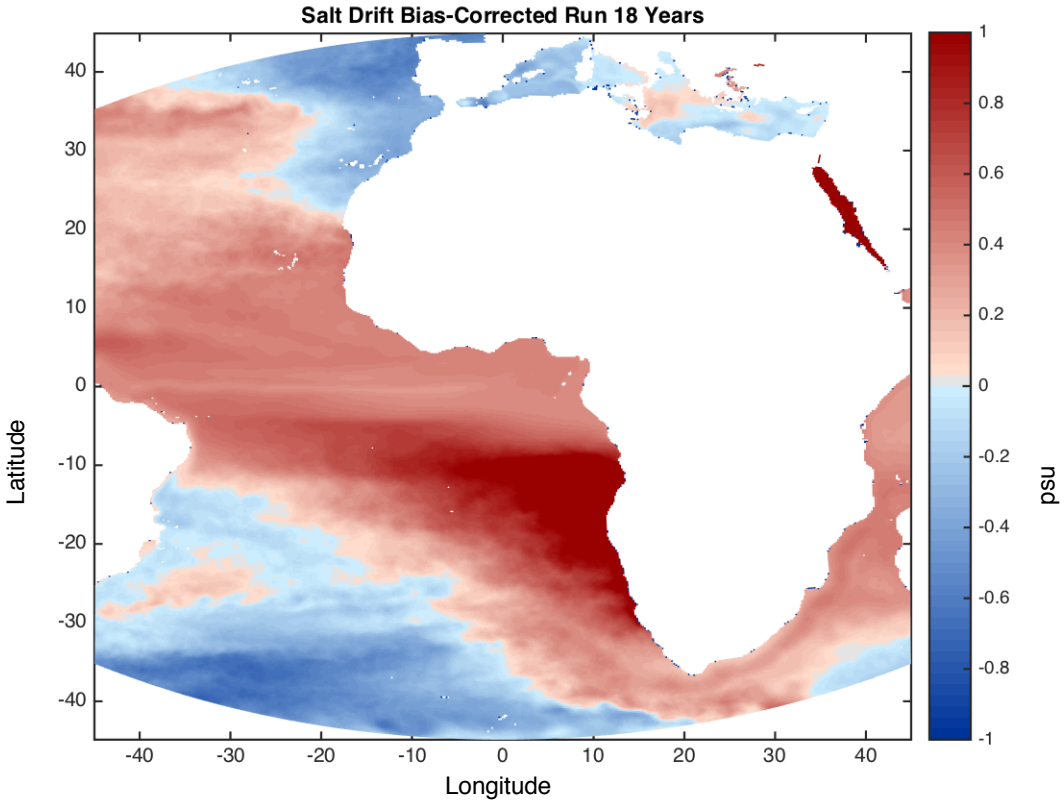

Figure 3.3Resulting change in salinity after 18 model years in the bias-corrected NCAR experiment. The bias-corrected ocean and atmosphere were produced by adding the Pliocene Modern difference of the coupled NCAR simulation experiments to the modern NCEP reanalysis ocean and atmosphere and then re-gridding the resulting bias-corrected model\to the MITgcm cube-sphere dimensions.

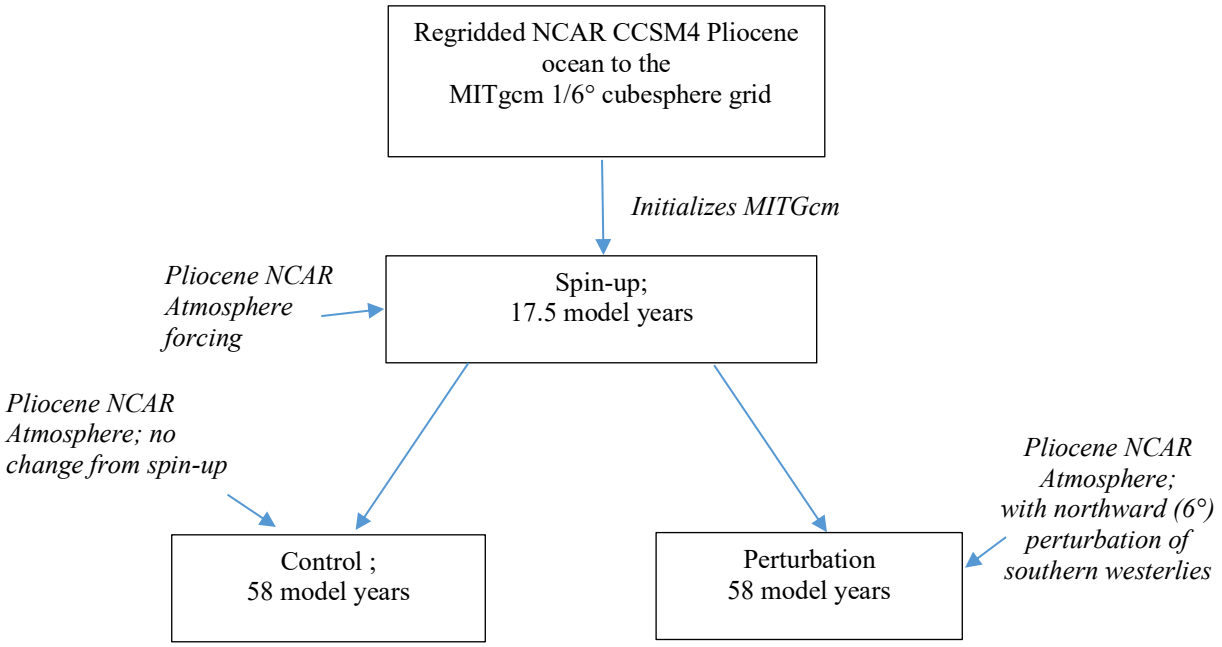

Figure 3.4 Flowchart showing the experiment setup of the CCSM4-based experiment; showing the re-gridding and spin-up

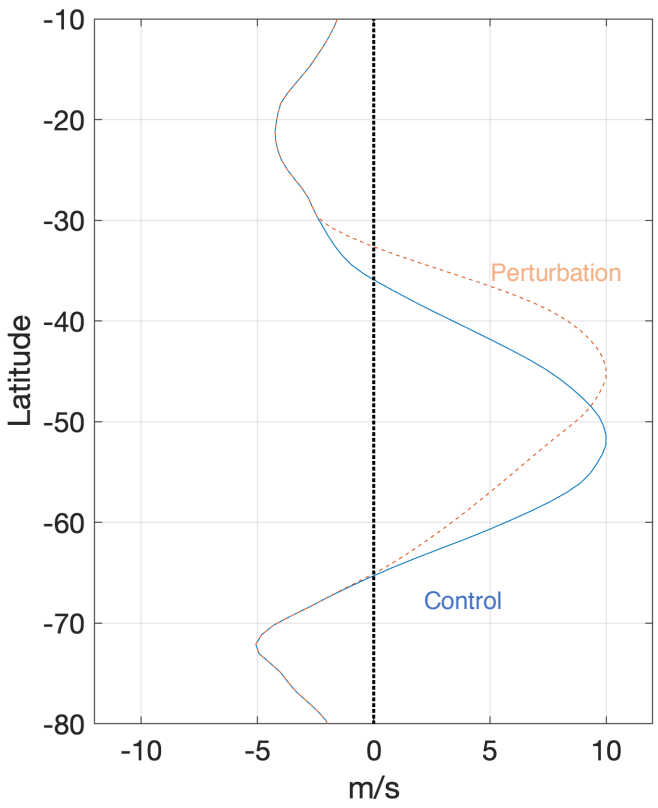

Figure 3.5 Wind shift used in the NCAR initialized experiments. Zonal wind velocity averages between 70°W to 40°E plotted as a function of latitude. Blue line corresponds to the control or unperturbed wind; red dashed line the northward wind perturbation

CHAPTER 4

OCEAN PROPERTY RESULTS

4.1 Introduction

Shifting the southern hemisphere wind circulation in my MITgcm modeling experiment led to a global reorganization of the ocean circulation and properties, especially in the mid and high latitude Southern Ocean. The research goal of this project is whether southern hemisphere wind shifts in the Pliocene could affect heat transport into the northern hemisphere by changing the AMOC via the Agulhas Leakage. The Agulhas Leakage required specific measurement techniques to isolate carefully (discussed in the subsequent chapter). In this section, I will discuss any resulting simulated changes in ocean circulation and stratification that could potentially affect the AMOC. Some general global ocean changes to give a broad overview will also be discussed. I will focus on changes in the high-latitude Southern Ocean and North Atlantic; where the AMOC upwelling and downwelling. This will allow me to infer the changes in the AMOC strength. In the subsequent results chapter, I will discuss the Agulhas Leakage changes.

In the southern hemisphere, shifting the southern westerlies directly impacts the strength of the underlying Antarctic Circumpolar Current (ACC). In the Pliocene, the core of the southern westerly wind belt was centered over the latitude of the peak of the Antarctic Circumpolar Current strength, like today. Shifting the southern westerlies away from this latitude decreases the surface forcing on the ACC, affecting upwelling in the southern polar oceans (Russell et al., 2006, Spence 2014). This alters the southern limb of the Atlantic Meridional Overturning Circulation (AMOC).

The northern, descending limb of the Meridional Overturning Circulation (Figure 2.2) is in the subpolar North Atlantic and the site of North Atlantic Deep Water (NADW) formation. Changes in the density stratification of the high-latitude North Atlantic have the potential to impact NADW formation. The salt and heat anomalies transported by the Agulhas Leakage are partly model dependent, so I measured the Agulhas volume transport changes rather than the salt and heat transported by the Agulhas Leakage directly. In the next section, I discuss general ocean circulation and property changes caused the northward westerly shift, particularly those that could change the MOC.

The northward wind perturbation (experiment #3) reorganized the Southern Hemisphere wind belts, leading to rapid changes in surface conditions but slower deep water changes. As expected, the Southern Ocean gyres narrowed in north-south extent; shown in the mean sea surface height changes (Figure 4.1). The retroflection region narrowed, leaving less of a path for the Agulhas water to leak into the Atlantic. The sea surface height also showed a slight increase, suggesting a faster current speed off the Cape of Good Hope. This implies that more of the Agulhas Current recirculates into the Indian Ocean, as the mean current flow generally follows the contours of sea surface height. Meanwhile, the Antarctic Circumpolar Current shows a sharp decrease in sea surface height, suggesting less Ekman-driven upwelling (Figure 4.1). Given the decreased wind stress curl over the Southern Ocean from the northward wind perturbation, a decline in Ekman-driven upwelling was expected. Globally, the perturbation resulted in the surface ocean freshening everywhere except for the Southern Ocean and a few other areas. These areas include sections of the subtropical Southern Hemisphere oceans and the North Atlantic, some of which contain North Atlantic deep-water sinking sites. The details of the spatial

ocean changes are discussed below.

4.2 Southern Ocean Changes

In the NCAR CSSM4 initialized control experiment (experiment #2), the latitude of the core of southern westerlies, which corresponds to the latitude of zero wind stress curl, aligns with the fastest core of the Antarctic Circumpolar Current. The winds are centered directly over the Drake Passage. Once the winds are shifted northward, land prevents the current from moving further northward, so the ACC passing through the Drake Passage receives a weaker wind forcing. This resulted in a slower Antarctic Circumpolar Current, potentially decreasing upwelling. By the end of my perturbation experiment, the flow through the Drake reached equilibrium, at a flux lower than the control simulation (110 Sv instead of 150 Sv). Further north, at the new latitude of the core of the southern westerlies, the current speed of the ocean increased in the South Atlantic and South Indian ocean.

The shifted wind stress curl caused ocean circulation changes which redistributed the salinity (Figure 4.2) and temperature (Figure 4.3) throughout the ocean. This redistribution altered the density stratification (

Figure 4.4) . A number of previous modeling studies (e.g. Gent et al., 2015; Swart and Fyfe, 2012; Sijp and England, 2009) have performed coarser resolution studies of a northward westerly perturbation; a recent study analyzed (Spence et al., 2014) the ocean response to a global southward wind perturbation.

The resulting modeled salinity change caused by the wind perturbation mirrored closely that of Sijp et al. (2008), with a few disagreements. Some of the deeper ocean discrepancies are likely due to the short duration of my integration. In addition, the lack of atmospheric coupling limited some feedbacks so a direct comparison to previously published literature is difficult. However, I observed many upper-ocean changes in response, some immediately; others in 20–40 model years. A global map is presented of the temperature, salinity and density changes of the north perturbation versus the control. For visualization purposes, I divided the ocean response into three levels: top 200 m, 200-700 m and 700 -1500 m, and present the depth integrated mean of the ocean for the surface and each of those three levels (see Figure 4.2, Figure 4.3,

Figure 4.4). Below 1500 m little significant change is observed so I do not map those depths.

The most consistent general ocean response was the salinity response, while the temperature response had more regional variation; other work, such as Sijp (2008) and Spence et al. (2014) found a clearer temperature response. At the ocean surface, most of the upwelling changes resulted in a freshening of much of the surface Southern Ocean (similar to the results found by Sijp et al., 2008), except for the southern edge of southern subtropical gyres; e.g., in the southern Indian Ocean gyre. This is due to the northward wind perturbation constricting the gyres, preventing less saline water to the south from mixing northward. The surface North Atlantic also became saltier, which is analyzed in the next section. Overall the near surface ocean (upper 200 m), followed a similar spatial pattern in salinity change, but additionally, part of the Southern Ocean centered around

the latitude of zero wind stress in the control also became saltier. Below (200–700 m), a much larger region of the Southern Ocean got saltier. Most of the rest of the ocean at this depth became marginally fresher (Figure 4.2). This shows the salt was not just re-distributed vertically in the Southern Ocean but distributed meridionally.

Temperature changes were less zonally uniform, and the causes for the changes are harder to diagnose. The ACC exhibited strong cooling; among the most significant temperature change globally (Figure 4.3). Below 200 m, the ACC cooled consistently across the globe (zonally); yet closer to the surface, the changes are more varied. Strangely, Spence (2014) found a similar ACC cooling after a *southward* wind perturbation, but I am unsure why they don't have opposite results. North of the ACC into the Indian Ocean gyre and Agulhas retroflection, below 200 m, the ocean exhibited a warming.

Trends in sea surface temperatures presented a less clear signal, but with a moderate warming of 0.5–1.0°C in the region of the Antarctic Circumpolar Current from latitudes 55°S to 60°S, which is just to the south of the latitude of zero-stress wind curl in the perturbation experiment (Figure 4.3). The Southern Ocean to the north, that region that sees increased Westerlies from the northward perturbation, showed a substantial cooling of 1.0–1.5°C. In general, the sea surface temperature at the latitudes where the Westerlies were formerly centered (in the control experiment) became warmer in the perturbation experiment; presumably from a reduction in Ekman-driven upwelling. South of the latitude of maximum ACC strength, close to the Antarctic coast, there was a systematic surface cooling. These regions also exhibit a sea ice expansion **(**Figure 4.5). In these

higher latitudes, the weaker meridional wind stress results in less upwelling**,** leading to cooler surface temperatures. The same region below 200 m cools (Figure 4.3). The reverse pattern appears in the Southern Ocean north of 45°S: the surface and near-surface (from the surface down to 200 meters) moderately cools, but warming occurs at depth (Figure 4.3).

Overall, the northward wind perturbation caused a re-arrangement of Atlantic Ocean density. I see a symmetrical response around the wind perturbation change. The upper level of regions where the northward perturbation increased the wind stress (about 42°S to 34°S) became more dense (

Figure 4.4) at its upper level (≤100 m), while below 100 m they became less dense, implying the water column became less stratified and vertical mixing increased in response to the wind shift. To the south, where the perturbation caused wind stress to decrease, the opposite occurred: the upper 100 m of the ocean became less dense through a combination of warmer ocean temperatures in some parts of the Southern Ocean and a much fresher ocean overall, while below 100 m, the ocean density in this region increased. This led to a more stratified Southern Ocean overall. The greatest freshening in the Southern Ocean occurred south of 58°S, where sea ice also expanded (Figure 4.5).

Away from the Antarctic coast, roughly north of 60°S and south of 45°S most of the high latitude Southern Ocean, including the Antarctic Circumpolar current becomes slightly more density stratified (

Figure 4.4). Roughly below 200 m, this region of the Southern Ocean in the northern

perturbation experiment becomes less dense, while water above 200 m becomes denser. The salinity showed a similar vertical change, implying that salinity redistribution rather than temperature is mainly responsible for density stratification. Looking more closely at a Southern Ocean region with the largest temperature and salinity changes; roughly from 60 to 43°S from the South American coast to 45°E (just east of the Cape of Good Hope) had an above average stratification change; the region of the Southern Ocean that a pronounced cooling below 200 m also became much less stratified. The increased stratification of the high latitude Southern Ocean suggests the Southern Ocean limb of the AMOC may be affected.

4.3 North Atlantic response

Overall in the North Atlantic, I saw a freshening and decrease in density in all water masses down to 1200 m (

Figure 4.4). A region of the subpolar and polar North Atlantic, extending from the coast of Labrador northeastwards toward Iceland, was a significant exception to this trend of substantial salinification near the surface. In this region, warming canceled out the densification due to salinification, resulting in little net density change, except at the very surface (

Figure 4.4). These regions correspond to the main areas with the highest mixed layer depth (> 1000 m) in my ocean model. This was determined using the same convention used by de Boyer Montégut (2004), whereby I defined sinking to occur wherever the Mixed Layer Depth exceeded 1000 m. The mixed layer depth is the depth at which the

ocean is 0.03 kg m^{-3} denser than the surface. A very deep mixed layer would allow for deep convection, allowing surface waters to sink. Thus, the regions of increased surface salinity in the perturbation experiment match the areas of North Atlantic deep-water formation. The fact that this change is limited to these areas suggest the strength of the AMOC has been affected by my perturbation.

The two main regions of North Atlantic Deep Water (NADW) formation in both the model and observed today are in the Greenland-Icelandic Sea and the Labrador Sea. The Greenland-Iceland Sea lies to the east of Greenland and north of Iceland from 65-80°N and 20°W to 20°E. The Labrador Sea is east of Labrador, between 50 to 65°N, west of 20°W (Heuzé, 2017). Both of these regions (Figure 4.6) showed a very small change in density stratification (see Figure 4.7) in the perturbation experiment, and again more change in salt stratification. While there was little significant change in the stratification of NADW formation sites, the overall mean could mask seasonal and localized changes. Deep water formation only occurred seasonally and not in the entire area of the region each season, therefore only stratification changes that affected the ocean enough to trigger or halt convection are relevant in the amount of deep-water formation changes.

The MITgcm experiments produce most of the deep-water formation in the Greenland Nordic Seas (about 7/8th) with the remainder in the Labrador Sea. Today, deep water formation is observed in both seas. Deep-water formation, using the previously described 1000 m threshold, occurred in my model every year but mostly during four months of the year in both the control and northward wind perturbation experiments. It did not occur across the entire region in the Greenland-Iceland Nordic Sea as defined by Figure 4.6 but

rather in small regions, varying annually. A map displaying the location and frequency of deep water formation (again where the modeled mixed layer depth > 1000 m) in the North Atlantic in the last five years of both the perturbation and control experiment is shown in Figure 4.8, with a difference plot in Figure 4.9. In the perturbation, the area of convection shrunk but convection occurred more frequently than the control at the same model timestep. Overall, totaled over the modeled five-year period, the perturbation convected over a 20% smaller area than the control, as the decrease in additional area convected in the perturbation experiment is larger than the frequency increase in a few spots. It is noteworthy that the small areas where the perturbation convects deep water more frequently than the control are among the few spots in the upper ocean (Figure 4.6) that become densified, and therefore less stratified in the perturbation. In contrast, over most of the North Atlantic with the potential to become deep water formation sites, the upper ocean became less dense and the vertical water more stratified. These sites all exhibit less frequent deep-water formation.

My outcome of deep-water formation rate change should be taken as a representation of possible ocean changes, but not taken literally due to high model uncertainty. The locations of deep-water formation in my experiment are in the same regions the coarser resolution modern-day CCSM4 simulates deep water formation. Models of the modern ocean vary in where they represent convection sites (Huezé, 2017). Observed deep water formation is highly variable today as well and does not occur every year in the real ocean (Oka et al., 2006, Yeager and Danabasoglu, 2013). Many models including the CCSM4 simulate the observed magnitude closely, but with differing, more regular patterns convecting in the same region every season. This is perhaps related to the low resolution

of most global coupled models, as well as their crude parameterizations of sub-grid scale processes, especially vertical mixing (Jungclaus et al., 2013). While in the real ocean, sinking is controlled by surface buoyancy forcing, Heuzé (2017) found little connection in ocean models between buoyancy forcing and deep convection in the North Atlantic. This suggests that it may not be useful to rely on modeled surface buoyancy anomalies to represent sinking locations of production rates of deep-water formation.

Equatorward of the NADW formation, substantial salinity changes are observed. As the ocean alterations originate in the South Atlantic, I may expect the tropical and subtropical North Atlantic changes to lead changes in North Atlantic. The density stratification changes could be from either a change in salt and heat transport from the South Atlantic or from dynamically induced circulation changes from the Southern Ocean. To investigate how temporally associated the North Atlantic changes are with the Southern Ocean circulation changes, I compared how much the salinity and temperatures changes in the North Atlantic lagged the Southern Ocean. The absolute change in heat and salinity is somewhat confounded as the MITgcm underwent model drift during the length of the simulation, so disentangling the perturbation-induced change from drift is not completely straightforward.

4.4 Timing of the response

The Southern Ocean responded quickly to a zonal shift in westerlies; below surface (200 m) becomes colder and more saline, while the upper ocean showed the opposite but a more spatially varied response. The surface to 200 m became fresher quickly, with a decrease of about 0.15 psu in 6 model years. The perturbation had a quick response in 10

model years while continuing to freshen at a slower rate. It continued to freshen more slowly, losing an additional 0.05 psu in the subsequent 30 model years. The Southern Ocean below 200 m gained salt at a slower but steady rate, however at that depth, the ocean took longer to reach an equilibrium, with the control simulation freshened until model year 40. The increase in salinity in the perturbation experiment slowed after 40 model years but still continued. Below a water depth of 700 m, the control had much less drift and the magnitude of the drift was much slower than the perturbation - control changes. While the perturbation signal is strong and several times larger than the model drift, the North Atlantic signal is less clear. The northward wind perturbation across the Southern Ocean produced a much more gradual response, while the control displayed minor drift in salinity and temperature; it's unclear if the North Atlantic continued to drift or is displaying internal variability.

Salinity changes are apparent in the North Atlantic within 10 model-years. I see a faster change in salinity at lower latitudes, with salinity changes at 8°N leading those at 30°N. The Atlantic Ocean across 8°N has an Atlantic-wide layer between about 500 m to 1,000 m water depth that becomes saltier in the perturbation. It is a transient response, and by 50 model-years it had mostly disappeared (Figure 4.10). This suggests some of the mid-depth ocean response could be a dynamical response, rather than due to Agulhas driven buoyancy forcing.

The magnitude of the subpolar North Atlantic salinity and temperatures due to the wind perturbation relative to model drift and internal variability is small. The trend showed a slow but steady divergence in the North Atlantic in contrast to the fast response of the

Southern Ocean. The surface changed much earlier than the deeper ocean, which suggested the primary driver of North Atlantic changes are surface fluxes rather than vertical mixing of deep-water circulation.

The North Atlantic changes in ocean stratification had a significant impact on the salinity distribution of the North Atlantic, with the largest changes in the Gulf Stream region, but also a significant impact further north in the regions of North Atlantic deep water formation (Figure 4.2). Changes in the density stratification of the subpolar North Atlantic gyres are of interest in studies of ocean-driven global climate impacts, because they influence southern to northern hemisphere heat transport. Evidence tying the North Atlantic changes to Agulhas Leakage changes are unclear. The changes appear to have occurred too early to have been caused by the Agulhas Leakage alterations, suggesting dynamical changes were more likely. However, since the changes were mainly surface makes a surface flux causation more likely.

4.5 Atlantic Meridional Overturning Circulation (AMOC)

A comparison of AMOC near the end of the unperturbed wind experiment and northward wind perturbation is shown in Figure 4.11 and Figure 4.12. The small changes observed in the deep-water sinking were insufficient to significantly alter the AMOC. Most modeling experiments investigating AMOC changes typically required much longer model integrations than was possible in my high-resolution study. The trade-off of high-resolution modeling is the additional computation time required for the same amount of model time; I am unable to run the simulations long enough for the deep ocean to

respond. However, I do see a small decrease in northward surface transport of the AMOC of about 0.5 Sv (Figure 4.13). Biastoch and Böning (2013) performed an experiment involving a smaller southward shift and found an increase in the upper branch of the AMOC of about 0.6 Sv at 6°N.

While the AMOC changes are not clearly within the timeframe of my experiment, I have shown the deep-water sinking sites became more stratified in response to the wind perturbation. Salinity and density anomalies further south in the Atlantic preceded North Atlantic shifts. Again, my main research interest is whether the Agulhas Leakage has the ability to alter the North Atlantic. In the subsequent section I will investigate whether (1) the perturbation was able to affect the Agulhas Leakage magnitude (2) The Agulhas Leakage changes affect the North Atlantic and can therefore be tied to the observed North Atlantic change.

4.6 Figures

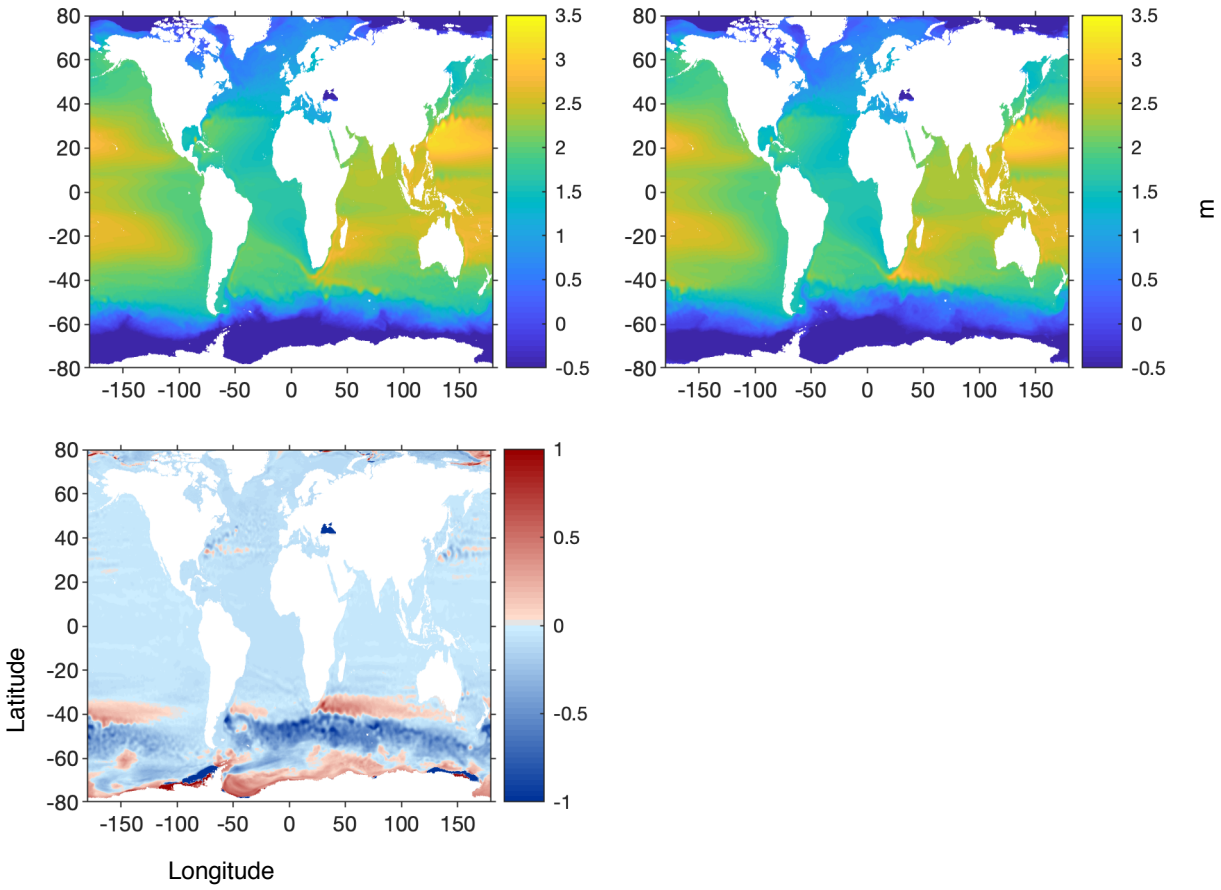

Figure 4.1 The Sea Height averaged 50-55 model-years after the start of the perturbation experiment. Comparison of mean Sea Surface Height in the control (top left) and northward wind perturbation (top right) experiments. Difference plot shown on the bottom left.

The sea surface heights indicates the ocean circulation, as the ocean circulation roughly follows lines of constant of sea surface height. The perturbation narrows the southward extent of the south Atlantic and Indian Ocean gyres, narrowing the width of the Agulhas Leakage.

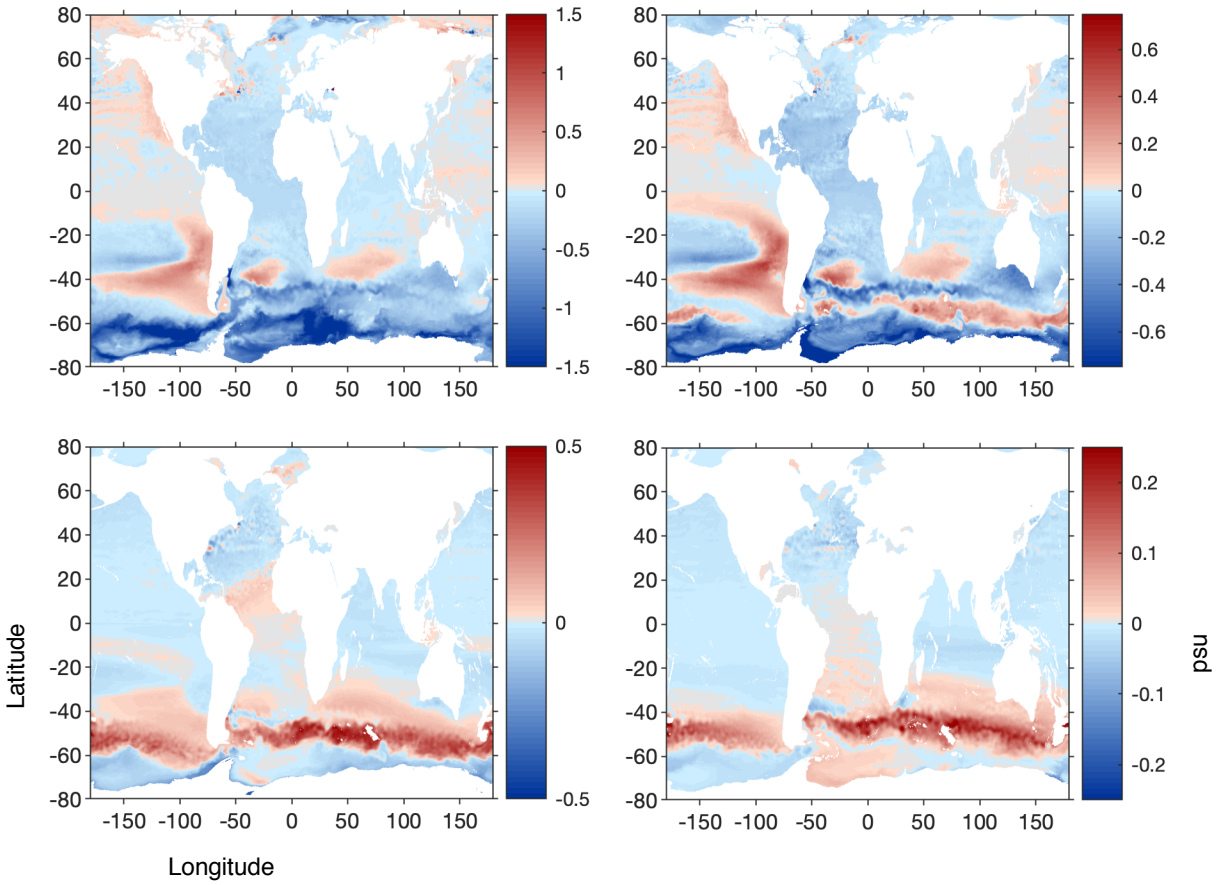

Figure 4.2 The depth-averaged salinity difference between the northward perturbation simulation and the control simulation averaged over 50-55 model-years after experiment initialization. Each plot displays the salinity averaged over a different depth. Top left: surface changes; Top right: upper 200 m; Bottom left: 200–700 m; Bottom right, 700–1500 m.

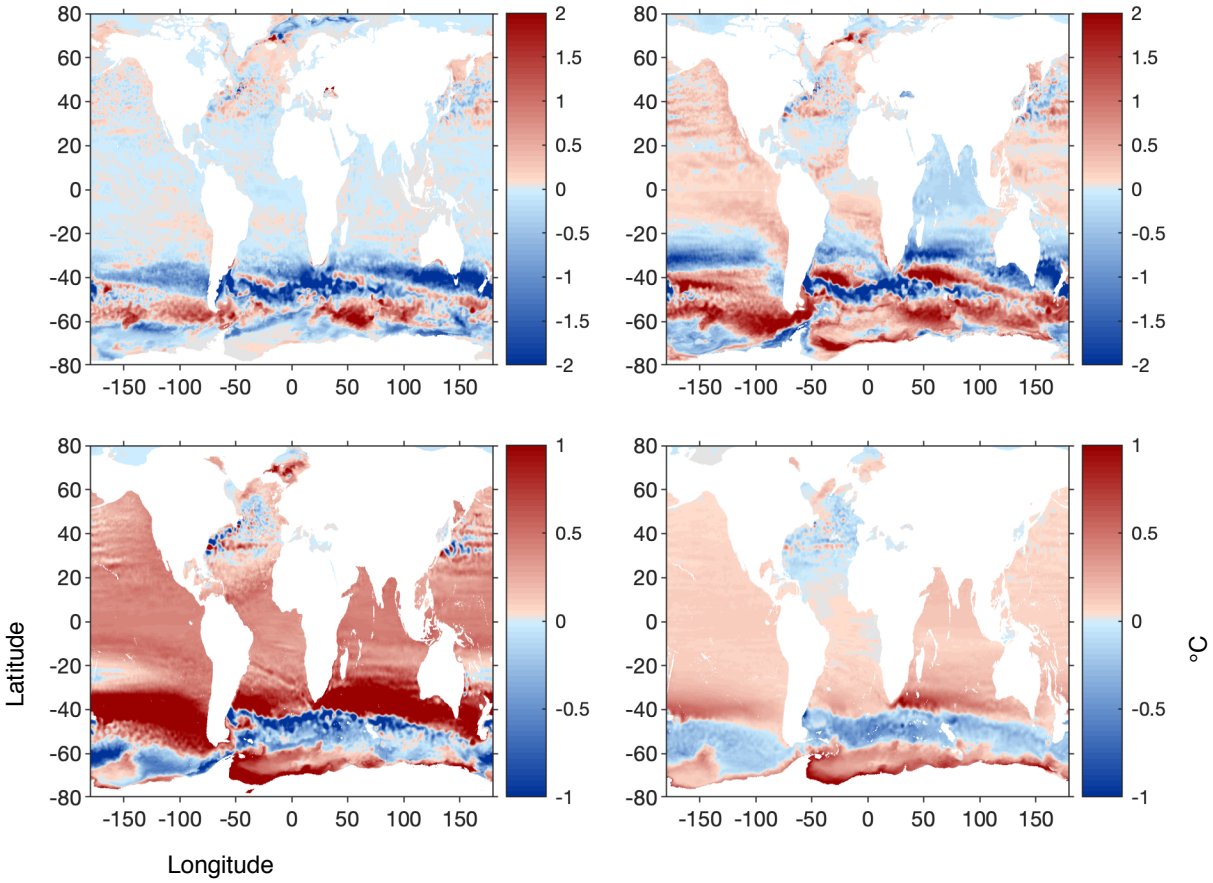

Figure 4.3 The depth-averaged temperature difference between the northward perturbation simulation and the control simulation averaged over 50-55 model-years after experiment initialization. Each plot displays the temperature averaged over a different depth. Top left: surface changes; Top right: upper 200 m; Bottom left: 200–700 m; Bottom right, 700–1500 m.

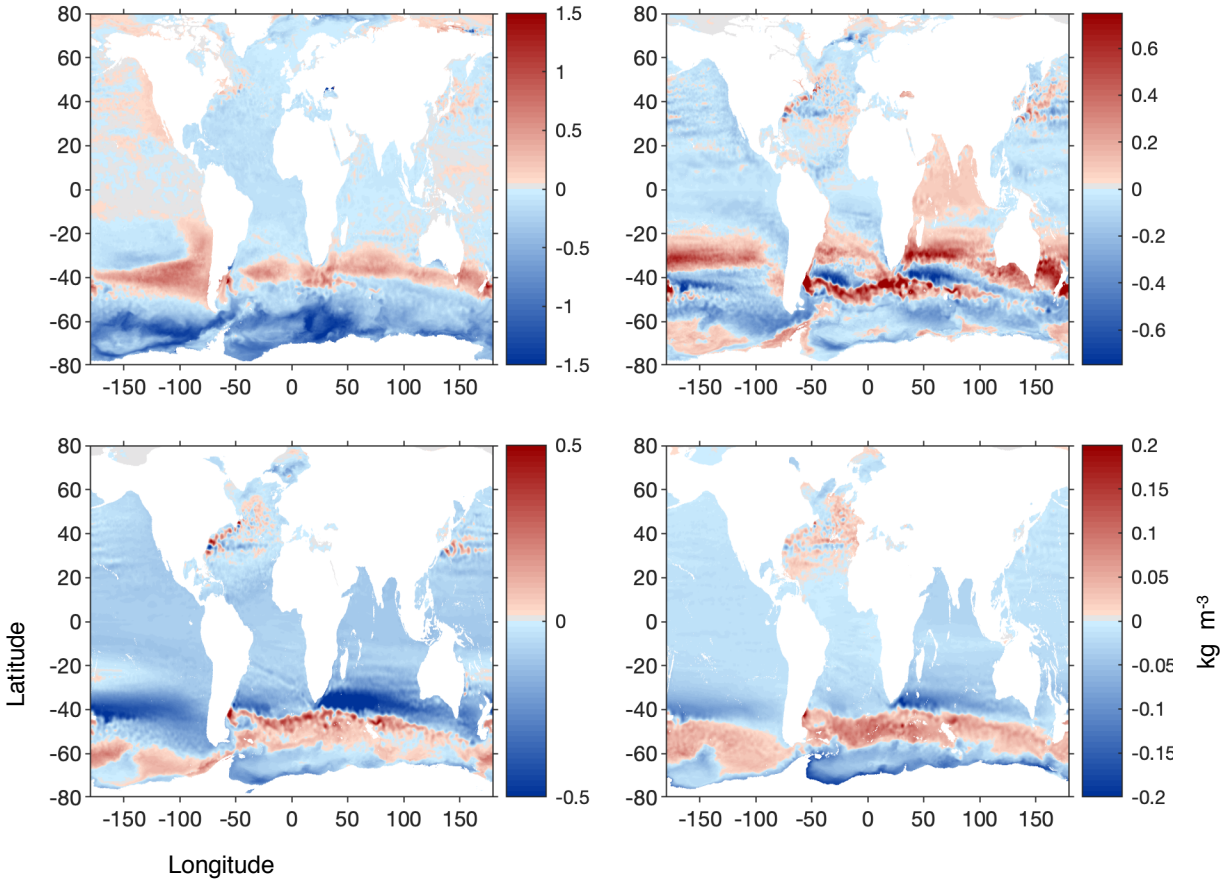

Figure 4.4 The depth-averaged density difference between the northward perturbation simulation and the control simulation averaged over 50-55 model-years after experiment initialization. Each plot displays the density averaged over a different depth. Top left: surface changes; Top right: upper 200 m; Bottom left: 200–700 m; Bottom right, 700–1500 m.

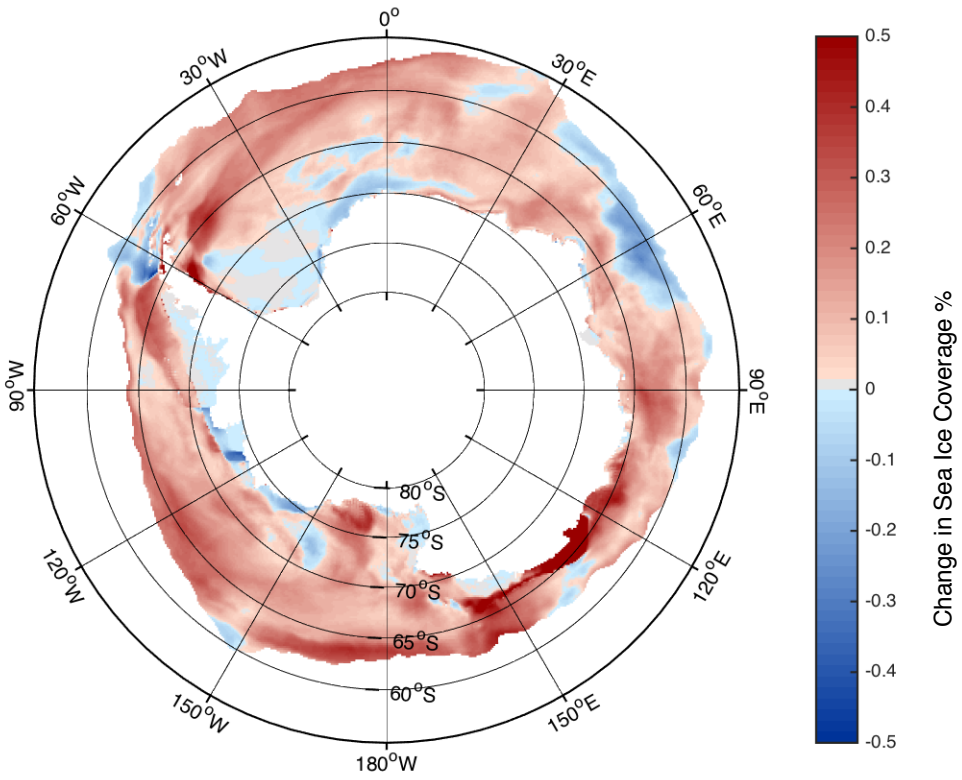

Figure 4.5 A map of the change in annual sea ice coverage between the northward wind perturbation and the control simulation. The change in annual sea ice coverage is an annual average difference in the proportion of the year covered with sea ice. Average was computed over model years 50-55 after the start of the perturbation branch-off. Cells with no sea ice in both experiments are set to unshaded.

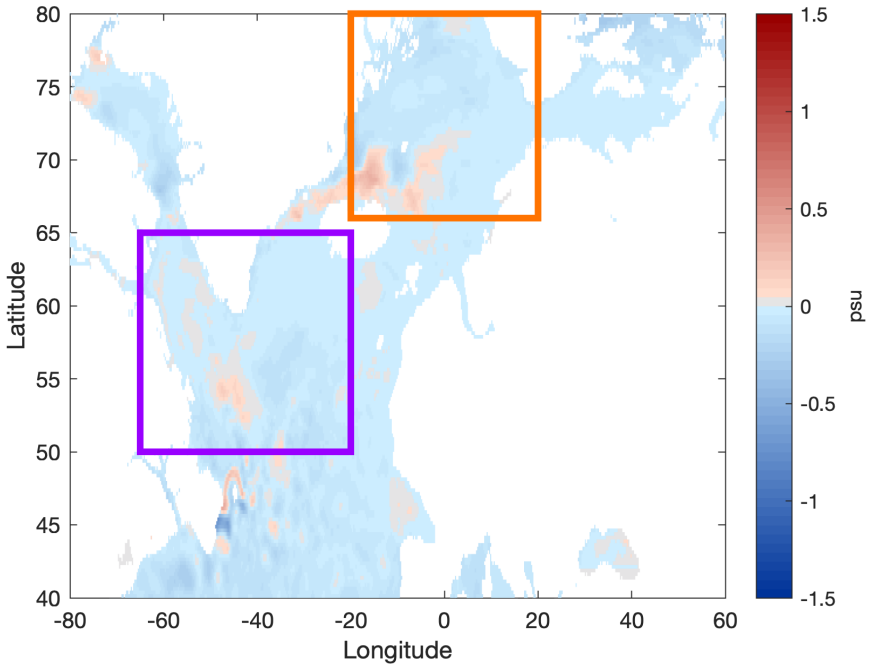

Figure 4.6 The depth-averaged salinity difference between the northward perturbation experiment and the control in the upper 200 m, averaged over model-years 50–55 after experiment initialization. The two rectangles represent regions of the North Atlantic where nearly all North Atlantic Deep Water (NADW) is formed (Heuzé 2015). The purple box shows the boundaries of the Labrador Sea region; the orange box, the boundaries of the Greenland-Icelandic Sea Region. These regions are used for measuring stratification changes in the regions of deep water formation. For example, stratification changes in the Greenland-Icelandic Sea Region (ornage) is shown in Figure 4.7

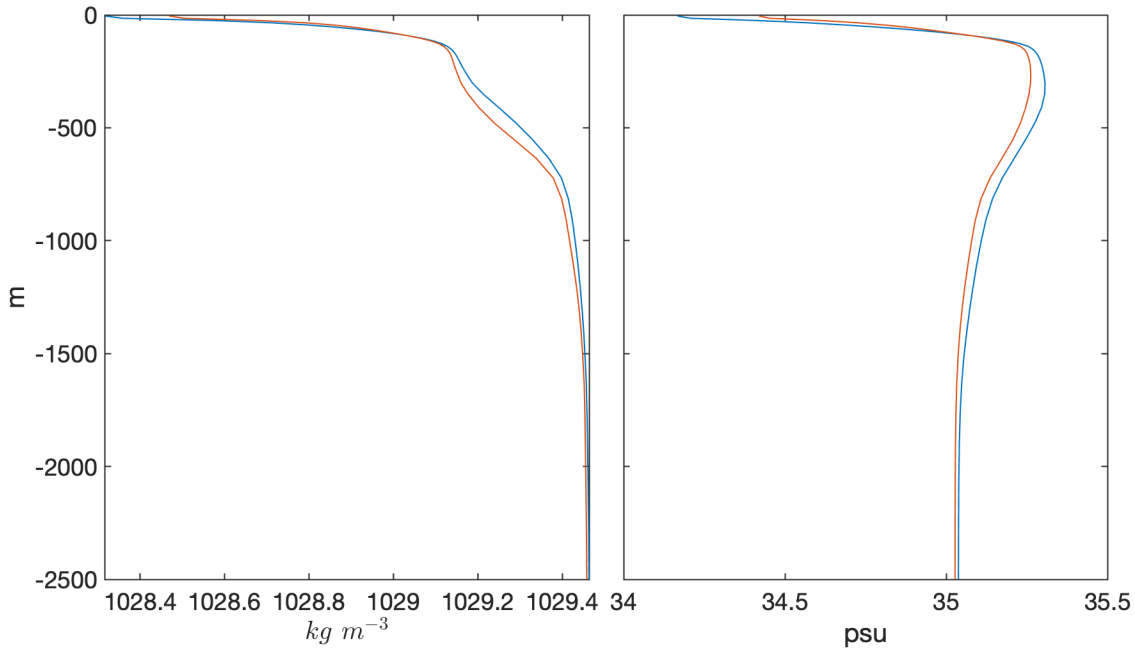

Figure 4.7 Vertical profile of salt (left) density (right) in the Greenland-Iceland-Nordic Sea region, the region highlighted in orange in Figure 4.6. Control shown by the blue line, perturbation by the orange line

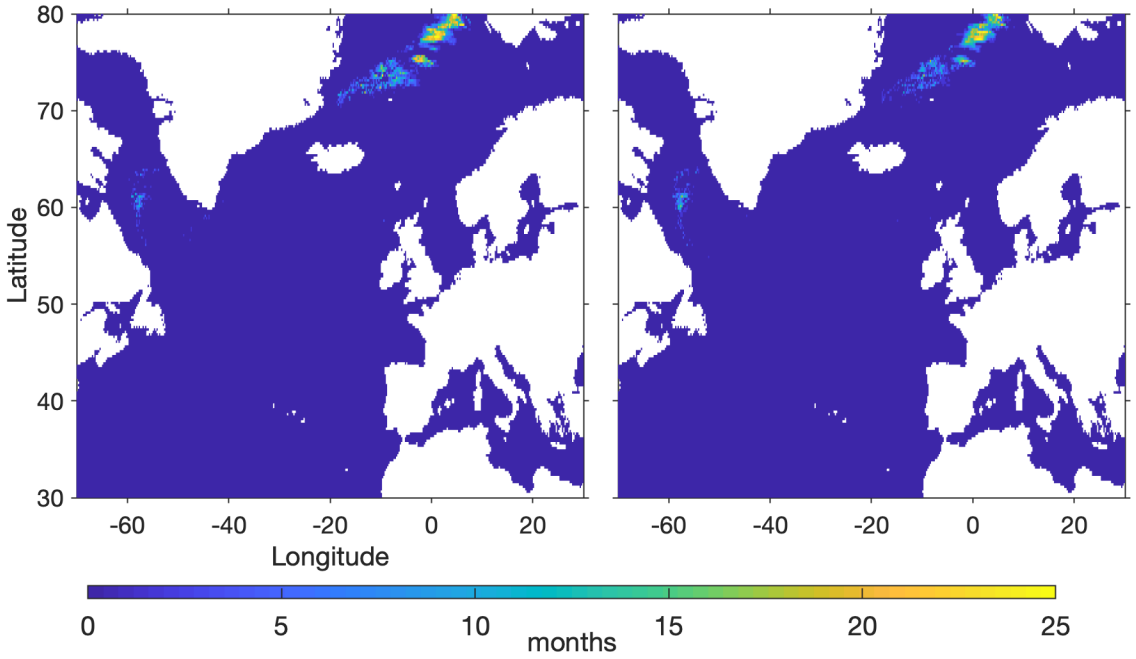

Figure 4.8 Number of months in the last five years of the experiments that the mixed layer depth was deeper than > 1000 m. A mixed layer depth > 1000 m indicates the ocean stratification is low enough to convect and form North Atlantic Deep Water (see text).Control on left, perturbation on right

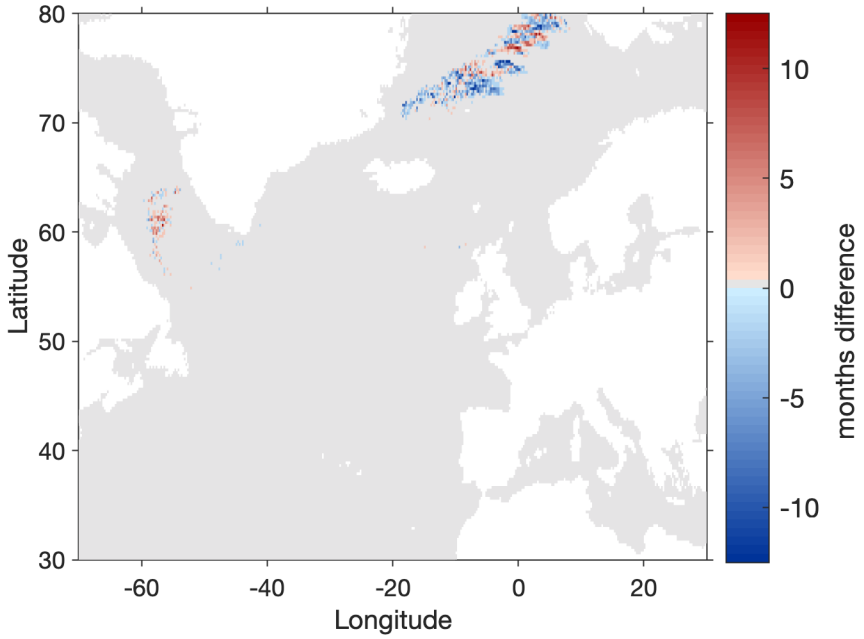

Figure 4.9 The change in number of months (northward wind perturbation – control) in the last five of years of the experiment the mixed layer depth was deeper than 1000 m.. A mixed layer depth > 1000 m indicates the ocean stratification is low enough to convect and form North Atlantic Deep Water (see text).

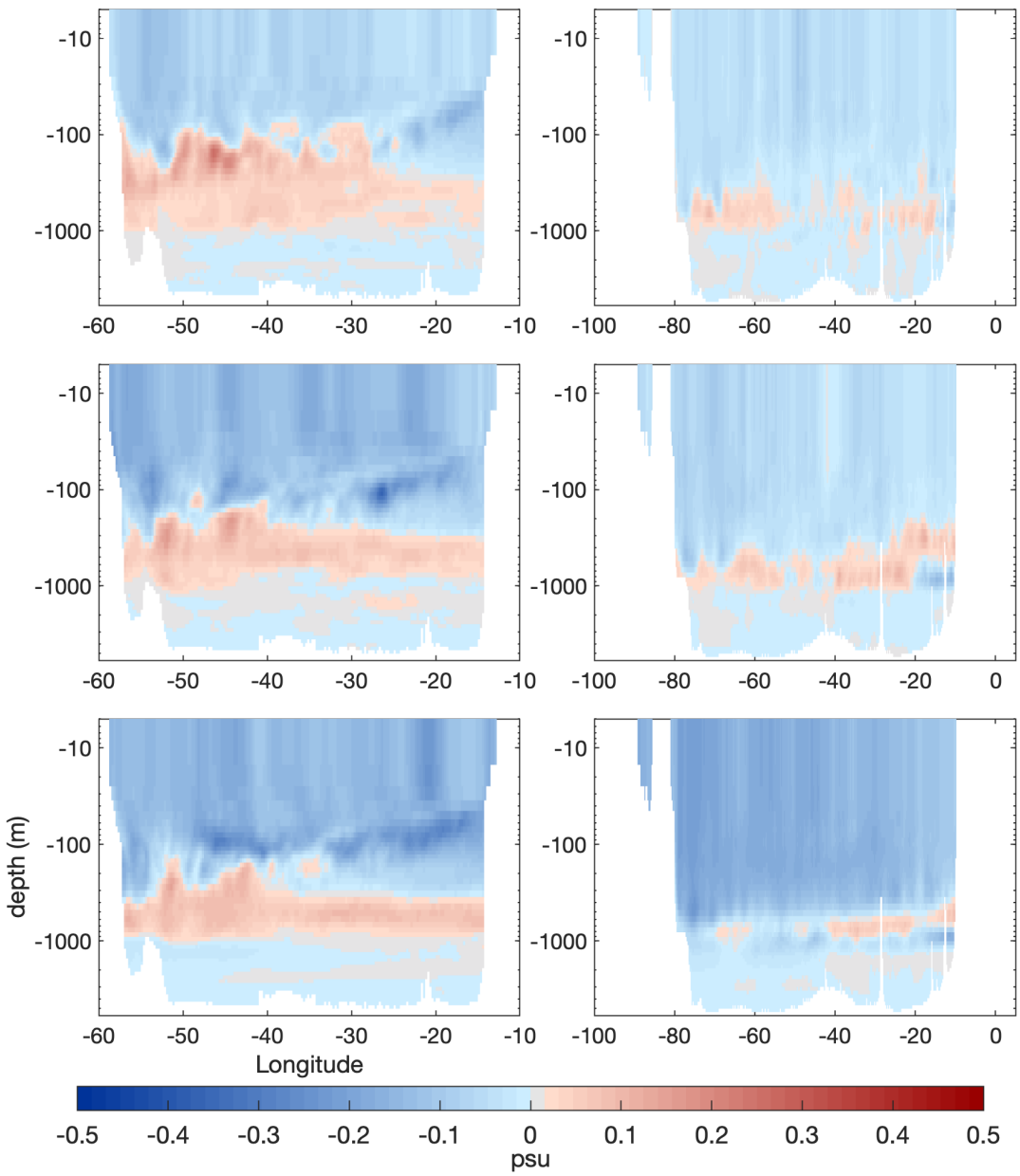

Figure 4.10 Latitudinal cross-sections of the Atlantic Ocean northward wind perturbation simulation and control salinity simulation differences between the perturbation and control experiments, ordered in increasing model time. Depth, plotted on a log scale, is on the y-axis; longitude is on the x-axis. Top plots show the salinity difference 12-15 model-years after the start of the perturbation experiment. Middle plots, 22-25 model-years., Bottom plots display the last five year of the simulation (53-58). Left plots are of an Atlantic cross-section at 8°N; right, cross-section at 30°N. There is a steady decline in salinity in the perturbation relative to the control, with the region of increased salinity in the perturbation at 500–1000 m in the 30°N cross-section nearly disappearing by the end of the experiment

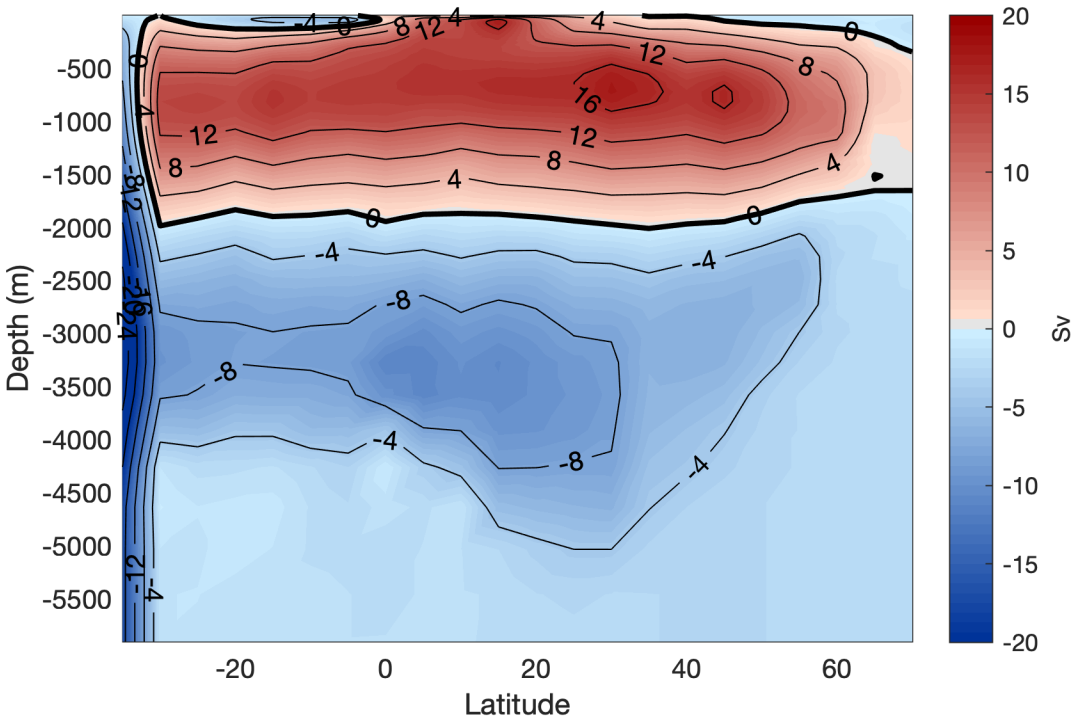

Figure 4.11 Atlantic MOC overturning function in the last 5 model years of the control experiment

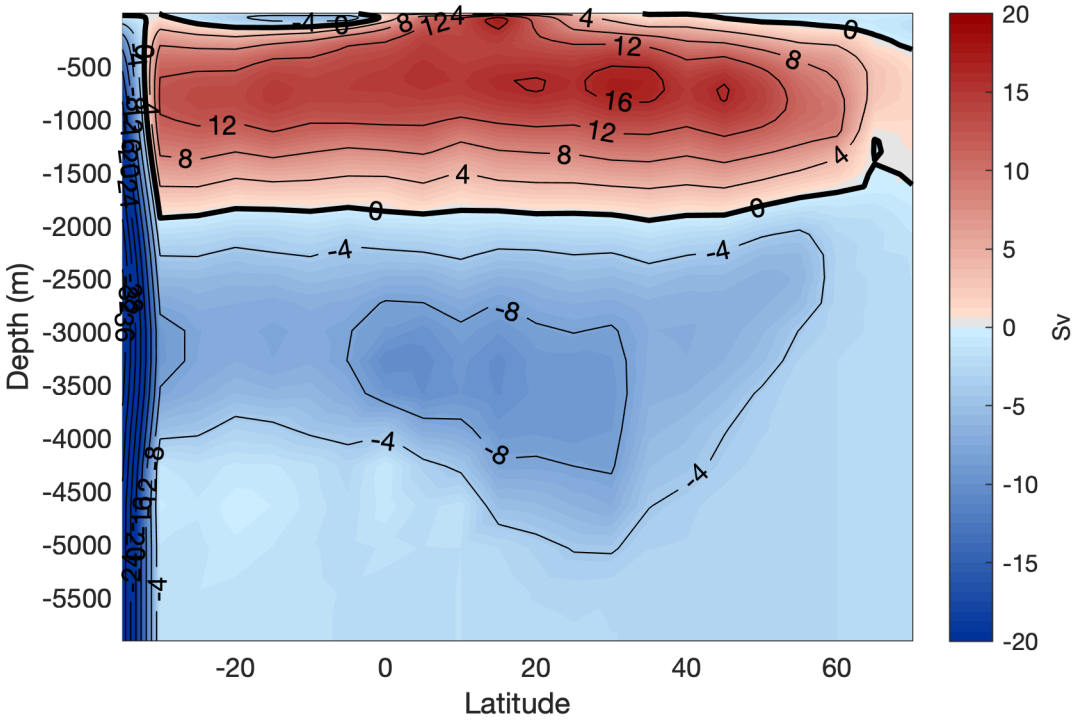

Figure 4.12Atlantic MOC in the last 5 model years of the northward wind perturbation experiment

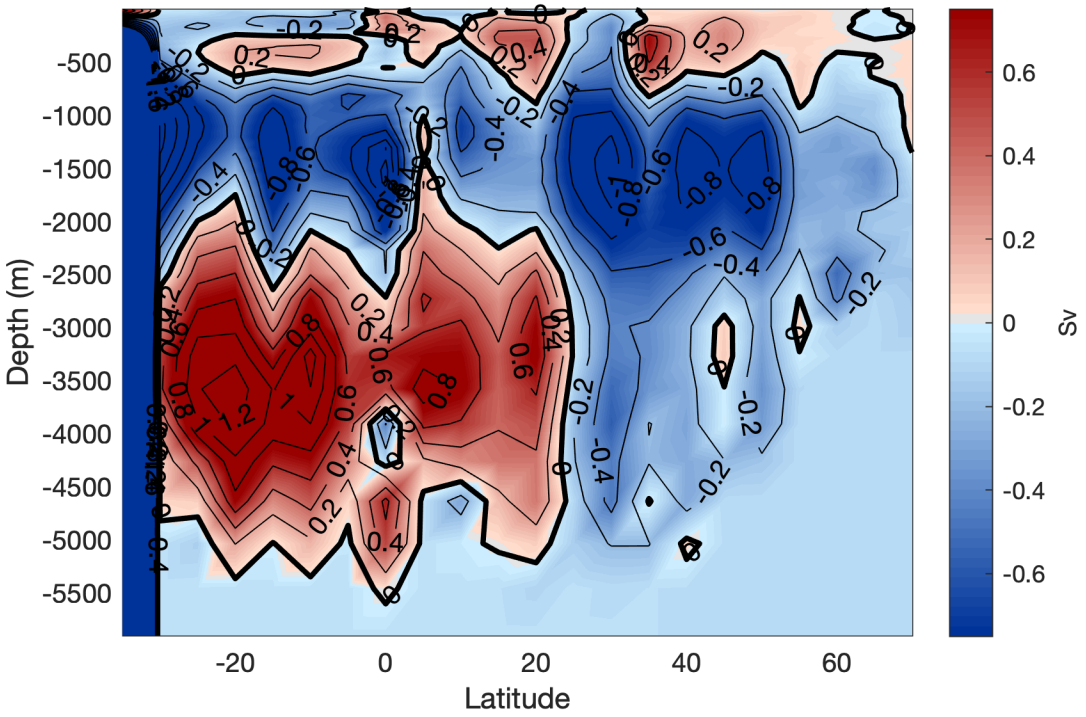

Figure 4.13 Difference in MOC in the last 5 years of the experiment; positive numbers represent increased clockwise rotation (or decreased counter-clockwise rotation)

CHAPTER 5

AGULHAS MEASUREMENT

5.1 Introduction

Measuring the Agulhas Leakage in both the real ocean and in ocean models is not straightforward. It is difficult to distinguish leakage waters from other waters in nearby currents, and small-scale features make it hard to determine the overall velocity. The two methods of determining ocean current transport are an Eulerian framework, which involves summing the total net volume of water transported through a boundary; and a Lagrangian framework, where virtual particles are seeded into the simulation and tracked (van Sebille et al., 2010). The Lagrangian method is the more widely used method for Agulhas Leakage tracking (Cheng et al., 2016). The Lagrangian method has the advantage of not requiring a property-based threshold and is less liable to track non-Leakage water by mistake. However, this method is computationally expensive and since it represents Agulhas Leakage as non-diffusive point particles, it does not depict the transfer of heat and salt anomalies by diffusion.

To calculate the flux of water entering by the Eulerian method, the area of water passing through a defined boundary is multiplied by the velocity of water passing through the boundary. The transect chosen to track the Agulhas Leakage should be a line just to the west of the Cape of Good Hope, so that all Agulhas waters entering the Atlantic would pass through the transect while Agulhas water retroflecting back into the Indian Ocean would not reach the transect. To isolate Agulhas waters, a water property threshold is defined based on a function of salt, temperature and depth. This has several

complications: Agulhas water properties change with depth, are somewhat model dependent, and may be different from today in the Pliocene. Alternatively, rather than isolating Agulhas Leakage water by ocean properties, the Agulhas Leakage can be isolated directly by tagging the Agulhas water in the model with a passive tracer, allowing the route and volume of Agulhas Leakage water to be tracked in the ocean model.

To gain a more complete perspective on changes in the Agulhas Leakage in my experiments, I use both measurement methods. The details of each method are discussed in subsequent subsections. I also performed an additional Agulhas Leakage measurement; counting the number of eddies that are spun off the retroflection and enter the South Atlantic. While roughly only 50% of the leakage is enclosed within eddies (Loveday et al., 2015), making this measure in isolation incomplete, eddy tracking is a convenient tool for several reasons. First, tracking eddies is useful because they contain only Agulhas water, providing an unambiguous Agulhas measure unlike Eulerian methods. Second, eddies provide a Lagrangian tracking that is less noisy than point particle tracking. The two measures should also be correlated, providing a check for the accuracy of the Lagrangian measure.

5.2 Lagrangian Particle Tracking (LPT).

To quantify changes in the influence of the southern Indian Ocean on the South Atlantic, I used Lagrangian Particle Tracking (LPT). As particle tracking is non-diffusive and measures different ocean motions, the results differed somewhat from the passive tracer experiments. A comparison of the particle and passive tracer measures are discussed in

the next chapter, as well as the implications of salt and heat transport and density anomalies around North Atlantic sites of deep-water formation.

Lagrangian particle tracking can either be performed offline, after the simulation has been run using saved 3-D velocity outputs, or online during simulation runtime. Lagrangian particle tracking adds several computational downsides. First, online tracking can impact simulation speed. Additionally, it cannot be used on simulation results that did not have a Lagrangian package tuned on. I set the MITgcm simulations to output full-depth mean ocean velocities at a monthly frequency, as higher frequency saves would produce an unmanageable amount of data, making storage difficult and processing tedious. Monthly mean velocities are too infrequent to be useful for tracking particle motion; ocean velocities change greatly in a shortly distance, especially where eddies compose much of the motion. Therefore, I used an online Lagrangian particle tracking package.

The particle tracking package used here is a modified version of the MITberg, an iceberg package for the MITgcm cubesphere written by Hill and Condron (2014); it was originally written for the purpose of tracking icebergs in the North Atlantic and has been used in meltwater experiments to track iceberg motion during the Last Glacial Maximum (Condron and Winsor, 2012). Each particle is meant to represent an "iceberg". These icebergs can be set to not add any freshwater or melt into the surrounding ocean, so they are functionally Lagrangian particles. Several modifications were made to the particle tracking scheme. This included the capability to allow particle motion between all cubefaces of the model grid domain, to allow them to be a useful Lagrangian particle tracker anywhere on the globe. Secondly, a modification was made to allow the passive

tracers to be released at any vertical level of the ocean, rather than just the surface level as it was originally written. This allows the motion and flux of Agulhas Leakage to be tracked at any ocean depth.

I used particle tracking in the NCAR control and northward perturbation experiments, while the IPSL and modern reanalysis-forced experiments were performed without particle tracking. In the experiments with particle tracking, The Agulhas Current is "seeded" with particles along a cross-section at 32°S similar to Loveday et al. (2014), Weijer and van Sebille (2014), and Durgadoo et al. (2013), extending from the coast to 35 °E and down to 1100 m. The location and depth of this cross-section were chosen to be sufficiently upstream of the Cape of Good Hope to capture nearly all the Agulhas Current water before the current separates into leakage and retroflection but close enough to the Cape for particles to reach the retroflection region quickly, capturing any fast leakage response in the simulation. The flow across the cross-section is 65-70 Sv in the control experiment**,** matching observed modern fluxes of the Agulhas Current (Beal and Bryden, 1999; Hermes et al., 2007)

The particles were seeded in 100 release sites in the cross-section shown in Figure 5.1. The release sites were determined such that each particle represented an equal amount of Agulhas Current and was created as follows. The Agulhas Current particle release cross-section was divided into four levels, each containing equal flux. Since the ocean has faster currents near the surface, the particle levels closer to the surface represent less ocean thickness. The particles were released at the flux-weighted vertical center of each depth level. Within each depth level, the same procedure was used to subdivide the

current into leakage sites horizontally. The current was divided into 25 regions of equal mean flux, with the flux calculated from two-year mean of the control simulation,10 model-years from the beginning of the spin-up period. While the perturbation simulation has a 15% weaker Agulhas Current and a slightly different flux profile, I use the same release sites for a simpler comparison. The deepest depth of the current level corresponded to the lowest depth of Agulhas Leakage eddies, which allowed the entire depth of eddies to be tracked. The vertical centers of the four vertical levels are at 55, 172**,** 350 and 722 meters.

Since each particle represented 1/100th of the total Agulhas Current, and the Agulhas Current has an annual mean of 70 Sv, each particle represented 0.07 Sv of transport. New particles were added at the particle release points ten times a year, or every 36 days, and then advected by the local ocean current velocity. So, a total of 1000 particles were released every year, with 250 particles in each vertical level. The first particles were released 3 model years after the perturbation or 20.5 model years from the beginning of the spin-up period; their motion integrated at the same timestep as the model timestep of 600 seconds. Each particle's position and velocity was tracked along a unique ID and its release date, tagging where each water mass travels.

5.2.1 Lagrangian Particle Measurement

To measure how much Agulhas water mass leaked into the Atlantic or enters the North Atlantic, I defined crossing barriers to count particles entering a specific ocean region. The timing when particles cross the barriers was also accounted for. The boundary for defining if Agulhas water had leaked and exited the Agulhas Region was set far enough

west from the point of mean retroflection that most particles crossing the barrier enter the Atlantic Ocean, instead of soon retroflecting and re-entering the Agulhas region. I considered a particle to be leaked if it crossed my defined barrier just to the west of the Cape of Good Hope at 19°W, extending from the cape to 50°S. The barrier together with a sample of particle paths of one year after release are shown in Figure 5.1. Most retroflected particles did not cross the barrier. However, due to the nonlinearity of ocean motion and eddy motion superimposed on the general circulation, many particles entered the Atlantic, then changed direction and returned to the Indian Ocean. To prevent the counting of particles that are in the Atlantic Ocean only briefly, I ignored particles that returned to the Indian Ocean unless they were in the Atlantic Ocean for at least 5 years. I counted the time of last crossing as the time of leakage, similar to the method used by (Putrasahan et al., 2015). A significant number of particles crossed the Agulhas barrier and then reversed, returning back to the Indian Ocean. To show examples of typical tracks of this motion, a sample of 60 particles that did cross the barrier but then end in the Indian Ocean is shown in Figure 5.2.

The barrier used for counting the number of particles entering the North Atlantic is defined as the line across the ocean at 8°N. This barrier was chosen because the Atlantic is narrower at this latitude than further north or south, simplifying counting. Also, some particles that crossed the equator but then reversed direction, returning to the southern hemisphere. Setting the barrier at 8°N prevented motion within for example, the Caribbean Sea from being confused with particles entering or exiting the North Atlantic.

To calculate the time it took a particle to cross the Agulhas barrier or any other counting

barrier, I used the following procedure. I checked the trajectories of the particles in a two-month period and compiled a list of particles on the source side of the barrier at the beginning of the two-month period, and in the leaked, Atlantic-ward side at the end of the period. A small but significant number of particles traveled from their point of release to the Agulhas barrier in less than 2 months and therefore would not be counted by the method described (they were not in the ocean at the previous time of counting). Therefore, any particles released in the last two months were added to the list of particles in the source region. Then, for each particle in this list, I checked when the particle is closest to the barrier. So, multiple crossings within a two-month period were not tracked and a particle that crossed a barrier and then re-crossed (ending on the original side) is not counted twice. This rather cumbersome method was necessary since simply summing the total number of particles in a region would yield an underestimate, as non-moving particles stuck along the coastline were periodically removed, lowering the total from the true leakage amount. The number of particles that passed through the pre-defined barriers is summed annually, as particle variability at shorter timescales is very high.

5.2.2 Particle Leakage Results

The 6° northward wind perturbation resulted in a large decrease in Agulhas-sourced particles leaking into the Atlantic as well as entering the North Atlantic. The volume of particles that leaked in the northward wind perturbation experiment was reduced by 40–50% relative to the control simulation. The perturbation created a decrease in particle leakage quickly within one year. After that little trend was apparent. The Agulhas retroflection also reached equilibrium quickly. It took 5 years for the first leaked particles to reach the North Atlantic, but most took much longer. The details will be discussed in

the following subsections.

5.2.3 Simulated Particle Motion

The particles took a wide range of paths, with particle paths traversing through nearly all of the South Atlantic. However, most particles that entered the Atlantic Ocean tracked northwestwards, with most reaching the east coast of South America at or north of 20°S in the control simulation (Figure 5.3). Few particles turned southward upon reaching the South American coast; most moved eastward, while a minority continued northward, hugging the coast. The northward wind shift perturbation experiment produced far fewer particles leaking into the South Atlantic, and those that did leak continued northwestward over a much narrower range of pathways, with fewer particles south of 35°S, west of 0°W (roughly 2000 km downstream of the leakage barrier). Ten years of particle motion in the control and perturbation simulations is compared in Figure 5.3. The northward wind perturbation strongly choked off the Agulhas Leakage; limiting the Agulhas flux into the North Atlantic. Overall, particles in the control experiment followed a more southerly path, as would be expected from the change in sea surface height and implied currents.

5.2.4 Particle Leakage across the Agulhas Barrier

Particle speeds had a very wide distribution (Figure 5.4); particles underwent fast, circular motion if caught within an Agulhas ring, but much slower if not. An example of particle motion is shown in Figure 5.1, which shows the paths taken by all particles released in one year. A common track was a circular motion superimposed on the mean flow. The time it took a particle (Figure 5.5) to reach the Agulhas Leakage cross-section

from the release site had a modal peak of about 4 months, with an exponential decline in longer times; 80% of leaked particles reach the Agulhas Barrier in under 2 years.

The particles at depth were released five model years after the perturbation, so I was unable to gauge how quickly the ocean responded to the northward wind shift. After a year, the resulting particle fluxes through Agulhas Barrier were rather stable, with no statistically significant trend. The lack of any trend shows the deeper ocean was approaching equilibrium.

A depth-separated time series of Agulhas Leakage is presented in Figure 5.7. As expected, the overall result was a sharp reduction in Agulhas Leakage. The control experiment had an average of 267 particles leaked per year while the northward wind perturbation experiment had a leakage rate of 122 particles leaked per year. However, the details by depth are rather unexpected and counter-intuitive. Instead of the deeper levels showing less response to a change in surface winds, the opposite occurred, with the northward wind shift having a very large impact on the two deepest levels (350 and 722 m) but a minimal effect on the two shallower levels (55 and 172 m). In the control, a larger portion of particles at deeper depths leaked into the North Atlantic; about twice as many particles from the two deeper depths leaked compared to the two shallower levels. In the perturbation, the amount that leaked is about equal between the deeper and shallower layers.

The higher leakage at depth in the control experiment suggested a difference in current flow between depths was responsible for this depth pattern. One plausible explanation for the observed particle transport patterns with depth is that since the mean eastward flow of

the Agulhas Region decreases with depth, but the speed of Agulhas originated water, which is entering from a westward or southwestward direction, against the mean flow, does not decrease with depth as much. So, it is easier for Agulhas Water to overcome the opposing prevailing ocean water motion at deeper depth. The mean ocean flow near the Agulhas retroflection is eastward, only Agulhas water with high enough inertia to overcome the prevailing current flow leaked. A comparison of particle speed within the Agulhas retroflection region is shown in Figure 5.4. At depth, particles move at much slower speed and are more susceptible to changing ocean currents. A larger portion of particles at depth have a zonal (eastward) velocity low enough to leak, and more leaked at greater depth. However, the slow current speeds at depth result in particles staying within in the retroflection region for longer, making the deeper ocean in the retroflection region more sensitive to a change in current speed and therefore wind forcing. If the proposed reasoning is correct, the greater impact at depth is due to the Agulhas Leakage flowing against the mean local current. Further downstream, where particles would flow with the mean local current this depth pattern should weaken.

Further downstream in the South Atlantic, there was a significant difference in the number of particles that made it across the South Atlantic to the Brazilian coast between the control and perturbation NCAR-initialized experiments. This is of interest because once water reaches the South American coast, the prevailing current continues past the equator, allowing for an inter-hemispheric water mass pathway. Past the equator, some of the current water joins Gulf Stream, which influences the high latitude North Atlantic. The first particles reached the Brazil margin (around 20°S) at about 5 years after release at the uppermost ocean depth level (55 m), with a slowly increasing trend for the next 5-7

years. The time for the first particles for the particle at the next deeper two levels (172 m and 350 m) to arrive at the Brazil margin was 5-7 model years longer than the time it took the first particles from the shallowest level (55 m) to arrive. Additionally, particle flux increased more gradually at the deepest level (see Figure 5.6). After the first arrival of particles, the amount of particles reaching the South Atlantic cross-section (particles crossing north of 20°S) remained roughly constant with depth in both experiments with the exception of the deepest level (representing water at a depth of 722 m) where particles are slow to arrive due to slower ocean speeds. This contrasts with the pattern observed in the Agulhas retroflection region. In the South Atlantic cross-section, the deeper ocean did not have a larger response than the near surface ocean to the wind perturbation. Similar to the Agulhas Leakage changes, the northward perturbation had about half the particle volume of the control experiment.

The higher leakage rate with increasing depth in the unperturbed wind control experiment appears to reflect local dynamics within the retroflection. I investigated the leakage rate through the South Atlantic to check if the higher rate of deeper particles was limited to the Agulhas retroflection region or if it continued further downstream into the Atlantic.

The northward wind perturbation had a flux rate of about half of the control experiment, a very substantial slowdown in the Agulhas water mass influx. While the control shows a leakage rate higher with depth in the Agulhas retroflection region, further downstream in the South Atlantic, this is not the case. This implied that the deeper leaked particles tend not to reach the Brazilian coast or got caught in a western boundary current.

5.2.5 North Atlantic particles

About 2.4% of particles released entered the North Atlantic (defined by north of 8°N) in the control experiment, while 1.2% entered in the north perturbation wind experiment. Few of the deepest particles had time to reach the North Atlantic (Figure 5.8). The mean time for reaching the North Atlantic cross section from the Agulhas barrier was 14 model years with a very large variance. The northward perturbation experiment had a similar mean time. A histogram of the distribution of the times of when Agulhas particles were leaked and reached the North Atlantic is shown in Figure 5.9. A similar fraction of Agulhas Leakage particles reached the North Atlantic cross-section in the northward wind perturbation as the control experiment; however, the northward wind perturbation had a much lower Agulhas Leakage flux overall. However, the proportions of deeper to shallower particles shifted.

Few particles that reached the North Atlantic travel further north than 40°N, nor entered the North Atlantic Deep Water (NADW) formation sites such as the Greenland Iceland Seas and Subpolar Gyres (shown in Figure 5.2). Rather than continuing northward, most particles tracked eastward. The lack of particles reaching the NADW formation sites implied the only method for Agulhas density anomalies to reach the NADW is via diffusion. Regardless, most heat or salinity anomalies would have largely diffused by the time a particle (or a water parcel) reached the North Atlantic and only a small fraction of particles reached into the North Atlantic. In the next section, the impact of the Agulhas Leakage on the North Atlantic considering diffusive processes is discussed.

5.3 Passive tracers

As mentioned earlier in the section, the Eulerian flux of an ocean current is calculated directly by measuring the total ocean water flux across a defined boundary. A threshold based on salt and temperature properties is required to isolate the ocean current of interest. One drawback of measuring salt and heat changes directly to quantify the impact of the Agulhas Leakage is that the measure is dependent upon model biases. Given the large salinity biases (Figure 3.1) of my starting model, the CCSM4, the actual water properties for a Eulerian analysis of Agulhas Leakage threshold would need to be changed (bias-corrected) from the usual modern-day threshold. Another issue is that both the prevailing salt and heat in ocean current water changes quickly as it moves, making it difficult to track an ocean current. Putrasahan et al. (2015) proposed using a quantity named “spice”, which is a linear combination of temperature and salinity, orthogonal to density. Spice has the benefit of being conserved over longer distances. Agulhas Leakage water stands out for having anomalously high “spice”, with observations indicating a suitable threshold for what spice values should count as Agulhas Leakage. However, due to salinity and temperature biases in ocean models, a new spice threshold needs to be determined that matches the Agulhas Leakage properties in my modeling experiments. The spice threshold used by Putrasahan et al. (2015) was unable to capture Agulhas water in my Pliocene simulations but was successful in isolating Agulhas water in a short modern reanalysis-forced MITgcm experiment I performed. While the spice measurement technique was useful as a check for gauging if the MITgcm is capable of simulating the Agulhas Leakage accurately, an alternative passive tracer technique is needed to measure the leakage in my Pliocene model. While I could have altered the salt

and heat threshold to match my model's Agulhas Leakage properties, determining the correct threshold may be difficult. The unrealistically low salinity contrast between Agulhas water and the surrounding water in the CCSM4 added to the difficulty. So, rather than use a property-based threshold, I used a passive water mass tracer to “tag” Agulhas Current water.

A passive tracer is an additional field in the ocean model, which does not affect model physics or ocean properties like temperature and salinity. However, like heat and salt, the tracer is advected and diffused. Passive tracers are commonly used in ocean models to track the concentration of dissolved matter in the ocean such organic carbon. To release and track the tracers, I used the MITgcm package PTracers. In this package, the passive tracers advect and diffuse with the same timestep as the model integration timestep. The diffusivity of passive tracers is useful for understanding how much Agulhas water diffuses into distant waters far from the North Atlantic. After longer distances Agulhas-derived waters mix into surrounding waters, affecting the local water properties but are no longer a distinct water mass. The tracer concentration value can range from 0 to 1, with 1 corresponding to an ocean made up entirely of the tagged water mass, and zero containing none of the water mass. To track the path of Agulhas water, I set the tracer value of the Agulhas Current to one from the surface to a depth of 1500 m, corresponding to the deepest depths the Agulhas Current reaches in the model, and initialized the rest of the ocean to zero. During the model integration when the tracer is enabled, the tracer concentration over the entire full-depth ocean was saved monthly. Throughout the tracer experiment, the tracer concentration in the Agulhas Current source region was nudged back to a value of one at the end of each model year, while the rest of the ocean slowly

accumulated tracer. A nudged passive tracer experiment to track Agulhas Current was also performed by Loveday et al. (2014), running their experiment for five years. I tried multiple experiments, defining the Agulhas Current region differently. The passive tracer experiments are listed below in Table 5.1, described where and the ocean is initialized:

Experiment	Region tagged initially (all north of 32°S in Indian Ocean)	Initialized (relative to perturbation start)
1	Within 10° of southern African coast	2 model-years before
2	Entire Indian Ocean	2 model-years before
3	Within 10° of southern African coast	47 model-years after

Table 5.1 List of Agulhas Tracer experiments

All regions had a southern boundary at 32°S, same as the cross-section of Lagrangian particle release. The "within 10° of southern African coast" region was bounded in the north at 8°S and only water within 10° of the east coast of Africa was tagged. This is large enough to encompass all waters the Agulhas Current passes. The initial region tagged for these experiments is shown in Figure 5.10.

Tracer experiment 1 was started two model years before the northward wind perturbation experiment was branched off from the control simulation. This timing was chosen so that at the time of the perturbation, there would already be some passive tracer-tagged Agulhas Leakage water present in the leakage region, so the tracer response would be visible. I added tracers only two years before the perturbation in avoid over-saturating the global ocean with tracer water.

In its original configuration, the MITgcm PTracer package does not restore the passive

tracer during the simulation. I attempted an experiment with no nudging of PTracers and found the tracer dissipated too quickly to be useful for Agulhas Leakage measurement. An Agulhas Leakage experiment initialized to the region described in (1) diffused out of the region within 3-4 years, leading to the Agulhas Current having a near zero passive tracer value. An Agulhas Leakage experiment (2), the Indian Ocean was tagged with Agulhas water which allowed the Agulhas Current to maintain a high passive tracer value, due to recirculation within the Indian Ocean gyre. However, tagging the entire Indian Ocean with a passive tracer resulted in too much passive tracer representing non-Agulhas water. Eventually, some tracer from the Indian Ocean exited into the Antarctic Circumpolar Current, and from there some entered the Atlantic Ocean (Figure 5.12). Since in this setup much of the tracer in the Atlantic Ocean did not represent water that directly entered the Atlantic via the Agulhas Leakage, this was not a useful method for measuring the leakage and I did not continue this tracer experiment. Neither of PTracer experiment 1 or 2 were ideal: either the tracer was lost too quickly out of the Agulhas Region, making it difficult to track the current, or too much tracer water was marked.

To better track Agulhas Leakage water for the length of the model experiments, I used the region defined in (1) but continuously nudged the source region to a value of 1. The tracer source is still limited to the Agulhas Current and the Agulhas Current is a tracer source for the length of the tracer experiment. However, this led to an issue that made interpreting the tracer value challenging. Nudging the Agulhas Current region to a value of 1 (100% tracer concentration) resulted in the Agulhas Leakage appearing to accumulate throughout the global ocean, since tracer was always added to the simulation and never removed (non-conservative). The passive tracer value did not accurately reflect

concentration of Agulhas Leakage water due to this accumulation. However, it was not an ideal measure for total tracer accumulation either. In high Agulhas tracer regions, the tracer saturated (approaches 1) and no longer increased as quickly; once the passive tracer value approaches 1, passive tracer cannot diffuse into it. Over time, the passive tracer content of the waters near the Agulhas Leakage saturated to almost 1, becoming indistinguishable from Agulhas Current water despite having received an influx of water mass from other sources such as the Antarctic circumpolar current and the south Indian Ocean. Areas of the ocean that received an influx of Agulhas water at a slower rate were less affected by this saturation problem. The nudged tracer experiment of Loveday et al. (2014) was performed for only five years, so there was less of a saturation problem in their study.

Nevertheless, despite the drawbacks of the non-restoring tracer setup, I found that restoration (nudging) was the best way for passive tracers to both provide a longer-term measure of the Agulhas Leakage as well as a good measure of Agulhas water mass diffusion into the North Atlantic ocean. Because of the saturation problem, I used the passive tracer mainly to measure the influx of Agulhas water mass to areas to where Agulhas Leakage tracer concentrations are not near a value of 1; in particular, for the quantity of Agulhas water entering the North Atlantic. Because a grid cell cannot have a tracer value higher than 1, the increase in total tracer content in the ocean slowed with model time, leading to the measure no longer reflecting the same dynamics as at the beginning of the tracer experiment. This effect produced a loss of accuracy with time. A passive tracer derived Agulhas Leakage time series is shown in Figure 5.11, but due to this saturation, its accuracy after 15-20 model years is questionable. The tracer-derived

Agulhas Leakage flux is defined here as the net monthly increase in Agulhas tracer volume in the Atlantic. The tracer volume in the Atlantic was calculated by summing over the tracer content of each grid cell in the Atlantic Ocean; where the grid cell tracer content is equal to the cell volume multiplied by the passive tracer value. The Atlantic - Indian Ocean boundary was defined by the barrier used for particle counting (Figure 5.1) the west of where most of the Agulhas Current retroflects.

To obtain an accurate tracer-derived measure of the Agulhas Leakage later in the model simulation when the saturation issue became problematic, I started two additional passive tracer experiments 47 model years after the start of the perturbation, since the earlier ones have run for too long and have the saturation issues described above. One (experiment #3) uses the same tracer-injection region as the earlier experiment (1), while the other used a much narrower tracer source region (experiment 4), using the same Agulhas Current cross-section used to measure the Agulhas Leakage in particle release counting. The resulting tracer volume from experiment #4 into the Agulhas Leakage was very small, with very little tracer tagged water reaching the Agulhas Leakage in the remaining 10-15 model years of the experiment. Therefore, I did not use this tracer experiment in my conclusions nor discuss its results.

5.3.1 Passive Tracer Results

Significant tracer differences between the two experiments appeared quickly. As expected, the control experiment had more tracer-marked leakage water than the northward wind perturbation experiment. The amount of tracer water in the northward perturbation differed greatly everywhere downstream from the source region, including

the area immediately south of the source region before the Cape of Good Hope.

Within one model month, the perturbation altered the upper ocean passive tracer distribution; although one month was insufficient to impact the overall Atlantic tracer content. Within three years of the perturbation, there was an appreciable difference in passive tracer water transported compared to the control. After five years, the average leakage transported in the perturbation experiment was significantly less than in the control; the north perturbation averaged 11 Sv and the control averaged 13 Sv (Figure 5.11). These values are close to other published values of modern-day Agulhas Leakage, which is about 15 Sv (Richardson et al., 2007, De Ruijter et al., 1999).

After 15 model years, the passive tracer values near the Agulhas Region saturated to near 1 in both control and wind-perturbation experiments. As the entire region eventually saturated, both the perturbation and control tracer-derived leakage values also converged to nearly the same value.

As tracer diffusion decreased later in the simulation, both the total tracer content in the global ocean increased at a slower rate and the Agulhas-derived leakage rate also declined later in the tracer experiment. However, the total North Atlantic-wide tracer content in both experiments showed no significant decrease in accumulation rate, showing the saturation issue was not adversely affecting the North Atlantic results.

The tracer results did not follow the same patterns observed in particles; the change in leakage from control to perturbation was much smaller measured by tracers than particles. This suggests that diffusive processes are not as strongly impacted by a

meridional shift in southern westerlies. Additionally, the tracers did not exhibit the unexpected response of the particles, where water mass at deeper depths in the ocean showed a larger response. Unlike particles, the evolving tracer distribution revealed that the deeper ocean has a slower leakage rate than the shallower ocean depths, which is expected as the overall ocean speeds are faster at shallower depths, allowing for more mixing and diffusion.

5.3.2 Spatial and Temporal Patterns in Tracer Results

While the first tracer reached the North Atlantic (north of 8°N) around 3 years after its release, a significant difference between the control and northward perturbation was not observed until at least 10 years after the start of the perturbation (Figure 5.15). This is similar to the median time for particles to reach the North Atlantic (Figure 5.9). The tracer differences were global; less Agulhas-influenced water entered the North Atlantic, while more entered the Antarctic Circumpolar Current. Figure 5.10 shows the change in tracer concentration after 53 model years.

The region of the North Atlantic with the largest difference in tracer concentration followed the path of the Gulf Stream. After 50 model years, the region of the North Atlantic in and around deep water formation sites displayed a difference in tracer concentrations (Figure 5.10), however the difference was larger south of 45°N. Like the impact on tracer concentration, the wind perturbation had a significant impact on the salinity distribution of the North Atlantic, with the largest changes in the Gulf Stream region (Figure 4.2). Resulting changes in the density stratification of the subpolar North Atlantic gyres are important because they can have an impact on the AMOC (e.g. Arzel et

al., 2008; Huezé 2017; de Boer 2008). In turn, changes in the AMOC influence global climate via the redistribution of heat (e.g. Rahmstorf and England, 1997; Cheng et al., 2007, Zhang and Delworth, 2005; Vellinga and Wood, 2002; Sgubin, 2017). However due to the early onset of salinity changes, preceding the tracer concentration changes, it is unclear if the salinity changes were caused by the reduced Agulhas Leakage in the wind-perturbation experiment, but the vertical profile of the salinity changes suggest that surface ocean processes dominate the connection between the leakage and the North Atlantic.

5.3.3 Long-Term Passive Tracer Results

An additional passive tracer experiment was started late in the model simulation (model-year 47). In another ocean modeling study, Durgadoo et al. (2015) found only a transient response in the Agulhas Leakage after a large southward wind perturbation, and by 50 model years most of the response disappeared. The purpose of this later passive tracer experiment was to verify if the perturbation response was transient. Initially, there was little significant difference between the perturbation and control until after 6 model-years, as it took time for tracers to accumulate. Afterwards, there was a significant difference in Agulhas Leakage flux between the perturbation and control, showing the response continued after 50 model-years (Figure 5.16).

Ten model years after this model year-47tracer experiment, there were some differences in the amount of passive tracer that reached the North Atlantic, but most of the changes in the South Atlantic did not have time to reach the North Atlantic (Figure 5.14). The leakage rate differences into the North Atlantic were small in this experiment (Figure

5.17) even while those in the South Atlantic are clearly visible.

5.4 Eddies and Eddy tracking

Roughly half of the Agulhas Leakage is carried by eddies, also called Agulhas rings (Loveday et al., 2015) into the South Atlantic. These rings extend down to depth of at least 1000 m (Putrasahan et al., 2015). The rings are a near circular, rotating mass of water. Even though only part of the Agulhas Leakage is contained within eddies, eddies are easy to track, and their rotation minimizes diffusion, allowing them to keep Agulhas water properties for longer than non-eddy water.

A script was written to identify the Agulhas eddies in the modeled ocean, and track their path using the monthly 3-D ocean velocity data files. The script also measures the salinity and volume of the eddy every month the eddy is identified. Potential eddies in the ocean were found by finding closed vorticity contours of the surface ocean above a chosen vorticity threshold of 1.2 sec^{-1}. The threshold was chosen to best capture rotating water bodies in the model output while not capturing non-linearities unrelated to eddies. If the region enclosed within the vorticity contour was both of sufficiently large area and nearly circular, the region was marked as an eddy. Below the surface, the lateral boundary of the eddy was determined using the same vorticity threshold as the surface down to 1300 m, where most eddies become indistinguishable from their surrounding waters. By this method, the full depth of the eddy is found.

From the mean velocity of the ocean in the region, a probable location for where the eddy would be in the next month was determined. If an eddy was found in the predicted region

in the next month, it was assigned to be that eddy's location in the next month. In this way, eddies are tracked. In the few cases where multiple eddies were in close proximity, the eddy chosen was the one closest to the predicted position.

Interestingly, in both the control and perturbation runs, the Agulhas Leakage eddies followed a very similar path and then weakened below the defined eddy detection threshold in roughly the same region of the South Atlantic (Figure 5.18). As eddies crossed the Atlantic, they slowly shrank in width and eventually either became too small to detect, or lost their circular shape. Most went below the detection limit not far from the Brazil Current, which meant that most of the waters initially contained in eddies would be entrained by the current and advected northward.

The number of eddies leaking into the South Atlantic was significantly higher in control, confirming that a northward westerly wind shift leads to a decrease in Agulhas Leakage. Also informative were the salt anomalies contained in the eddies. In both experiments, the eddies carried an excess of salt compared to the surrounding waters. Importantly, this showed that despite the large salinity biases of the CCSM4, the Agulhas Leakage in the model still carried a positive salt anomaly into the Atlantic. At a glance, the eddies varied and do not always look distinctive in a salinity map; but their salinity anomalies became clear in difference plots. A histogram of the salt excess of eddies entering the South Atlantic (crossing of 17°W), is shown in Figure 5.19. The eddies are on average 0.1 psu more saline than the surrounding waters.

5.5 Figures

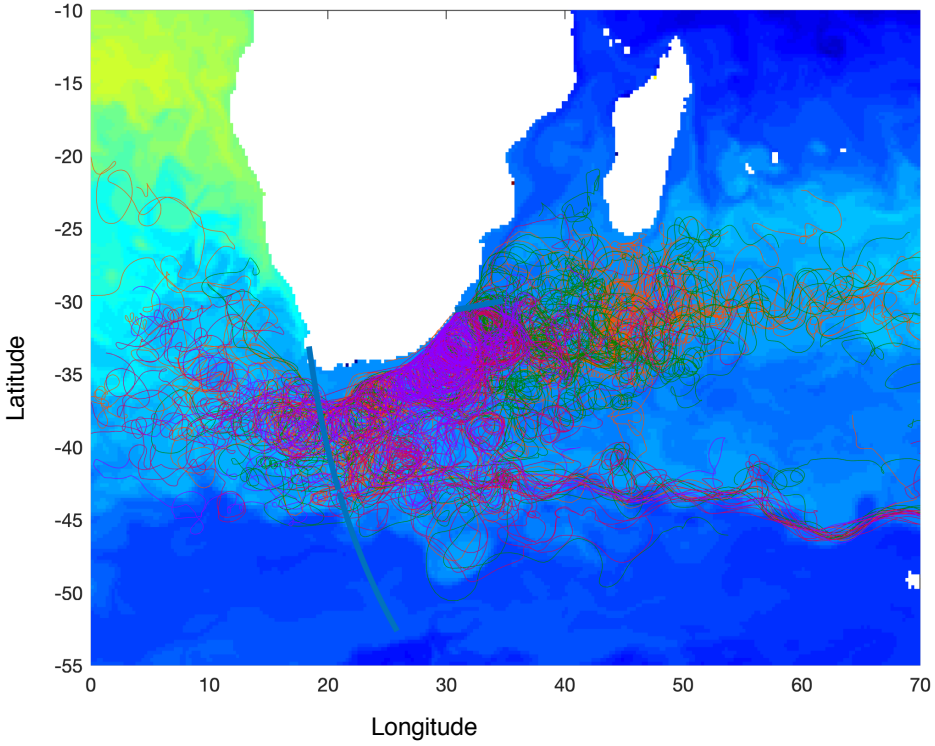

Figure 5.1 Motion of particles released in one-year in the control simulation. Prevailing ocean current speed is sufficiently fast that many reach the Agulhas retroflection within a year. Individual water mass movement is often non-linear, with eddy motion creating ring-like motions superimposed on the general flow. The blue line extending from the east coast of Africa represents the Agulhas particle release. The blue line starting at the Cape of Good Hope extending southeastward is the leakage line, used in counting Agulhas Leakage water. This is used in both tracer and particle measurements

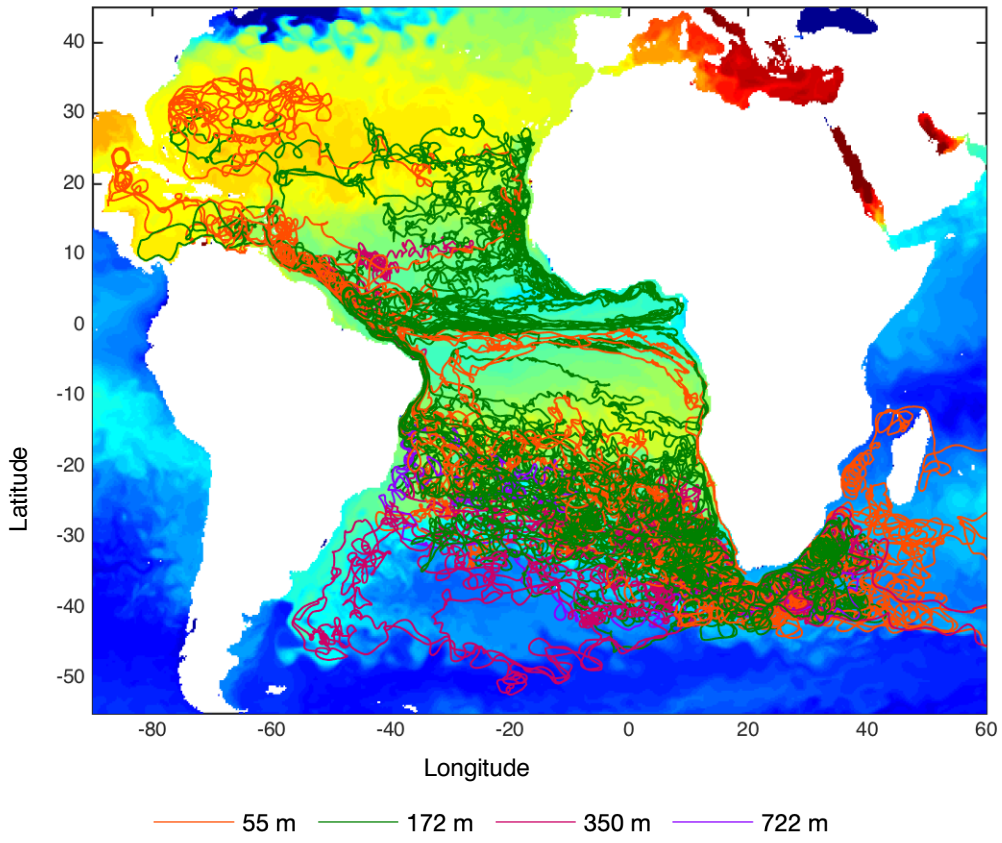

Figure 5.2 The path of 60 particles released at model-year 25, colored by depth level, that reached the North Atlantic in the control simulation. The colors represent particle at different depth levels, labeled in the above legend

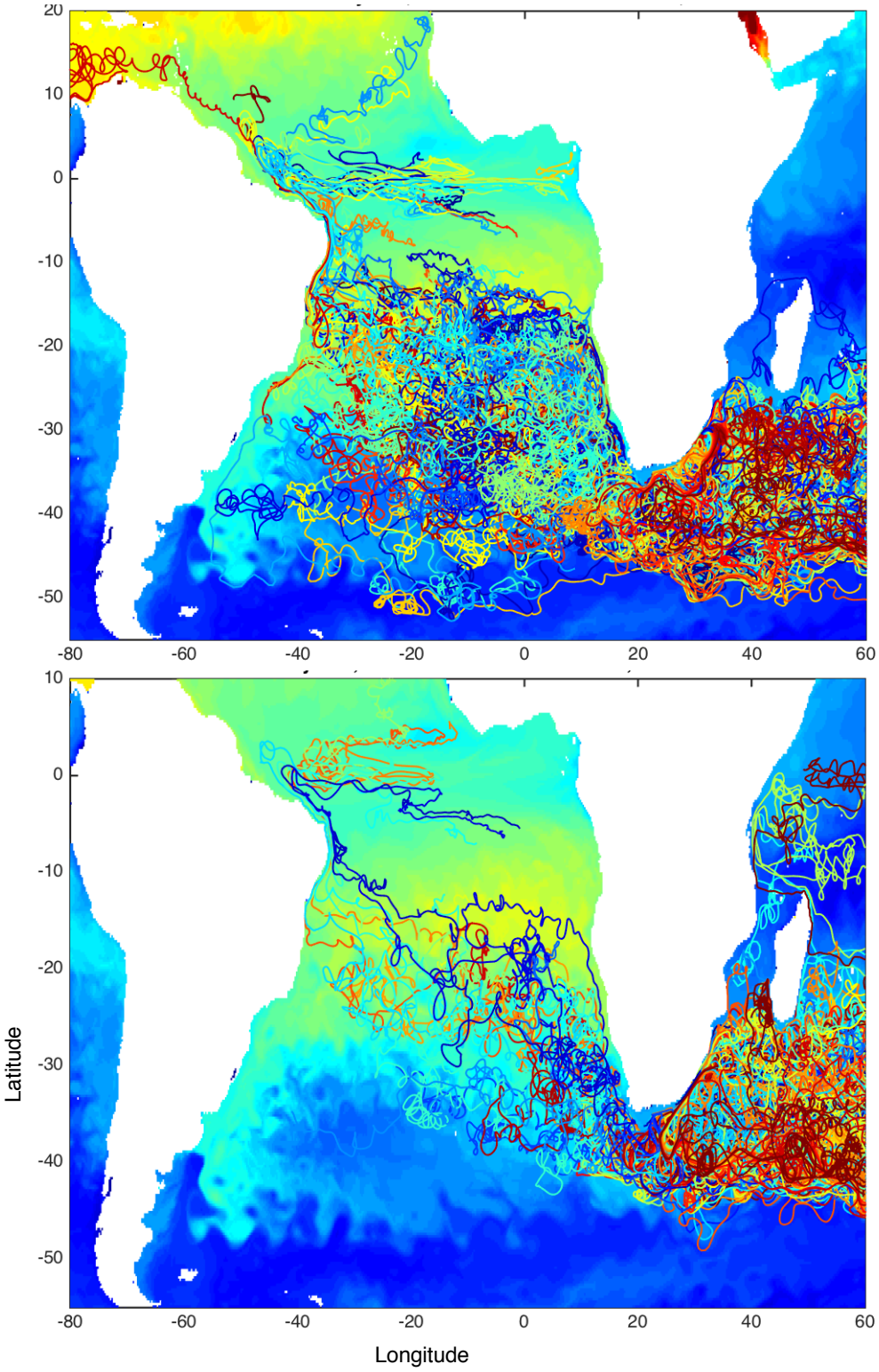

Figure 5.3 The paths of particles released in the northward perturbation simulation (bottom) and control simulation (top); paths for 10 years of particle motion, all released 20 years after the start of the applied perturbation.

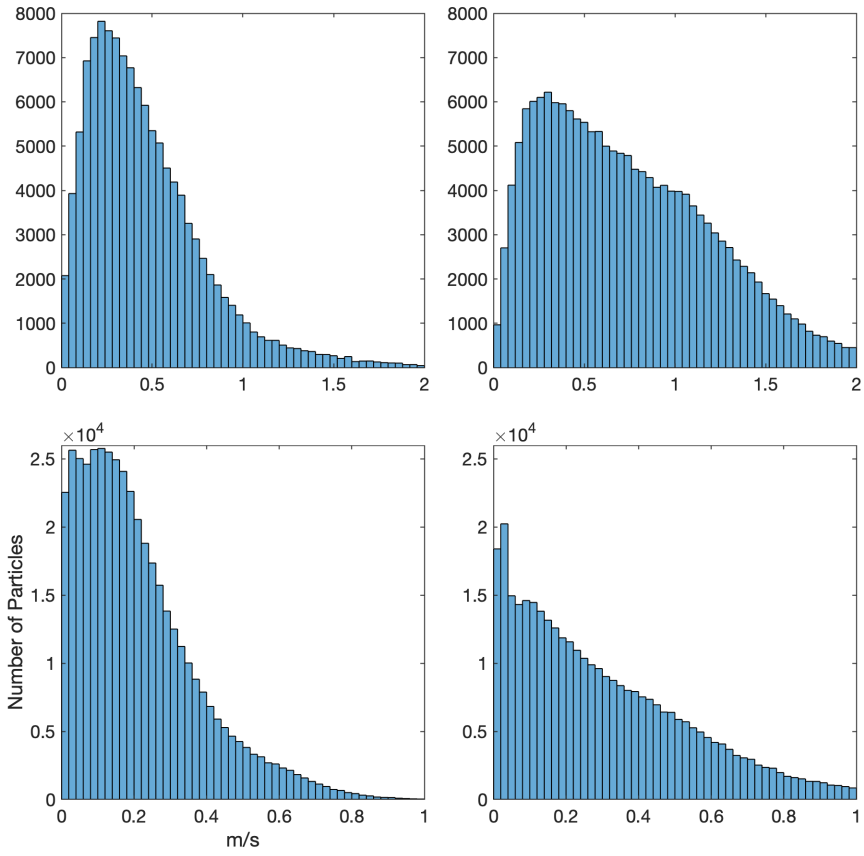

Figure 5.4 Histograms of particle speed in the Agulhas retroflection region (18–28°E, 35–41°S),. Histograms on the left are from the control simulation, histograms on the right are from the northward wind perturbation. Top, shallowest layer of particles (55 m); bottom, deepest layer of particles (722 m)

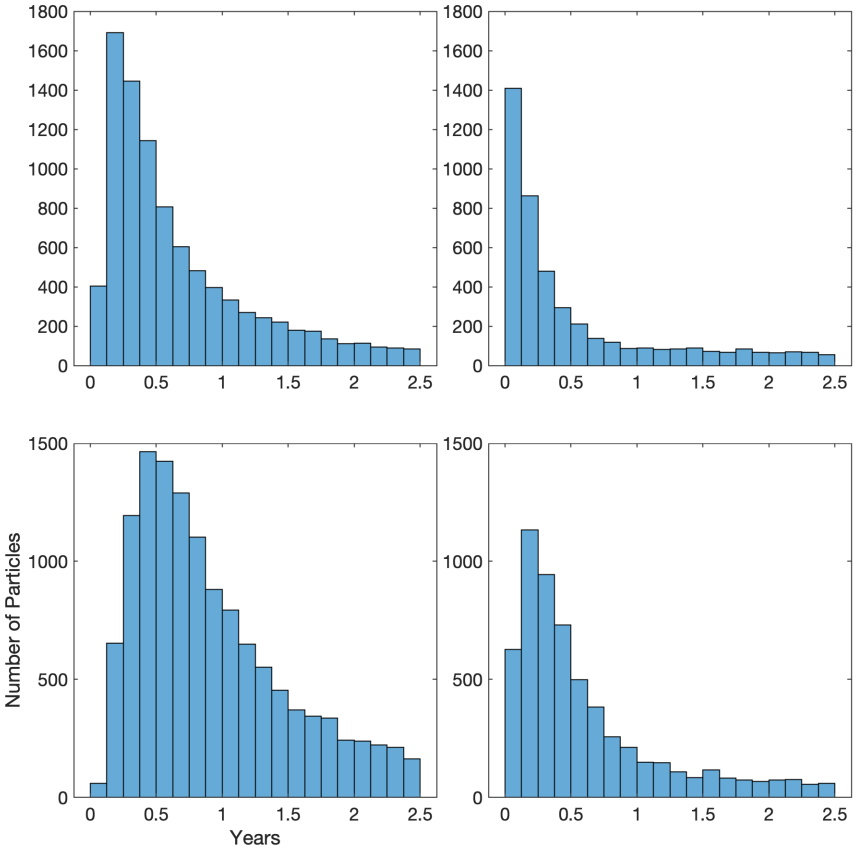

Figure 5.5 Histogram of time for particles to travel from the particle release site to the Agulhas Leakage cross-section (shown in Figure 5.1)by particle ocean depth. The two deepest levels(350 and 722 m) are shown on the lower plots, the two uppermost) levels (55 and 172 m) are shown on the upper plots. Histograms on the left show the control. Histograms on the left control simulation, the northward wind perturbation is shown on the right. Histograms are of particles released 40–50 model-years after the start of the wind perturbation experiment.

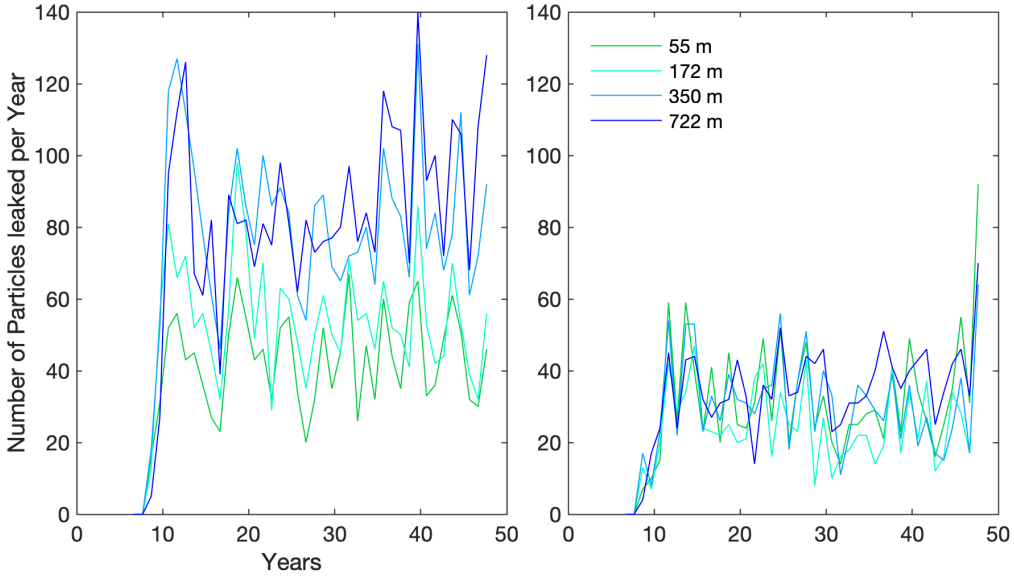

Figure 5.7 The number of particles that leak per year, crossing the section shown in Figure 5 1 by depth level; control simulation is on the left, northward wind perturbation is on the right. Model-years since the start of the spin-up initialization shown on the x-axis

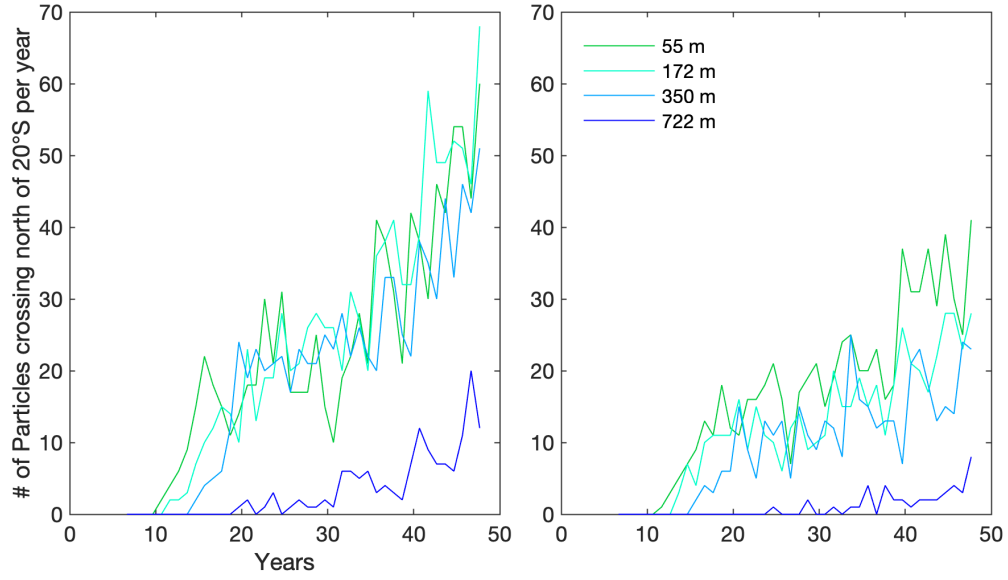

Figure 5.6 The number of particles that cross into the tropical South Atlantic (reaching north of 20°S) by depth level. The control simulation is on the left, northward wind perturbation is on right. Model-years since the start of the spin-up initialization are shown on the x-axis.

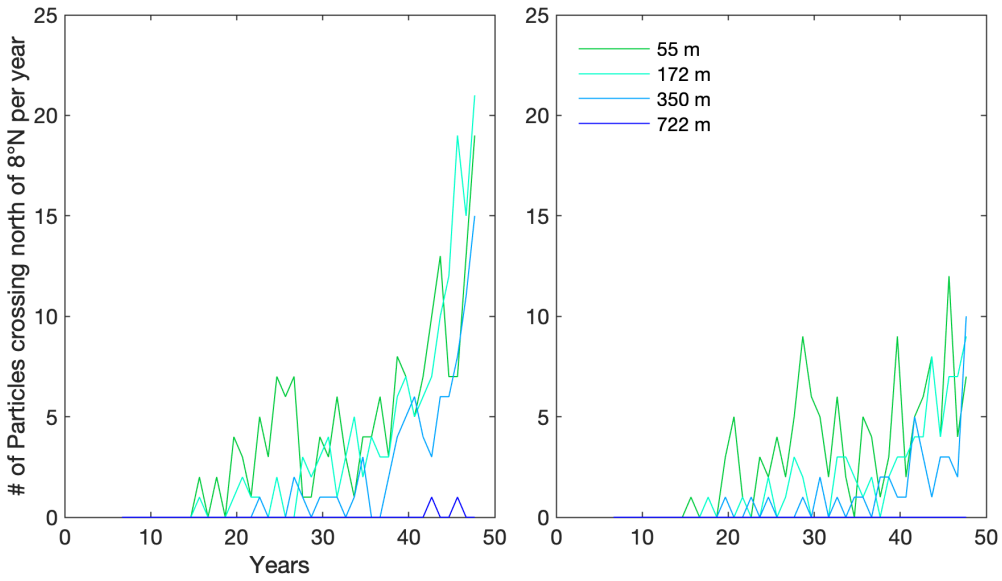

Figure 5.8 The number of particles that cross into the North Atlantic (north of 8°N) by depth level. The control simulation is on the left, the northward wind perturbation is on the right. Model-years since the start of the spin-up initialization shown are on the x-axis

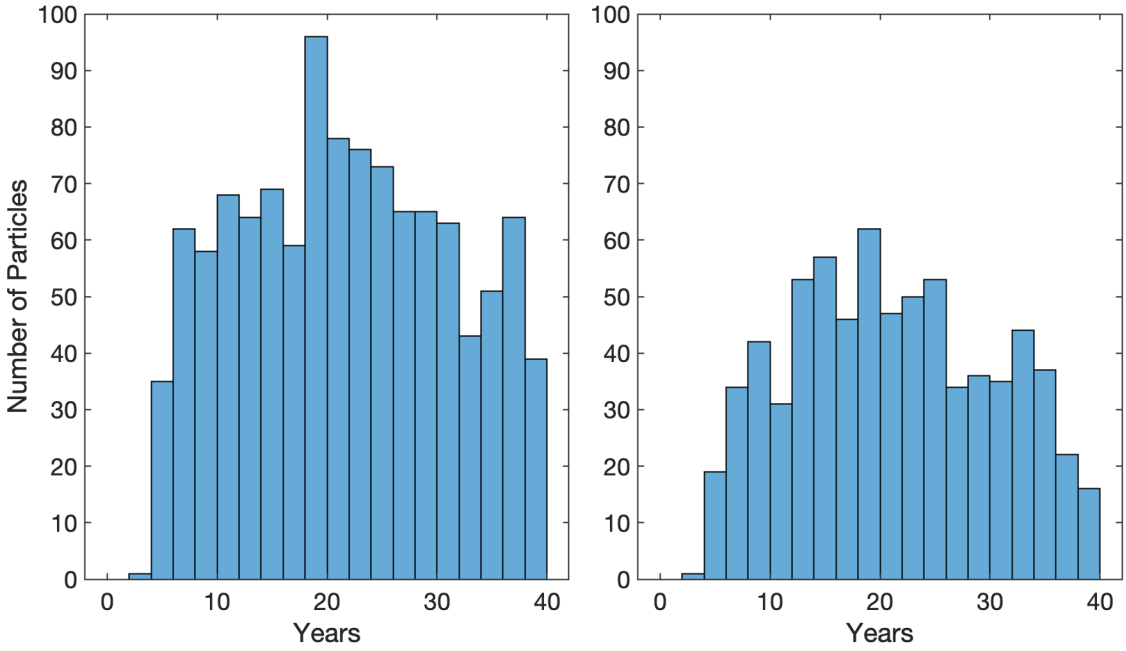

Figure 5.9 Histogram of time for particles to reach the North Atlantic after release, only of particles that reach the North Atlantic; control (left), north perturbation (right)

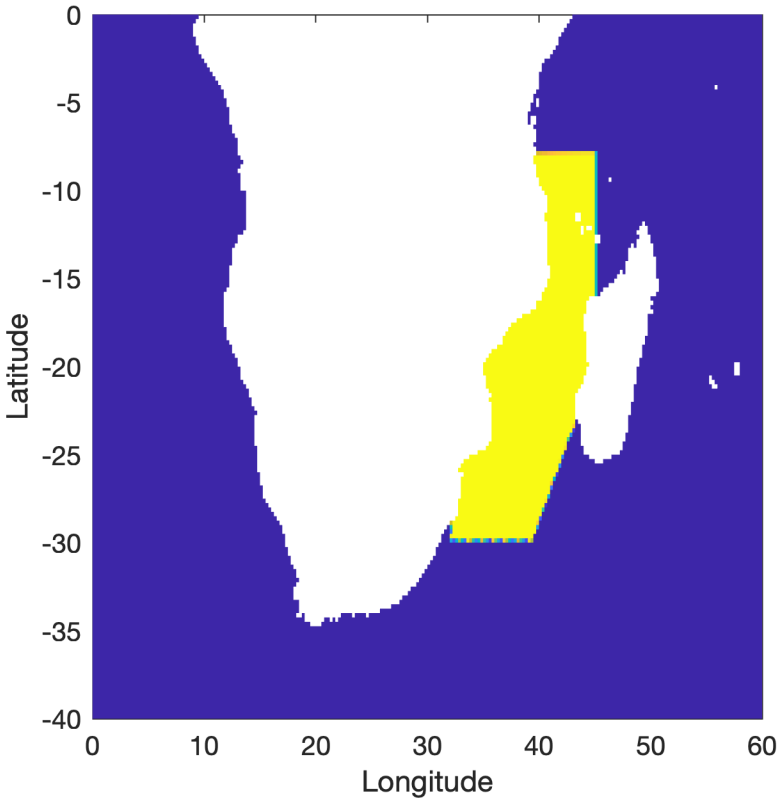

Figure 5.10 Region "Agulhas Current-only" tracer was initialized in tracer experiments 1 and 3. The ocean tagged as tracer water at the initial start of the experiment is colored in yellow; untagged water; dark blue.

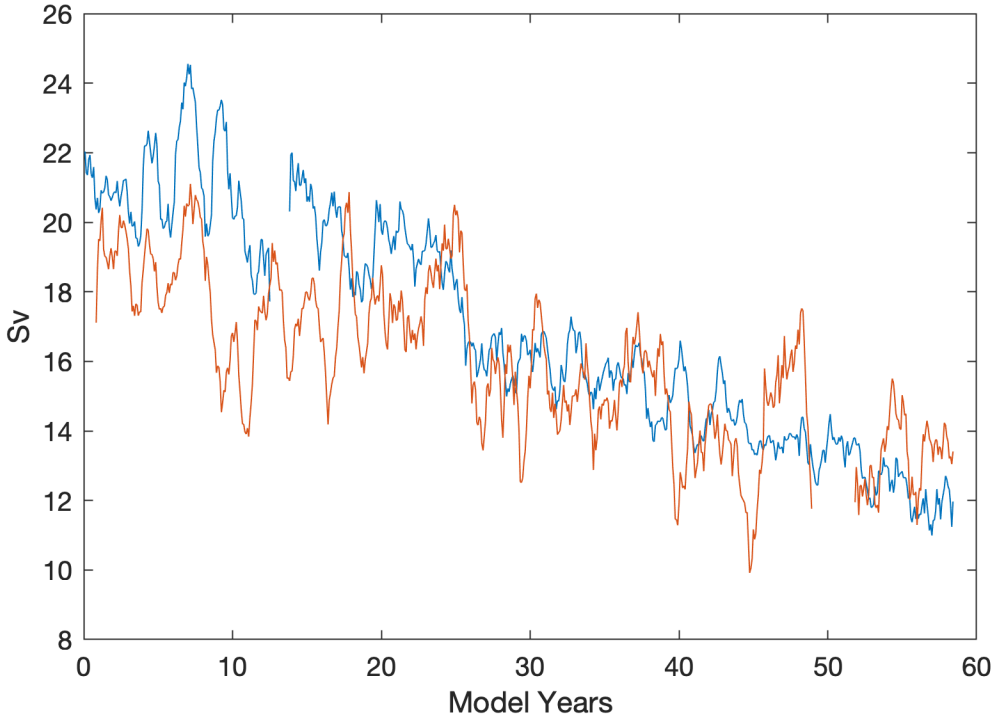

Figure 5.11 The amount of tracer-derived Agulhas Leakage water from the tracer release experiment initialized immediately before the start of the perturbation experiment. Blue is the control simulation, red is the northward wind perturbation simulation. A slow decline in the measurement occurs due to ocean saturation (see text). X-axis is time since start of perturbation experiment. Leakage is smoothed with a 12 month window.

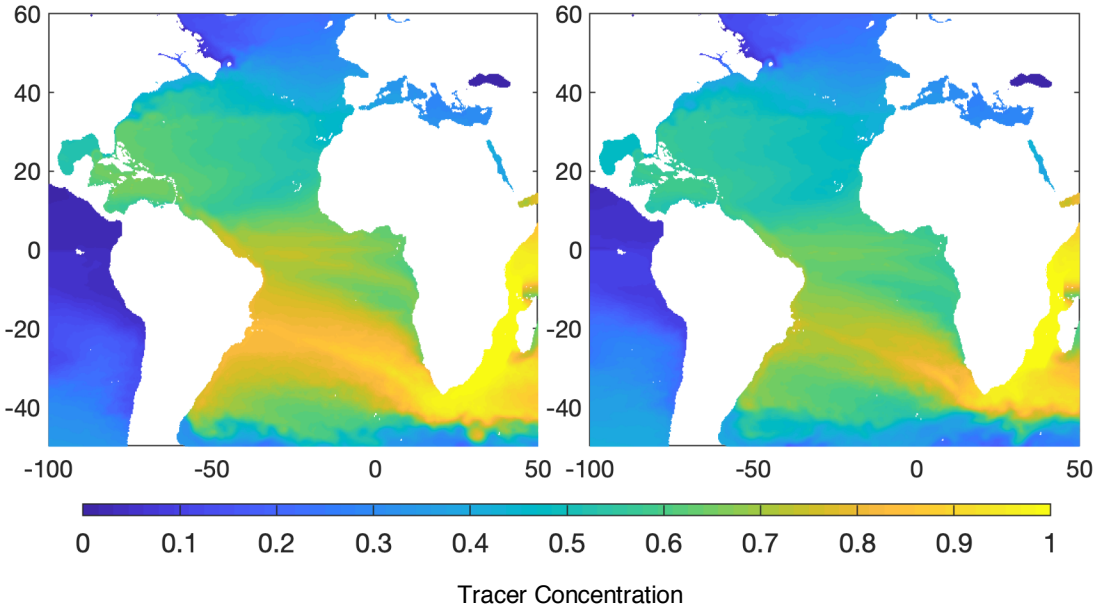

Figure 5.12 Tracer concentration after 10 model-years (2-year average) after the start of the second tracer experiment. Control, left; perturbation, right.

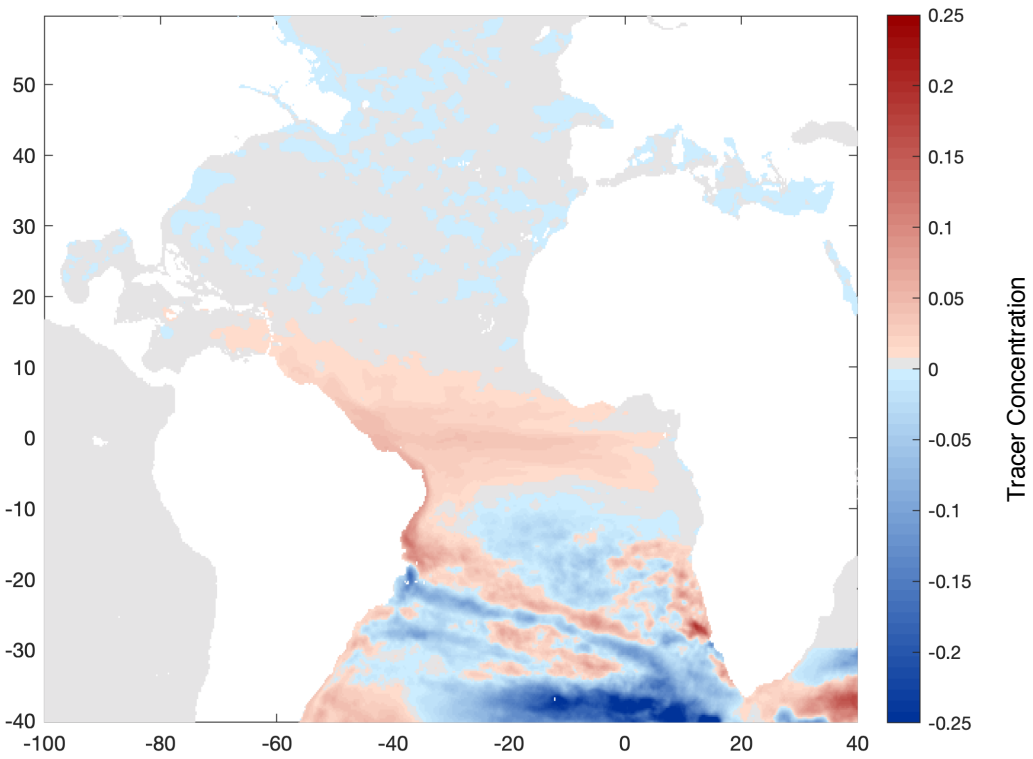

Figure 5.13 Tracer concentration difference between the north wind perturbation experiment and the model control, averaged model years 5–7 after the initialization of the first tracer experiment.

Note the first tracer experiment was initialized 2 years prior to the initialization of the perturbation experiment, so the above concentration map is 3–5 after the start of the perturbation experiment

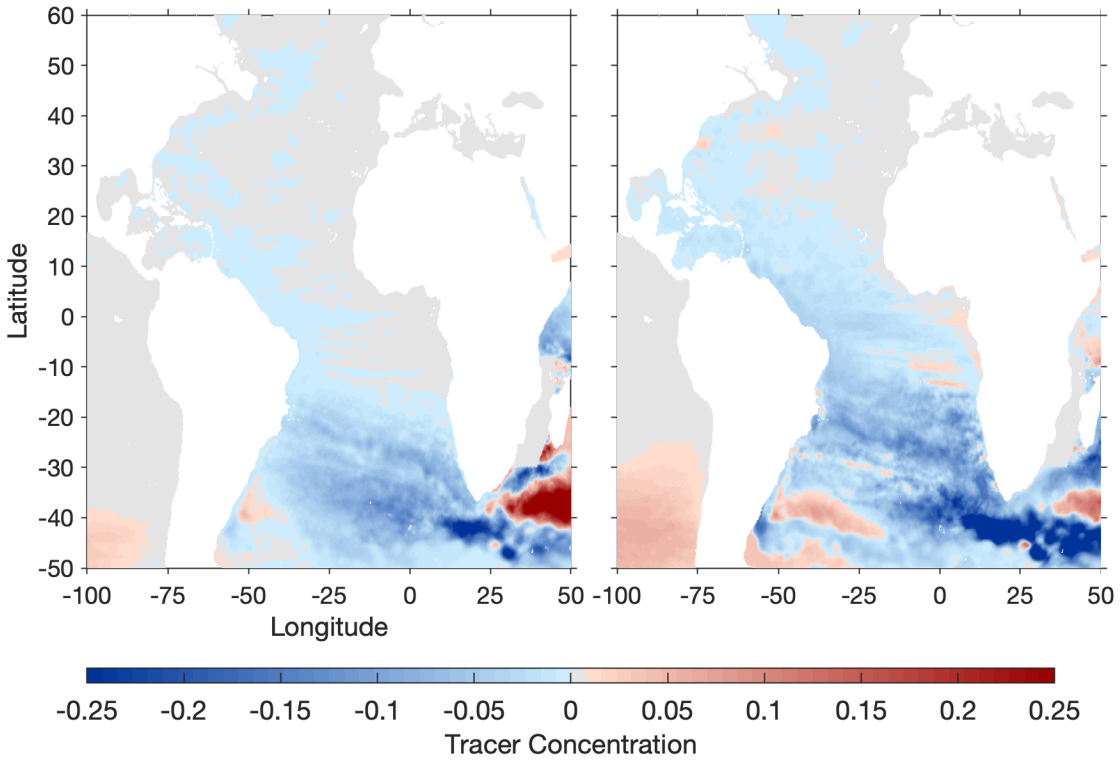

Figure 5.14 Tracer difference between the northward wind perturbation and the control, 9-11 model-years after the start of the second tracer experiment (47 model-years after the start of the north-wind perturbation experiment). Left plot is the tracer difference in depth averaged over the upper 222 m of ocean; right plot is the tracer difference depth-averaged over 222–1100 m

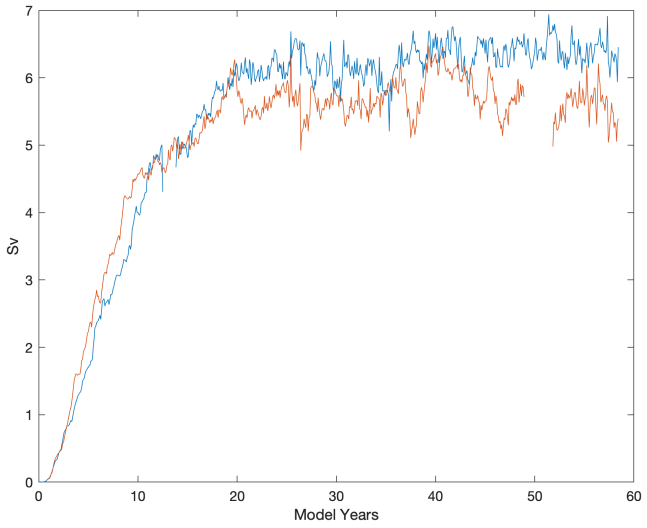

Figure 5.15 amount of Agulhas tagged water entering the North Atlantic (crossing 8°N) in Sverdrups in the first experiment; blue is control, red in northward wind perturbation. The x-axis is the time in model-years since the start of the perturbation experiment. Leakage is smoothed with a 12-month window.

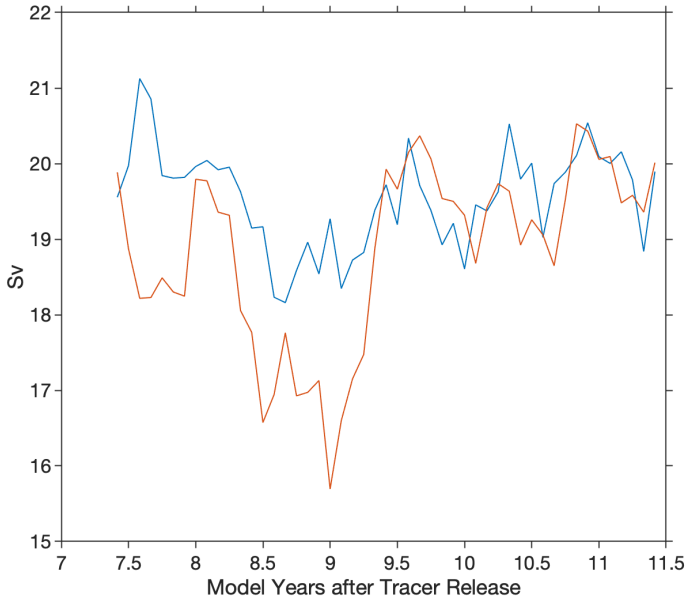

Figure 5.16 Agulhas Leakage rate in Sverdrups from the tracer experiment initialized 47 model years after the start of northward wind perturbation experiment; blue is the control, red is the north wind perturbation. The x-axis shows the time in model-years since the start of tracer release experiment, the leakage rate is shown on the y-axis. Agulhas leakage rate is smoothed with a 12-month window.

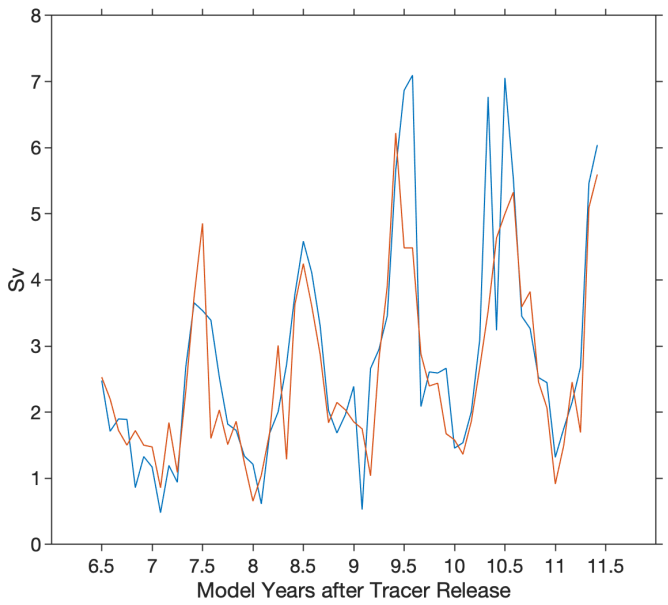

Figure 5.17 The rate of Agulhas Leakage entering the North Atlantic in Sverdrups from the second tracer experiment, which is initialized 47 model years after the start of perturbation experiment; blue is the control, red is the north wind perturbation simulation. The x-axis shows the time in model-years the since start of this tracer release experiment and the leakage rate is shown on the y-axis.

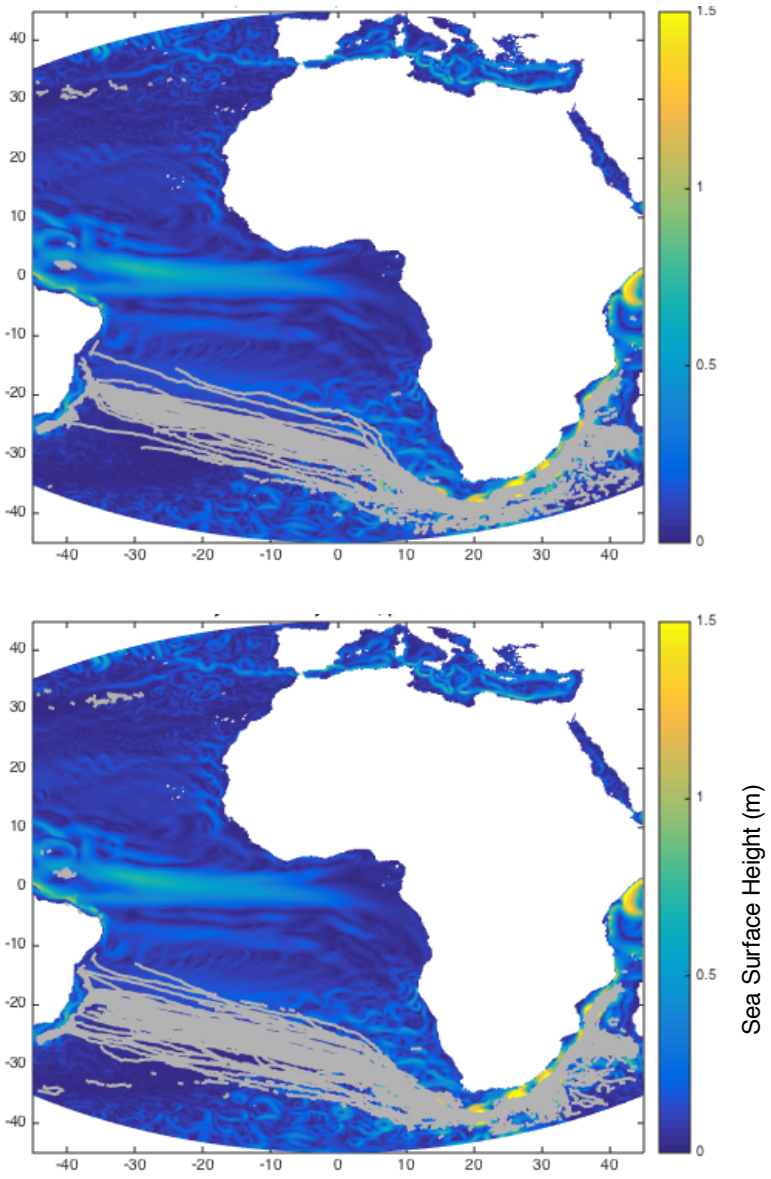

Figure 5.18 The paths of all eddies in the control experiment (top) and northward wind perturbation experiment (bottom) over 14 model-years. The eddy paths are shown as gray line overlying a colored map of sea surface height in m.

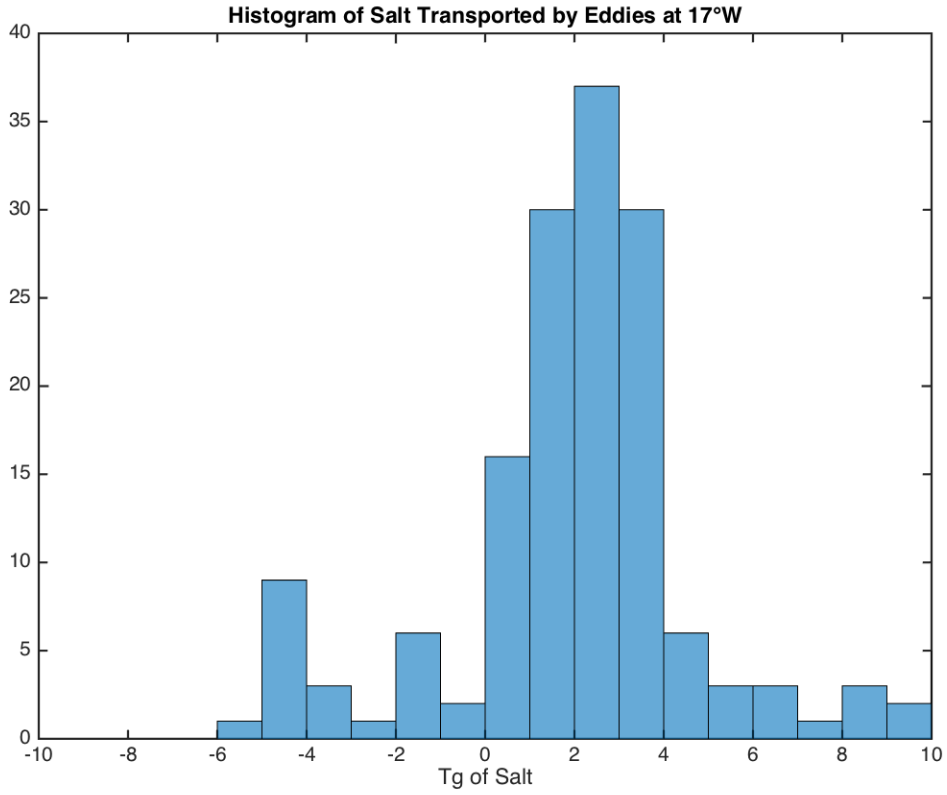

Figure 5.19 Histogram of the salinity excess of Agulhas-sourced eddies in the control simulation that go west of 17°W. Total salt eddy excess is calculated by subtracting the salinity of the eddy at 17°W by the regional average for its depth, then totaling over the entire volume of the eddy. Histogram counts number of eddies binned by salt excess.

CHAPTER 6

CONCLUSIONS AND OUTLOOK

In my experiment, I analyzed the resulting ocean flow in response to a northward shift in the southern westerlies on the backdrop of a modeled Pliocene ocean. The ocean response to changes in the overlying wind field was analyzed with techniques developed specifically to measure the Agulhas Leakage in a high-resolution ocean model. The goal of this modeling experiment was to determine whether a northward shift in the southern westerlies in the Pliocene would alter North Atlantic Deep (NADW) water formation via Agulhas Leakage changes. A decrease NADW weakens the AMOC and the global southern to northern oceanic hemispheric heat transport. To answer this question, it was broken down into two separate hypotheses:

1. The northward shift in southern westerlies at the end of the Pliocene results in a significant decrease in Agulhas Leakage volume

2. This decrease in Agulhas Leakage volume results in a slowdown of the AMOC

With a spin-up model time of 17.5 years followed by a relatively short 58 model years of simulation time with the developed Agulhas Leakage measurement techniques, there was a clear response in Agulhas Leakage volume, confirming (1). The upper level ocean had a response throughout the North Atlantic, but conclusions regarding the slower deep ocean and the meridional overturning response remain equivocal.

Underlying model biases, relatively small changes as well as insufficient modeling time for the deep ocean made interpreting the deep ocean response difficult. The medium resolution CCSM4 GCM used to initialize and force the offline, high resolution MITgcm ocean model simulations has a large salinity bias in the simulation of the modern ocean and a reduced Indian-to-Atlantic Ocean salinity contrast (Figure 3.2). As a result, the direct effects of southern Westerly wind changes on far-field changes in North Atlantic ocean stratification, stability and deep water production are difficult to diagnose directly. Nonetheless, changes in water mass and ocean properties are clearly seen in response to my prescribed northward shift on the southern westerlies. While the magnitude of the ocean property changes (mainly salinity) were biased, the observed changes do demonstrate the potential for Agulhas Leakages changes to alter the North Atlantic, and possibly the Atlantic Meridional Overturning Circulation (AMOC), and Northern Hemisphere climate. A small trend in AMOC weakening (~5%) is seen in the model, however the changes in the AMOC presented here are inconclusive, in part due to the relatively short duration of the model integration.

The Agulhas Leakage measurements do confirm that a shift in the southern westerlies affected the Agulhas Leakage volume, a substantial fraction of which reaches the North Atlantic. The amount reaching the North Atlantic was much higher when estimated by diffusive measures rather than Lagrangian (particle-based) techniques that tracked water transport directly. However, the change in water mass volume reaching the North Atlantic between the perturbation and control experiments was much smaller in the diffusive measures than the particle-based measures. Few Agulhas Leakage particles reached the North Atlantic, and none reached the sites of deep-water formation in the North Atlantic.

However, diffusive measures show a substantial volume of Agulhas Leakage reached the high-latitude North Atlantic, demonstrating that the Agulhas system is able to influence the North Atlantic indirectly.

In addition to the direct Agulhas impacts, there is a significant alteration of North Atlantic salinity and heat content in the model experiment with the northward wind perturbation experiment. While it is difficult to attribute these changes to the Agulhas Leakage, given the only ocean forcing changes downstream are in the South Atlantic, an Agulhas-related forcing is highly likely due to the accompanied changes in water mass properties. Both the timing and spatial pattern of the ocean's response to the northward wind shift demonstrated by diffusive ocean tracers of Agulhas Leakage water correlates with North Atlantic salinity changes, further validating the influence of the Agulhas on the North Atlantic. The correlation has some discrepancies, suggesting dynamical effects are playing an additional role. For example, changes in North Atlantic water properties preceded major changes in Agulhas tracer concentration in the same region. While tracer concentration in the North Atlantic steadily increased after the wind perturbation, the salinity difference in the North Atlantic followed a rather different trend; starting relatively quickly only 10 years after the perturbation, and then becoming much larger 30 years after the perturbation. The entire North Atlantic also adjusted quite quickly to the southern westerly wind change.

Agulhas-tagged passive tracer water reaching the North Atlantic (north of 8°N) was reduced by ~1 Sv in response to the northward shift of the Southern Westerlies. Agulhas sourced eddies in the South Atlantic are more saline than their surroundings, those

entering the South Atlantic vary in their salinity, but they average ~0.1 psu more saline than the surrounding waters. Assuming the eddy salinity excess of 0.1 psu reflects the Agulhas water reaching the South Atlantic, an 1 Sv reduction of Agulhas waters would result in a decrease of 0.1 psu*1 Sv reduction in salt flux into the North Atlantic. However, this may be a large underestimate, due to the salinity bias in the CCSM4.

Only a small (~5%) change in the AMOC was observed (Figure 4.13), both the northward perturbation and the control has a mean AMOC of 20 Sv**.** Both the perturbation and control were run for 58 model years, which is short compared to many other studies using coarse-resolution models that do not resolve the eddies being quantified here. The small impact on the AMOC was not completely unexpected as there was insufficient time for the deep ocean to approach equilibrium ($10^{2\text{-}3}$ years). The model salinity bias is also a factor in the lack of an AMOC response. However, there was a small but significant change in the northward transport of the near surface layers and in North Atlantic mixed-layer thickness. Some previous work has found an AMOC response to a perturbation on similarly short model timescales. For example, Gent and Danabasoglu (2011) found a southern hemisphere response to increased wind stress in less than 100 years using the CCSM4, Delworth and Zhang (2008) found a response with a much coarser resolution (2°) ocean model. Within 50 model years, Biastoch and Böning (2013) and Durgadoo et al. (2013) found small changes in the upper branch of the Atlantic AMOC with an alteration of the southern westerlies via the Agulhas Leakage. However, their model domain did not extend northward of 20°N, so they could not measure changes in the North Atlantic sinking sites.

To investigate high latitude impacts on the AMOC that may only be visible after a much longer integration time, a coarser-resolution simulation would be needed to be computationally practical to run. To continue the simulation for a longer model time, the last output from my high-resolution experiment could be re-gridded to a lower, coarser resolution. As mentioned, similar coarse-resolution experiments have been performed on a modern ocean. With the present results, I am unable to verify the hypothesis of McKay (2012), that a northward shift in the southern westerlies caused a slowdown in the AMOC and Northern Hemispheric cooling via the Agulhas Leakage. However, the fast response of the upper ocean to the wind experiment offers compelling evidence that the Agulhas Leakage and North Atlantic are strongly linked.

Despite the lack of a significant change in the AMOC in the model simulations presented here, the results do demonstrate that there is a direct connection between the Agulhas Leakage and the subpolar North Atlantic. While the model experiments show there is a connection between Southern Westerly changes and the North Atlantic, quantifying the potential for these changes to perturb the AMOC remains difficult. Multiple lines of evidence indicate there is a significant oceanic teleconnection between the Indian Ocean and North Atlantic. Southern hemisphere salt anomalies are clearly being imported to the North Atlantic via the Agulhas Leakage, and small changes in the northward Atlantic transport (upper limb of the AMOC), were found in my simulations, similar to those seen in (Biastoch et al., 2015). However, the changes are small, and it is unclear if they are statistically or climatically meaningful.

The regions where most sinking occurs in the North Atlantic, mainly the Greenland

Icelandic Nordic Sea Region, respond to the northward wind perturbation by becoming more stratified during the season deep water is usually formed. The perturbation experiment does shows a decrease in Agulhas tagged tracer water over the North Atlantic sinking sites.

These Pliocene ocean simulations are the first to be created at such a high spatial resolution. Regions of model disagreement or agreement with observed paleooceanographic proxy data could help indicate which regions of the Pliocene are well understood and where further research would be helpful. Unfortunately, there is limited paleooceanographic proxy evidence in the vicinity of the Agulhas retroflection of the late Pliocene. Most paleoceanographic data are from the Benguela Upwelling region. Petrick et al. (2015) and Karas et al. (2011) found much stronger upwelling in the Pliocene than modern. Petrick et al. (2015) found little cooling in the southern Benguela Upwelling region during the late Pliocene, while Karas et al. (2011) found a change further north. Comparing model and observationally derived temperatures is difficult because of model biases and ongoing uncertainties in proxy temperature reconstructions (Haywood et al., 2016). However, the modeled sea surface changes do demonstrate the northward wind perturbation resulted in the Agulhas Leakage becoming constricted, rather than shifting north to affect the Benguela region. This may confirm the changes seen by Petrick et al. (2015).

Comparing my results to global Pliocene temperature reconstructions such as from as the PRISM dataset (Dowsett et al., 2012), is difficult and would not be ideal, because PRISM represents a particular time slice in the Pliocene (the warm mid-Pliocene). Instead, this

study is focused on the cooling phase at the end of the Pliocene, when only a limited number of proxy studies are available. Furthermore, most Pliocene proxy-based temperature reconstructions average data over a large time interval, much of the PRISM dataset uses time slice of 240,000 years (Dowsett et al., 2012; Haywood et al., 2013), which would preclude most of the cooling trend.

Any additional proxy reconstructions of the late Pliocene, particularly both in the South Atlantic and North Atlantic near deep water formation site changes would be helpful in confirming the changes simulated here. Observations with the potential to confirm a correlation between decreased deep-water formation in the North Atlantic and reduced Agulhas Leakage would be especially helpful for comparing with the model results presented here. As mentioned above, simulating changes in the AMOC requires hundreds of years of model time, an order of magnitude longer than the simulations presented here. Continuing the wind perturbation experiment would certainly help ascertain whether there is any additional AMOC responses and whether the small response already observed is non-transient. With the enormous computational cost of high-resolution modeling, an extension experiment would need to be much lower resolution to cover hundreds of model-years. The purpose of using a high-resolution ocean model was to accurately capture the eddies and filaments of the Agulhas Leakage; coarse-resolution models are unable to accurately model the dynamics of the Agulhas Leakage. In a subsequent coarse-resolution follow-up, the area of interest is in changes in North Atlantic Deep Water and the Atlantic-basin wide circulation rather than changes in the Agulhas Leakage. Once the Agulhas Leakage has reached equilibrium from the wind shift, a coarse resolution parameterization, could be implemented from the high-

resolution results, so the coarse resolution has the correct leakage impacts that are entering the Atlantic Ocean.

By both my Lagrangian and Eulerian measures demonstrate that the Agulhas Leakage has reached an equilibrium by the end of the 17 year spin up period. Recent work including by Durgadoo et al. (2013) and Biastoch and Böning (2013) also found the Agulhas Leakage reached equilibrium within 50 model-years, so the length of my high-resolution experiment should be sufficient. Similar to their work, I have shown the Agulhas Leakage responded to shifts in the southern westerlies. However, unlike Durgadoo et al. (2013), my Agulhas Leakage response is not transient and there is no recovery towards the pre-shift state. This is either from differing models or because I applied a large northward wind perturbation. It is possible that a 6° northward wind perturbation has a longer last-lasting impact than simply changes in strength or southward shifts in the westerlies, as applied in other studies.

I have shown a northward wind perturbation of the southern westerlies results in a significant slowdown of the Agulhas Leakage and subsequent decrease in salt input into the South Atlantic. While we do see a significant change in North Atlantic vertical mixing, we are unable to ascertain if there were resulting changes in the AMOC due to model salinity biases and insufficient modeling time.

REFERENCES

Arzel, Olivier, Matthew H. England, and Willem P. Sijp. 2008. "Reduced Stability of the Atlantic Meridional Overturning Circulation Due to Wind Stress Feedback during Glacial Times." *Journal of Climate* 21 (23): 6260–82. https://doi.org/10.1175/2008JCLI2291.1.

Bailey, Ian, Georgia M. Hole, Gavin L. Foster, Paul A. Wilson, Craig D. Storey, Clive N. Trueman, and Maureen E. Raymo. 2013. "An Alternative Suggestion for the Pliocene Onset of Major Northern Hemisphere Glaciation Based on the Geochemical Provenance of North Atlantic Ocean Ice-Rafted Debris." *Quaternary Science Reviews* 75: 181–94. https://doi.org/10.1016/j.quascirev.2013.06.004.

Bard, Edouard, and Rosalind E.M. Rickaby. 2009. "Migration of the Subtropical Front as a Modulator of Glacial Climate." *Nature* 460 (7253): 380–83. https://doi.org/10.1038/nature08189.

Beal, Lisa M., and Harry L. Bryden. 1999. "The Velocity and Vorticity Structure of the Agulhas Current at 32°S." *Journal of Geophysical Research: Oceans* 104 (C3): 5151–76. https://doi.org/10.1029/1998jc900056.

Beal, Lisa M., Wilhelmus P.M. De Ruijter, Arne Biastoch, Rainer Zahn, Meghan Cronin, Juliet Hermes, Johann Lutjeharms, et al., 2011. "On the Role of the Agulhas System in Ocean Circulation and Climate." *Nature* 472 (7344): 429–36. https://doi.org/10.1038/nature09983.

Biastoch, A., L. M. Beal, J. R. E. Lutjeharms, and T. G. D. Casal. 2009. "Variability and Coherence of the Agulhas Undercurrent in a High-Resolution Ocean General Circulation Model." *Journal of Physical Oceanography* 39 (10): 2417–35. https://doi.org/10.1175/2009jpo4184.1.

Biastoch, Arne, and Claus W. Böning. 2013. "Anthropogenic Impact on Agulhas Leakage." *Geophysical Research Letters* 40 (6): 1138–43. https://doi.org/10.1002/grl.50243.

Biastoch, Arne, Jonathan V. Durgadoo, Adele K. Morrison, Erik Van Sebille, Wilbert Weijer, and Stephen M. Griffies. 2015. "Atlantic Multi-Decadal Oscillation Covaries with Agulhas Leakage." *Nature Communications* 6: 1–7. https://doi.org/10.1038/ncomms10082.

Bishop, Stuart P., Peter R. Gent, Frank O. Bryan, Andrew F. Thompson, Matthew C. Long, and Ryan Abernathey. 2016. "Southern Ocean Overturning Compensation in an Eddy-Resolving Climate Simulation." *Journal of Physical Oceanography* 46 (5): 1575–92. https://doi.org/10.1175/JPO-D-15-0177.1.

Boer, A. M. de, J. R. Toggweiler, and D. M. Sigman. 2008. "Atlantic Dominance of the Meridional Overturning Circulation." *Journal of Physical Oceanography* 38 (2): 435–50. https://doi.org/10.1175/2007jpo3731.1.

Boer, Agatha M. De, Robert M. Graham, Matthew D. Thomas, and Karen E. Kohfeld. 2013. “The Control of the Southern Hemisphere Westerlies on the Position of the Subtropical Front.” *Journal of Geophysical Research: Oceans* 118 (10): 5669–75. https://doi.org/10.1002/jgrc.20407.

Boyer Montégut, Clément de, Gurvan Madec, Albert S. Fischer, Alban Lazar, and Daniele Iudicone. 2004. “Mixed Layer Depth over the Global Ocean: An Examination of Profile Data and a Profile-Based Climatology.” *Journal of Geophysical Research C: Oceans* 109 (12): 1–20. https://doi.org/10.1029/2004JC002378.

Bragg, F. J., D. J. Lunt, and A. M. Haywood. 2012. “Mid-Pliocene Climate Modelled Using the UK Hadley Centre Model: PlioMIP Experiments 1 and 2.” *Geoscientific Model Development* 5 (5): 1109–25. https://doi.org/10.5194/gmd-5-1109-2012.

Brierley, Christopher M., and Alexey V. Fedorov. 2010. “Relative Importance of Meridional and Zonal Sea Surface Temperature Gradients for the Onset of the Ice Ages and Pliocene-Pleistocene Climate Evolution.” *Paleoceanography* 25 (2): 1–16. https://doi.org/10.1029/2009PA001809.

Brummer, Geert-Jan A., Ralph R. Schneider, Gerald M. Ganssen, Wilhelmus P. M. de Ruijter, Frank J. C. Peeters, Dick Kroon, Els Ufkes, and Ruth Acheson. 2004. “Vigorous Exchange between the Indian and Atlantic Oceans at the End of the Past Five Glacial Periods.” *Nature* 430 (7000): 661–65. https://doi.org/10.1038/nature02785.

Buckley, Martha W, and John Marshall. 2015. “Circulation : A Review.” *Reviews of Geophysics* 54: 5–63. https://doi.org/10.1002/2015RG000493.Received.

Burke, K D, J W Williams, M A Chandler, A M Haywood, D J Lunt, and B L Otto-bliesner. 2018. “Pliocene and Eocene Provide Best Analogs for Near- Future Climates” 115 (52). https://doi.org/10.1073/pnas.1809600115.

Caley, Thibaut, Jacques Giraudeau, Bruno Malaizé, Linda Rossignol, and Catherine Pierre. 2012. “Agulhas Leakage as a Key Process in the Modes of Quaternary Climate Changes” 109 (18). https://doi.org/10.1073/pnas.1115545109.

Caley, Thibaut, Frank J.C. Peeters, Arne Biastoch, Linda Rossignol, Erik Van Sebille, Jonathan Durgadoo, Bruno Malaizé, Jacques Giraudeau, Kristina Arthur, and Rainer Zahn. 2014. “Quantitative Estimate of the Paleo-Agulhas Leakage.” *Geophysical Research Letters* 41 (4): 1238–46. https://doi.org/10.1002/2014GL059278.

Castellanos, Paola, E. J.D. Campos, J. Piera, O. T. Sato, and M. A.F. Silva Dias. 2017. “Impacts of Agulhas Leakage on the Tropical Atlantic Western Boundary Systems.” *Journal of Climate* 30 (17): 6645–59. https://doi.org/10.1175/JCLI-D-15-0878.1.

Chavaillaz, Y., F. Codron, and M. Kageyama. 2013. “Southern Westerlies in LGM and Future (RCP4.5) Climates.” *Climate of the Past* 9 (2): 517–24. https://doi.org/10.5194/cp-9-517-2013.

Cheng, Yu, Dian Putrasahan, Lisa Beal, and Ben Kirtman. 2016. “Quantifying Agulhas Leakage in a High-Resolution Climate Model.” *Journal of Climate* 29 (19): 6881–92. https://doi.org/10.1175/JCLI-D-15-0568.1.

Condron, Alan, and Peter Winsor. 2012. “Meltwater Routing and the Younger Dryas” 109 (49): 1–6. https://doi.org/10.1073/pnas.1207381109.

Cunningham, Stuart A., and Robert Marsh. 2010. “Observing and Modeling Changes in the Atlantic MOC.” *Wiley Interdisciplinary Reviews: Climate Change* 1 (2): 180–91. https://doi.org/10.1002/wcc.22.

Danabasoglu, Gokhan, Susan C. Bates, Bruce P. Briegleb, Steven R. Jayne, Markus Jochum, William G. Large, Synte Peacock, and Steve G. Yeager. 2012. “The CCSM4 Ocean Component.” *Journal of Climate* 25 (5): 1361–89. https://doi.org/10.1175/JCLI-D-11-00091.1.

Dekens, Petra S., Ana Christina Ravelo, and Matthew D. McCarthy. 2007. “Warm Upwelling Regions in the Pliocene Warm Period.” *Paleoceanography* 22 (3): 1–12. https://doi.org/10.1029/2006PA001394.

Delworth, Thomas L., and Fanrong Zeng. 2008. “Simulated Impact of Altered Southern Hemisphere Winds on the Atlantic Meridional Overturning Circulation.” *Geophysical Research Letters* 35 (20): 1–5. https://doi.org/10.1029/2008GL035166.

Dencausse, Guillaume, Michel Arhan, and Sabrina Speich. 2010. “Author ’ s Accepted Manuscript Routes of Agulhas Rings in the Southeastern Cape Basin.” *Deep-Sea Research Part I* 57 (11): 1406–21. https://doi.org/10.1016/j.dsr.2010.07.008.

Dowsett Harry J, Robinson Marci M., Stoll Danielle K., Foley Kevin M., Johnson Andrew L A., Williams Mark, and Riesselman Christina R. 2013. “The PRISM (Pliocene Palaeoclimate) Reconstruction: Time for a Paradigm Shift.” *Philosophical Transactions of the Royal Society A: Mathematical, Physical and Engineering Sciences* 371 (2001): 20120524. https://doi.org/10.1098/rsta.2012.0524.

Dowsett, Harry J, Kevin M Foley, Danielle K Stoll, Mark A Chandler, Linda E Sohl, Mats Bentsen, Bette L Otto-Bliesner, et al., 2013. “Sea Surface Temperature of the Mid-Piacenzian Ocean: A Data-Model Comparison.” *Scientific Reports* 3 (June): 2013. https://doi.org/10.1038/srep02013.

Durgadoo, Jonathan V., Benjamin R. Loveday, Chris J. C. Reason, Pierrick Penven, and Arne Biastoch. 2013. “Agulhas Leakage Predominantly Responds to the Southern Hemisphere Westerlies.” *Journal of Physical Oceanography* 43 (10): 2113–31. https://doi.org/10.1175/JPO-D-13-047.1.

Dutton, A., A. E. Carlson, A. J. Long, G. A. Milne, P. U. Clark, R. DeConto, B. P. Horton, S. Rahmstorf, and M. E. Raymo. 2015. “Sea-Level Rise Due to Polar Ice-Sheet Mass Loss during Past Warm Periods.” *Science* 349 (6244). https://doi.org/10.1126/science.aaa4019.

Flores, José Abel, Rainer Gersonde, and F. Javier Sierro. 1999. "Pleistocene Fluctuations in the Agulhas Current Retroflection Based on the Calcareous Plankton Record." *Marine Micropaleontology* 37 (1): 1–22. https://doi.org/10.1016/S0377-8398(99)00012-2.

Franzese, Allison M., Sidney R. Hemming, Steven L. Goldstein, and Robert F. Anderson. 2006. "Reduced Agulhas Leakage during the Last Glacial Maximum Inferred from an Integrated Provenance and Flux Study." *Earth and Planetary Science Letters* 250 (1–2): 72–88. https://doi.org/10.1016/j.epsl.2006.07.002.

Gent, Peter R. 2015. "Effects of Southern Hemisphere Wind Changes on the Meridional Overturning Circulation in Ocean Models." *Annual Review of Marine Science* 8 (1): 79–94. https://doi.org/10.1146/annurev-marine-122414-033929.

Gent, Peter R., and Gokhan Danabasoglu. 2011. "Response to Increasing Southern Hemisphere Winds in CCSM4." *Journal of Climate* 24 (19): 4992–98. https://doi.org/10.1175/JCLI-D-10-05011.1.

Gent, Peter R., Gokhan Danabasoglu, Leo J. Donner, Marika M. Holland, Elizabeth C. Hunke, Steve R. Jayne, David M. Lawrence, et al., 2011. "The Community Climate System Model Version 4." *Journal of Climate* 24 (19): 4973–91. https://doi.org/10.1175/2011JCLI4083.1.

Gordon, Arnold L. 2003. "Oceanography: The Brawniest Retroflection." *Nature* 421 (2): 904–5. https://doi.org/10.1038/421904a.

Haug, Gerald H, Andrey Ganopolski, Daniel M Sigman, Antoni Rosell-Mele, George E A Swann, Ralf Tiedemann, Samuel L Jaccard, et al., 2005. "North Pacific Seasonality and the Glaciation of North America 2.7 Million Years Ago." *Nature* 433 (7028): 821–25. https://doi.org/10.1038/nature03332.

Haywood, A. M., H. J. Dowsett, B. Otto-Bliesner, M. A. Chandler, A. M. Dolan, D. J. Hill, D. J. Lunt, et al., 2010. "Pliocene Model Intercomparison Project (PlioMIP): Experimental Design and Boundary Conditions (Experiment 1)." *Geoscientific Model Development* 3 (1): 227–42. https://doi.org/10.5194/gmd-3-227-2010.

Haywood, A. M., D. J. Hill, A. M. Dolan, B. L. Otto-Bliesner, F. Bragg, W. L. Chan, M. A. Chandler, et al., 2013. "Large-Scale Features of Pliocene Climate: Results from the Pliocene Model Intercomparison Project." *Climate of the Past* 9 (1): 191–209. https://doi.org/10.5194/cp-9-191-2013.

Haywood, Alan M., Harry J. Dowsett, and Aisling M. Dolan. 2016. "Integrating Geological Archives and Climate Models for the Mid-Pliocene Warm Period." *Nature Communications* 7 (May 2015): 1–14. https://doi.org/10.1038/ncomms10646.

Hermes, J. C., C. J.C. Reason, and J. R.E. Lutjeharms. 2007. "Modeling the Variability of the Greater Agulhas Current System." *Journal of Climate* 20 (13): 3131–46. https://doi.org/10.1175/JCLI4154.1.

Heuzé, Céline. 2017. “North Atlantic Deep Water Formation and AMOC in CMIP5 Models.” *Ocean Science* 13 (4): 609–22. https://doi.org/10.5194/os-13-609-2017.

Hill, Daniel J. 2015. “The Non-Analogue Nature of Pliocene Temperature Gradients.” *Earth and Planetary Science Letters* 425: 232–41. https://doi.org/10.1016/j.epsl.2015.05.044.

Hill, Jenna C, and Alan Condron. 2014. “Subtropical Iceberg Scours and Meltwater Routing in the Deglacial Western North Atlantic.” Nature Geoscience 7 (October): 806. https://doi.org/10.1038/ngeo2267.Hogg, Andrew McC., Paul Spence, Oleg A. Saenko, and Stephanie M. Downes. 2016. “The Energetics of Southern Ocean Upwelling.” *Journal of Physical Oceanography* 47 (1): 135–53. https://doi.org/10.1175/jpo-d-16-0176.1.

Jungclaus, J. H., N. Fischer, H. Haak, K. Lohmann, J. Marotzke, D. Matei, U. Mikolajewicz, D. Notz, and J. S. Von Storch. 2013. “Characteristics of the Ocean Simulations in the Max Planck Institute Ocean Model (MPIOM) the Ocean Component of the MPI-Earth System Model.” *Journal of Advances in Modeling Earth Systems* 5 (2): 422–46. https://doi.org/10.1002/jame.20023.

Karas, Cyrus, Dirk Nürnberg, Ralf Tiedemann, and Dieter Garbe-Schönberg. 2011. “Pliocene Indonesian Throughflow and Leeuwin Current Dynamics: Implications for Indian Ocean Polar Heat Flux.” *Paleoceanography* 26 (2). https://doi.org/10.1029/2010PA001949.

Kelly, Kathryn A., Kyla Drushka, Lu Anne Thompson, Dewi Le Bars, and Elaine L. McDonagh. 2016. “Impact of Slowdown of Atlantic Overturning Circulation on Heat and Freshwater Transports.” *Geophysical Research Letters* 43 (14): 7625–31. https://doi.org/10.1002/2016GL069789.

Kemp, A. E.S., I. Grigorov, R. B. Pearce, and A. C. Naveira Garabato. 2010. “Migration of the Antarctic Polar Front through the Mid-Pleistocene Transition: Evidence and Climatic Implications.” Quaternary Science Reviews 29 (17–18): 1993–2009. https://doi.org/10.1016/j.quascirev.2010.04.027. Kohfeld, K E, R M Graham, A M de Boer, L C Sime, E W Wolff, C Le Quéré, and L Bopp. 2013. “Southern Hemisphere Westerly Wind Changes during the Last Glacial Maximum: Paleo-Data Synthesis.” *Quaternary Science Reviews* 68: 76–95. https://doi.org/https://doi.org/10.1016/j.quascirev.2013.01.017.

Kuhlbrodt, T, A Griesel, M Montoya, A Levermann, M Hofmann, and S Rahmstorf. 2007. “On the Driving Processes of the Atlantic Meridional Overturning Circulation.” *Reviews of Geophysics* 45 (2). https://doi.org/10.1029/2004RG000166.

Large, William G., Gokhan Danabasoglu, Scott C. Doney, and James C. McWilliams. 1997. “Sensitivity to Surface Forcing and Boundary Layer Mixing in a Global Ocean Model: Annual-Mean Climatology.” *Journal of Physical Oceanography* 27 (11): 2418–47. https://doi.org/10.1175/1520-0485(1997)027<2418:stsfab>2.0.co;2.

Lee, Shih Yu, John C.H. Chiang, Katsumi Matsumoto, and Kathy S. Tokos. 2011. "Southern Ocean Wind Response to North Atlantic Cooling and the Rise in Atmospheric CO<inf>2</Inf>: Modeling Perspective and Paleoceanographic Implications." *Paleoceanography* 26 (1): 1–16. https://doi.org/10.1029/2010PA002004.

Loveday, B. R., P. Penven, and C. J.C. Reason. 2015. "Southern Annular Mode and Westerly-Wind-Driven Changes in Indian-Atlantic Exchange Mechanisms." *Geophysical Research Letters* 42 (12): 4912–21. https://doi.org/10.1002/2015GL064256.

Loveday, Benjamin R., Jonathan V. Durgadoo, Chris J. C. Reason, Arne Biastoch, and Pierrick Penven. 2014. "Decoupling of the Agulhas Leakage from the Agulhas Current." *Journal of Physical Oceanography* 44 (7): 1776–97. https://doi.org/10.1175/JPO-D-13-093.1.

Lübbecke, Joke F., Jonathan V. Durgadoo, and Arne Biastoch. 2015. "Contribution of Increased Agulhas Leakage to Tropical Atlantic Warming." *Journal of Climate* 28 (24): 9697–9706. https://doi.org/10.1175/JCLI-D-15-0258.1.

Lumpkin, Rick, and Kevin Speer. 2007. "Global Ocean Meridional Overturning." *Journal of Physical Oceanography* 37 (10): 2550–62. https://doi.org/10.1175/jpo3130.1.

Lunt, Daniel J, Alan M Haywood, Gavin A Schmidt, Ulrich Salzmann, Paul J Valdes, and Harry J Dowsett. 2009. "Earth System Sensitivity Inferred from Pliocene Modelling and Data." Nature Geoscience 3 (December): 60. https://doi.org/10.1038/ngeo706.

Marino, Gianluca, Rainer Zahn, Martin Ziegler, Conor Purcell, Gregor Knorr, Ian R. Hall, Patrizia Ziveri, and Henry Elderfield. 2013. "Agulhas Salt-Leakage Oscillations during Abrupt Climate Changes of the Late Pleistocene." *Paleoceanography* 28 (3): 599–606. https://doi.org/10.1002/palo.20038.

McCarthy, G. D., B. A. King, P. Cipollini, E. L. McDonagh, J. R. Blundell, and A. Biastoch. 2012. "On the Sub-Decadal Variability of South Atlantic Antarctic Intermediate Water." *Geophysical Research Letters* 39 (10): 1–5. https://doi.org/10.1029/2012GL051270.

McClymont, Erin L, Antoni Rosell-Melé, Gerald H Haug, and Jerry M Lloyd. 2008. "Expansion of Subarctic Water Masses in the North Atlantic and Pacific Oceans and Implications for Mid-Pleistocene Ice Sheet Growth." *Paleoceanography* 23 (4). https://doi.org/10.1029/2008PA001622.

McKay, R., T. Naish, L. Carter, C. Riesselman, R. Dunbar, C. Sjunneskog, D. Winter, et al., 2012. "Antarctic and Southern Ocean Influences on Late Pliocene Global Cooling." *Proceedings of the National Academy of Sciences* 109 (17): 6423–28. https://doi.org/10.1073/pnas.1112248109.

Meehl, Gerald A, Warren M Washington, Julie M Arblaster, Aixue Hu, Haiyan Teng, Claudia Tebaldi, Benjamin N Sanderson, et al., 2011. "Climate System Response to External Forcings and Climate Change Projections in CCSM4." *Journal of Climate* 25 (11): 3661–83. https://doi.org/10.1175/JCLI-D-11-00240.1.

Meinshausen, Malte, S. J. Smith, K. Calvin, J. S. Daniel, M. L.T. Kainuma, J. Lamarque, K. Matsumoto, et al., 2011. "The RCP Greenhouse Gas Concentrations and Their Extensions from 1765 to 2300." *Climatic Change* 109 (1): 213–41. https://doi.org/10.1007/s10584-011-0156-z.

Miller, Kenneth G., James D. Wright, James V. Browning, Andrew Kulpecz, Michelle Kominz, Tim R. Naish, Benjamin S. Cramer, Yair Rosenthal, W. Richard Peltier, and Sindia Sosdian. 2012. "High Tide of the Warm Pliocene: Implications of Global Sea Level for Antarctic Deglaciation." *Geology* 40 (5): 407–10. https://doi.org/10.1130/G32869.1.

Morrison, Adele K., Thomas L. Frölicher, and Jorge L. Sarmiento. 2014. "Upwelling in the Southern Ocean." *Physics Today* 68 (1): 27–32. https://doi.org/10.1063/pt.3.2654.

Muglia, Juan, and Andreas Schmittner. 2015. "Glacial Atlantic Overturning Increased by Wind Stress in Climate Models." *Geophysical Research Letters* 42 (22): 9862–69. https://doi.org/10.1002/2015GL064583.

Naafs, B. David A., Jens Hefter, Gary Acton, Gerald H. Haug, Alfredo Martínez-Garcia, Richard Pancost, and Ruediger Stein. 2012. "Strengthening of North American Dust Sources during the Late Pliocene (2.7Ma)." *Earth and Planetary Science Letters* 317–318: 8–19. https://doi.org/10.1016/j.epsl.2011.11.026.

Naish, T, R Powell, R Levy, G Wilson, R Scherer, F Talarico, L Krissek, et al., 2009. "Obliquity-Paced Pliocene West Antarctic Ice Sheet Oscillations." *Nature* 458 (March): 322. https://doi.org/10.1038/nature07867.

Oka, A., Hasumi, H., Okada, N., and Suzuki, T. T., and Suzuki, T.: Deep convection seesaw controlled by freshwater trans- port through the Denmark Strait, Ocean Model., 15, 157–176, https://doi.org/10.1016/j.ocemod.2006.08.004, 2006.

Petrick, Benjamin, Erin L. McClymont, Sonja Felder, Gemma Rueda, Melanie J. Leng, and Antoni Rosell-Melé. 2015. "Late Pliocene Upwelling in the Southern Benguela Region." *Palaeogeography, Palaeoclimatology, Palaeoecology* 429: 62–71. https://doi.org/10.1016/j.palaeo.2015.03.042.

Pollard, David, and Robert M DeConto. 2009. "Modelling West Antarctic Ice Sheet Growth and Collapse through the Past Five Million Years." *Nature* 458 (March): 329. https://doi.org/10.1038/nature07809.

Putrasahan, D. A., Lisa M. Beal, Ben P. Kirtman, and Yu Cheng. 2015. "A New Eulerian Method to Estimate 'Spicy' Agulhas Leakage in Climate Models." *Geophysical Research Letters* 42 (11): 4532–39. https://doi.org/10.1002/2015GL064482.

Rahmstorf, Stefan, and Matthew H England. 1997. “Influence of Southern Hemisphere Winds on North Atlantic Deep Water Flow.” *Journal of Physical Oceanography* 27 (9): 2040–54. https://doi.org/10.1175/1520-0485(1997)027<2040:IOSHWO>2.0.CO;2.

Ravelo, Ana Christina, Dyke H. Andreasen, Mitchell Lyle, Annette Olivarez Lyle, and Michael W. Wara. 2004. “Regional Climate Shifts Caused by Gradual Global Cooling in the Pliocene Epoch.” *Nature* 429 (6989): 263–67. https://doi.org/10.1038/nature02567.

Raymo, M E. 1994. “THE INITIATION OF NORTHERN HEMISPHERE GLACIATION.” *Annual Review of Earth and Planetary Sciences* 22 (1): 353–83. https://doi.org/10.1146/annurev.ea.22.050194.002033.

Raymo, Maureen E., and Jerry X. Mitrovica. 2012. “Collapse of Polar Ice Sheets during the Stage 11 Interglacial.” *Nature* 483 (7390): 453–56. https://doi.org/10.1038/nature10891.

Riahi, Keywan, Shilpa Rao, Volker Krey, Cheolhung Cho, Vadim Chirkov, Guenther Fischer, Georg Kindermann, Nebojsa Nakicenovic, and Peter Rafaj. 2011. “RCP 8.5-A Scenario of Comparatively High Greenhouse Gas Emissions.” *Climatic Change* 109 (1): 33–57. https://doi.org/10.1007/s10584-011-0149-y.

Richardson, Philip L. 2007. “Agulhas Leakage into the Atlantic Estimated with Subsurface Floats and Surface Drifters.” *Deep-Sea Research Part I: Oceanographic Research Papers* 54 (8): 1361–89. https://doi.org/10.1016/j.dsr.2007.04.010.

Robinson, Marci M, United States, Geological Survey, Daniel Hill, Linda Sohl, and Mark Williams. 2010. “The PRISM3D Paleoenvironmental Reconstruction PRISM3 / GISS Topographic Reconstruction Data Series 419,” no. April 2017.

Rojas, Maisa, Patricio Moreno, Masa Kageyama, Michel Crucifix, Chris Hewitt, Ayako Abe-Ouchi, Rumi Ohgaito, Esther C. Brady, and Pandora Hope. 2009. “The Southern Westerlies during the Last Glacial Maximum in PMIP2 Simulations.” Climate Dynamics 32 (4): 525–48. https://doi.org/10.1007/s00382-008-0421-7.Rosenbloom, N. A., B. L. Otto-Bliesner, E. C. Brady, and P. J. Lawrence. 2013. “Simulating the Mid-Pliocene Warm Period with the CCSM4 Model.” *Geoscientific Model Development* 6 (2): 549–61. https://doi.org/10.5194/gmd-6-549-2013.

Rouault, Mathieu, Pierrick Penven, and Benjamin Pohl. 2009. “Warming in the Agulhas Current System since the 1980’s.” *Geophysical Research Letters* 36 (12): 1–5. https://doi.org/10.1029/2009GL037987.

Rovere, A., M. E. Raymo, J. X. Mitrovica, P. J. Hearty, M. J. O’Leary, and J. D. Inglis. 2014. “The Mid-Pliocene Sea-Level Conundrum: Glacial Isostasy, Eustasy and Dynamic Topography.” *Earth and Planetary Science Letters* 387: 27–33. https://doi.org/10.1016/j.epsl.2013.10.030.

Ruijter, W. P. M. de, A. Biastoch, S. S. Drijfhout, J. R. E. Lutjeharms, R. P. Matano, T. Pichevin, P. J. van Leeuwen, and W. Weijer. 1999. "Indian-Atlantic Interocean Exchange: Dynamics, Estimation and Impact." *Journal of Geophysical Research: Oceans* 104 (C9): 20885–910. https://doi.org/10.1029/1998jc900099.

Russell, Joellen L., Keith W. Dixon, Anand Gnanadesikan, Ronald J. Stouffer, and J. R. Toggweiler. 2006. "The Southern Hemisphere Westerlies in a Warming World: Propping Open the Door to the Deep Ocean." *Journal of Climate* 19 (24): 6382–90. https://doi.org/10.1175/JCLI3984.1.

Salzmann, U., A. M. Haywood, D. J. Lunt, P. J. Valdes, and D. J. Hill. 2008. "A New Global Biome Reconstruction and Data-Model Comparison for the Middle Pliocene." *Global Ecology and Biogeography* 17 (3): 432–47. https://doi.org/10.1111/j.1466-8238.2008.00381.x.

Schepper, Stijn De, Jeroen Groeneveld, Bernhard David A Naafs, Cedric Van Renterghem, Jan A I Hennissen, Martin J Head, and Stephen Louwye. 2013. "Oxygen Isotope Records of Foraminifera, and Alkenone and Mg/Ca-Based SST Estimates for ODP Hole 165-999A." In Supplement to: Northern Hemisphere Glaciation during the Globally Warm Early Late Pliocene. PloS ONE, 8(12), E81508, Https://Doi.Org/10.1371/Journal.Pone.0081508. PANGAEA. https://doi.org/10.1594/PANGAEA.804671.

Schouten, Mathijs W., Will P. M. de Ruijter, Peter Jan van Leeuwen, and Johann R. E. Lutjeharms. 2000. "Translation, Decay and Splitting of Agulhas Rings in the Southeastern Atlantic Ocean." Journal of Geophysical Research: Oceans 105 (C9): 21913–25. https://doi.org/10.1029/1999jc000046.

Scussolini, P., E. Van Sebille, and J. V. Durgadoo. 2013. "Paleo Agulhas Rings Enter the Subtropical Gyre during the Penultimate Deglaciation." Climate of the Past 9 (6): 2631–39. https://doi.org/10.5194/cp-9-2631-2013.

Sebille, E. Van, A. Biastoch, P. J. Van Leeuwen, and W. P.M. De Ruijter. 2009. "A Weaker Agulhas Current Leads to More Agulhas Leakage." *Geophysical Research Letters* 36 (3): 10–13. https://doi.org/10.1029/2008GL036614.

Sebille, Erik van, Peter Jan van Leeuwen, Arne Biastoch, and Wilhelmus P.M. de Ruijter. 2010. "Flux Comparison of Eulerian and Lagrangian Estimates of Agulhas Leakage: A Case Study Using a Numerical Model." *Deep-Sea Research Part I: Oceanographic Research Papers* 57 (3): 319–27. https://doi.org/10.1016/j.dsr.2009.12.006.

Sebille, Erik Van, Paolo Scussolini, Jonathan V. Durgadoo, Frank J.C. Peeters, Arne Biastoch, Wilbert Weijer, Chris Turney, Claire B. Paris, and Rainer Zahn. 2015. "Ocean Currents Generate Large Footprints in Marine Palaeoclimate Proxies." *Nature Communications* 6 (Ivm): 1–8. https://doi.org/10.1038/ncomms7521.

Sebille, Erik van, Stephen M. Griffies, Ryan Abernathey, Thomas P. Adams, Pavel Berloff, Arne Biastoch, Bruno Blanke, et al., 2018. “Lagrangian Ocean Analysis: Fundamentals and Practices.” Ocean Modelling 121 (July 2016): 49–75. https://doi.org/10.1016/j.ocemod.2017.11.008.

Shackleton, N., 1995. New data on the evolution of Pliocene climatic variability. In: Vrba, E., Denton, G., Partridge, T., Burckle, L. (Eds.), Paleoclimate and Evolution with Emphasis on Human Origins. Yale University Press, New Haven, CT, pp. 242–248.

Sijp, Willem P., and Matthew H. England. 2004. “Effect of the Drake Passage Throughflow on Global Climate.” *Journal of Physical Oceanography* 34 (5): 1254–66. https://doi.org/10.1175/1520-0485(2004)034<1254:eotdpt>2.0.co;2.

———. 2008. “The Effect of a Northward Shift in the Southern Hemisphere Westerlies on the Global Ocean.” *Progress in Oceanography* 79 (1): 1–19. https://doi.org/10.1016/j.pocean.2008.07.002.

Sime, Louise C, Karen E Kohfeld, Corinne Le Quéré, Eric W Wolff, Agatha M de Boer, Robert M Graham, and Laurent Bopp. 2013. “Southern Hemisphere Westerly Wind Changes during the Last Glacial Maximum: Model-Data Comparison.” *Quaternary Science Reviews* 64: 104–20. https://doi.org/https://doi.org/10.1016/j.quascirev.2012.12.008.

Simon, Margit H., Xun Gong, Ian R. Hall, Martin Ziegler, Stephen Barker, Gregor Knorr, Marcel T.J. Van Der Meer, Sebastian Kasper, and Stefan Schouten. 2015. “Salt Exchange in the Indian-Atlantic Ocean Gateway since the Last Glacial Maximum: A Compensating Effect between Agulhas Current Changes and Salinity Variations?” *Paleoceanography* 30 (10): 1318–27. https://doi.org/10.1002/2015PA002842.

Son, Seok Woo, Neil F. Tandon, Lorenzo M. Polvani, and Darryn W. Waugh. 2009. “Ozone Hole and Southern Hemisphere Climate Change.” *Geophysical Research Letters* 36 (15). https://doi.org/10.1029/2009GL038671.

Son, S W, E P Gerber, J Perlwitz, L M Polvani, N P Gillett, K H Seo, V Eyring, et al., 2010. “Impact of Stratospheric Ozone on Southern Hemisphere Circulation Change : A Multimodel Assessment” 115: 1–18. https://doi.org/10.1029/2010JD014271.

Souza, J. M.A.C., C. De Boyer Montégut, and P. Y. Le Traon. 2011. “Comparison between Three Implementations of Automatic Identification Algorithms for the Quantification and Characterization of Mesoscale Eddies in the South Atlantic Ocean.” *Ocean Science* 7 (3): 317–34. https://doi.org/10.5194/os-7-317-2011.

Spence, P., S. M. Griffies, M. H. England, A. M. C. Hogg, O. A. Saenko, and N. C. Jourdain (2014), Rapid subsurface warming and circulation changes of Antarctic coastal waters by poleward shifting winds, Geophys. Res. Lett., 41, 4601–4610, doi:10.1002/2014GL060613.

Spence, Paul, Ryan M. Holmes, Andrew Mc C. Hogg, Stephen M. Griffies, Kial D. Stewart, and Matthew H. England. 2017. “Localized Rapid Warming of West Antarctic Subsurface Waters by Remote Winds.” *Nature Climate Change* 7 (8): 595–603. https://doi.org/10.1038/NCLIMATE3335.

Swart, N. C., and J. C. Fyfe. 2012. “Observed and Simulated Changes in the Southern Hemisphere Surface Westerly Wind-Stress.” *Geophysical Research Letters* 39 (16): 6–11. https://doi.org/10.1029/2012GL052810.

Russell, Joellen L., Keith W. Dixon, Anand Gnanadesikan, Ronald J. Stouffer, and J. R. Toggweiler. 2006. “The Southern Hemisphere Westerlies in a Warming World: Propping Open the Door to the Deep Ocean.” *Journal of Climate* 19 (24): 6382–90. https://doi.org/10.1175/JCLI3984.1.

Turney, Chris S M, and Richard T. Jones. 2010. “Does the Agulhas Current Amplify Global Temperatures during Super-Interglacials?” *Journal of Quaternary Science* 25 (6): 839–43. https://doi.org/10.1002/jqs.1423.

Vellinga, Michael and Wood, Richard A. 2002. "Global climatic impacts of a collapse of the Atlantic thermohaline circulation" Clim. Change 54, (3): 251–267

Wang, Guojian, Wenju Cai, and Ariaan Purich. 2014. “Trends in Southern Hemisphere Wind-Driven Circulation in CMIP5 Models over the 21st Century: Ozone Recovery versus Greenhouse Forcing.” *Journal of Geophysical Research: Oceans* 119 (5): 2974–86. https://doi.org/10.1002/2013JC009589.

Watanabe, Tsuyoshi, Atsushi Suzuki, Shoshiro Minobe, Tatsunori Kawashima, Koji Kameo, Kayo Minoshima, Yolanda M Aguilar, et al., 2011. “Permanent El Niño during the Pliocene Warm Period Not Supported by Coral Evidence.” *Nature* 471 (March): 209. https://doi.org/10.1038/nature09777.

Weijer, Wilbert, Wilhelmus P.M. De Ruijter, Andreas Sterl, and Sybren S. Drijfhout. 2002. “Response of the Atlantic Overturning Circulation to South Atlantic Sources of Buoyancy.” *Global and Planetary Change* 34 (3–4): 293–311. https://doi.org/10.1016/S0921-8181(02)00121-2.

Weijer, Wilbert, and Erik van Sebille. 2014. “Impact of Agulhas Leakage on the Atlantic Overturning Circulation in the CCSM4.” *Journal of Climate* 27 (1): 101–10. https://doi.org/10.1175/JCLI-D-12-00714.1.

Willeit, Matteo, Andrey Ganopolski, Reinhard Calov, Alexander Robinson, and Mark Maslin. 2015. “The Role of CO<inf>2</Inf> Decline for the Onset of Northern Hemisphere Glaciation.” *Quaternary Science Reviews* 119: 22–34. https://doi.org/10.1016/j.quascirev.2015.04.015.

Xiangyu, L I, Jiang Dabang, Zhang Zhongshi, Zhang Ran, Tian Zhiping, and Y A N Qing. 2015. “Mid-Pliocene Westerlies from PlioMIP Simulations.” *Advances in Atmospheric Sciences* 32 (July): 909–23. https://doi.org/10.1007/s00376-014-4171-7.1.

Yang, Xiao Yi, Rui Xin Huang, and Dong Xiao Wang. 2007. “Decadal Changes of Wind Stress over the Southern Ocean Associated with Antarctic Ozone Depletion.” *Journal of Climate* 20 (14): 3395–3410. https://doi.org/10.1175/JCLI4195.1.

Yeager, Stephen and Danabasoglu, Gokhan. “The Origins of Late-Twentieth-Century Variations in the Large-Scale North Atlantic Circulation,” J*ournal of Climate* 27: 3222–47. https://doi.org/10.1175/JCLI-D-13-00125.1.

Zachos, James C, Gerald R Dickens, and Richard E Zeebe. 2008. “An Early Cenozoic Perspective on Greenhouse Warming and Carbon-Cycle Dynamics.” *Nature* 451 (January): 279. https://doi.org/10.1038/nature06588.

Zhang, Z. S., K. H. Nisancioglu, M. A. Chandler, A. M. Haywood, B. L. Otto-Bliesner, G. Ramstein, C. Stepanek, et al., 2013. “Mid-Pliocene Atlantic Meridional Overturning Circulation Not Unlike Modern.” *Climate of the Past* 9 (4): 1495–1504. https://doi.org/10.5194/cp-9-1495-2013.